Antibiotic resistance and pathogenicity in the Gram-negative bacteria *Pseudomonas aeruginosa* and *Klebsiella pneumoniae*

Von der Fakultät für Lebenswissenschaften
der Technischen Universität Carolo-Wilhelmina
zu Braunschweig
zur Erlangung des Grades eines
Doktor der Naturwissenschaften
(Dr. rer. nat.)
genehmigte

D i s s e r t a t i o n

von Sebastian Hans Günter Bruchmann
aus Northeim

1. Referent:	Professor Dr. Michael Steinert
2. Referentin:	Professorin Dr. Susanne Häußler
eingereicht am:	20.04.2015
mündliche Prüfung (Disputation) am:	01.09.2015

Druckjahr 2015

Vorveröffentlichungen der Dissertation

Teilergebnisse aus dieser Arbeit wurden mit Genehmigung der Fakultät für Lebenswissenschaften, vertreten durch den Mentor der Arbeit, in folgenden Beiträgen vorab veröffentlicht:

Publikationen

Bruchmann S., Muthukumarasamy U., Pohl S., Preusse M., Bielecka A., Nicolai T., Hamann I., Hillert R., Kola A., Gastmeier P., Eckweiler D., Häussler S. Deep transcriptome profiling of clinical Klebsiella pneumoniae isolates reveals strain- and sequence type-specific adaptation. Environmental Microbiology. 2015 Aug. doi: 10.1111/1462-2920.13016.

Bruchmann S., Dötsch A., Nouri B., Chaberny I.F., Häussler S. Quantitative contributions of target alteration and decreased drug accumulation to Pseudomonas aeruginosa fluoroquinolone resistance. Antimicrob Agents Chemother. 2013 Mar;57(3):1361-8.

Tagungsbeiträge

Bruchmann S., Chesnel D., Muthukumarasamy U., Bielecka A., Nicolai T., Eckweiler D., Häußler S. Whole-transcriptome sequencing of Klebsiella pneumoniae clinical isolates (Poster), 4th Joint Conference of the Association for General and Applied Microbiology (VAAM) and the Society of Hygiene and Microbiology (DGHM), Dresden (2014)

Bruchmann S., Schniederjans M., Khaledi A., Hornischer K., Pohl S., Dötsch A., Eckweiler D., Klawonn F., Häussler S. A comprehensive transcriptomic approach to unravel the antibiotic resistome of Pseudomonas aeruginosa clinical isolates (Vortrag und Poster). 8th European Cystic Fibrosis Young Investigator Meeting, Paris, Frankreich (2014)

Bruchmann S., Schniederjans M., Khaledi A., Hornischer K., Pohl S., Dötsch A., Eckweiler D., Klawonn F., Häussler S. A comprehensive transcriptomic approach to unravel the antibiotic resistome of *Pseudomonas aeruginosa* clinical isolates (Vortrag). 6th International PhD Symposium, HZI, Braunschweig (2013)

Bruchmann S., Dötsch A., Chaberny I.F., Häussler S. Target Alteration and Drug Efflux in *Pseudomonas aeruginosa* Fluoroquinolone Resistance (Poster). 5th Congress of European Microbiologists (FEMS), Leipzig (2013)

Bruchmann S., Dötsch A., Schniederjans M., Khaledi A., Häussler S. Prediction of antibiotic resistance in *Pseudomonas aeruginosa* based on genotypic data (Vortrag). 3rd Public Retreat HZI Graduate School, Bad Bevensen (2012)

Bruchmann S., Nouri B, Häussler S. Prediction of antibiotic resistance in *Pseudomonas aeruginosa* based on genotypic data (Poster). 5th International PhD Symposium, HZI, Braunschweig (2011)

Bruchmann S., Nouri B., Häussler S. Prediction of antibiotic resistance in *Pseudomonas aeruginosa* based on genotypic data (Poster). 2nd Public Retreat HZI Graduate School, Goslar-Hahnenklee (2011)

Zusammenfassung

Der dramatische Anstieg von Infektionen durch multiresistente, gramnegative Bakterien ist ein weltweites Problem, welches möglicherweise eine der größten Herausforderungen moderner Medizin darstellt. Bakterielle Krankheitserreger besitzen verschiedenste Mechanismen, um der Aktivität einer Vielzahl antimikrobieller Verbindungen zu widerstehen und zeigen eine alarmierende Zunahme von multi- oder sogar pan-resistenten Isolaten.

Die Ziele der vorliegenden Arbeit waren i) die molekularen Mechanismen der Fluorchinolonresistenz im opportunistischen Krankheitserreger *Pseudomonas aeruginosa* zu erklären und ii) die generelle Genexpression von *Klebsiella pneumoniae* zu beschreiben und mit den klinisch relevanten Phänotypen der Biofilmbildung, Virulenz und Antibiotikaresistenz zu korrelieren.

In diesem Zusammenhang untersuchten wir den quantitativen Einfluss von Mutationen und Veränderung der Expression von Effluxpumpen auf die Fluorchinolonresistenz in *Pseudomonas aeruginosa* durch die Verwendung einer Kombination von Resequenzierung, quantitativer realtime-PCR und Transkriptom-Sequenzierung (RNA-Seq) anhand einer Sammlung von 172 klinischen Isolaten. Diese umfassenden Daten zeigten die dominierende Rolle bestimmter Mutationen in *gyrA* und *parC*, während die Kombination mit weiteren Mutationen (zum Beispiel in *gyrB* und *parE*) oder verstärkter Efflux zwar eine additive Wirkung hatte, aber höchstwahrscheinlich nicht zum hohen Resistenzniveau in der Klinik beiträgt.

Darüber hinaus nutzen wir die Möglichkeiten hoch-auflösenden Transkriptom-Profilings mittels RNA-Seq um die generelle Gentranskription 37 klinischer *K. pneumoniae* Isolate unterschiedlichster Herkunft aufzuklären und identifizierten eine große Anzahl von 3346 Genen, die in allen Isolaten exprimiert wurden. Während dieses Kern-Transkriptom weitgehend homogen zwischen Isolaten des gleichen Sequenztypen war, variierte es deutlich zwischen Gruppen unterschiedlicher Sequenztypen. Diese detaillierten Informationen über differentiell exprimierte Gene wurde mit den klinisch relevanten Phänotypen der Biofilmbildung, bakterieller Virulenz und Antibiotikaresistenz verknüpft. Dieses erlaubte die Identifizierung eines Biofilm-spezifischen Genexpressionsprofil in der Gruppe der ST258-Isolate, welche hauptverantwortlich für die Verbreitung der KPC-Carbapenemase sind, als ein Sequenztyp-spezifisches Merkmal. Außerdem ergab die Analyse, dass die Antibiotikaresistenz durch das Auftreten nur weniger, dominanter Resistenzdeterminanten erläutert werden kann.

Insgesamt trägt diese Arbeit zu unserem Verständnis der molekularen Prozesse der Antibiotika-Resistenz und Pathogenität bei, welches zukünftig genutzt werden kann, um neue Strategien zur Diagnose und Behandlung bakterieller Infektionen zu entwickeln.

Abstract

The dramatic increase of infections caused by multidrug-resistant Gram-negative bacteria is an emerging global problem and possibly one of the greatest challenges of modern medicine. Bacterial pathogens devise various mechanisms to withstand the activity of a wide range of antimicrobial compounds and there is an alarming increase of multi- or even pandrug-resistant isolates.

The aims of this thesis were i) to elucidate the molecular mechanisms of fluoroquinolone resistance in the opportunistic pathogen *Pseudomonas aeruginosa* and ii) to describe the transcriptomic landscape of *Klebsiella pneumoniae* to correlate gene transcription with the clinical relevant phenotypes of biofilm formation, virulence and antibiotic resistance.

In this context, we evaluated the quantitative contributions of quinolone target alteration and efflux pump expression to fluoroquinolone resistance in *Pseudomonas aeruginosa* by applying a combination of directed resequencing methods, quantitative real-time PCRs and whole-transcriptome sequencing (RNA-Seq) on a broad and cross-sectional panel of 172 clinical isolates. This comprehensive data showed the role of distinct mutations in the quinolone resistance-determining regions of *gyrA* and *parC.* The combination with further mutations (e.g. in *gyrB* and *parE*) or enhanced efflux exhibited additive effects

Furthermore, we exploited the power of deep transcriptome profiling by RNA-seq to shed light on the transcriptomic landscape of 37 clinical *K. pneumoniae* isolates of diverse phylogenetic origin. We identified a large set of 3346 genes which were expressed in all isolates. While these core-transcriptome profiles were largely homogenous among isolates of the same sequence type, they varied substantially between groups of different sequence types. This detailed information on differentially expressed genes was linked with the clinically relevant phenotypes of biofilm formation, bacterial virulence and antibiotic resistance. This allowed the identification of a low biofilm-specific gene expression profile within the group of ST258 isolates, the dominant clonal lineage associated with KPC-carbapenemase spread, as a sequence type-specific trait. Moreover, the analysis revealed that antimicrobial resistance in this panel of clinical isolates can be explained by the occurrence of only a few dominant resistance determinants.

The results of this thesis contribute to our understanding of molecular processes leading to antibiotic resistance and pathogenicity which might be exploited in the future to design novel strategies to improve diagnosis and treatment of bacterial infections.

This research project has been supported by

the President`s Initiative and Networking Fund of the Helmholtz Association

of German Research Centers (HGF) under contract number VH-GS-202.

Table of Contents

List of Figures

List of Tables

List of Abbreviations

AAC	aminoglycoside N-acetyltransferase
AME	aminoglycoside-modifying enzyme
AMP	ampicillin
AMR	antimicrobial resistance
ANT	aminoglycoside O-nucleotidyltransferase
APH	aminoglycoside O-phosphotransferase
ARDB	antibiotic resistance genes database
bp	base pair(s)
CAZ	ceftazidime
CDC	U.S. Centers for Disease Control and Prevention
cDNA	complementary DNA
CF	cystic fibrosis
CFU	colony forming units
CIP	ciprofloxacin
CLSI	Clinical and Laboratory Standards Institute
COPD	chronic obstructive pulmonary disease
CXM	cefuroxime-axetil
dH_2O	deionized water
DSN	duplex-specific nuclease
E. coli	*Escherichia coli*
ESBL	extended-spectrum beta-lactamase
et al.	*et alii*
FDA	U.S. Food and Drug Administration
FDR	false discovery rate
GEN	gentamicin
GO	Gene Ontology
indel	insertion and deletion
IPM	imipenem
IPTG	isopropyl-β-d-thiogalactopyranoside
K. variicola	*Klebsiella variicola*
K. pneumoniae	*Klebsiella pneumoniae*
KPC	*Klebsiella pneumoniae* carbapenemase
LB	lysogeny broth
LVX	levofloxacin
m/v	mass per volume
MALDI-TOF	matrix-assisted laser desorption/ionization time-of-flight mass spectrometry
MATE	multidrug and toxic compound extrusion
MDR	multidrug resistant/resistance
MEM	meropenem
MEX	multidrug efflux
MFS	major facilitator superfamily
MH	Mueller Hinton

MIC	minimal inhibitory concentration
MLST	multilocus sequence typing
n.d.	not determined
NDM	New Delhi metallo-beta-lactamase
NIH	National Institutes of Health
nRPK	normalized reads per kilobase
OD	optical density
OMP	outer membrane proteins
P. aeruginosa	*Pseudomonas aeruginosa*
PBS	phosphate buffered saline
PBP	penicillin-binding protein
PCR	polymerase chain reaction
PLA	pyogenic liver abscess
PMQR	plasmid-mediated quinolone-resistance
PSQ	pyrosequencing
QRDR	quinolone resistance-determining region
qRT-PCR	quantitative real-time reverse transcription-PCR
RNA	ribonucleic acid
RND	resistance-nodulation division
RPG	reads per gene
rRNA	ribosomal RNA
S. aureus	*Staphylococcus aureus*
SAM	ampicillin-sulbactam
SMR	small multidrug resistance
SNP	single nucleotide polymorphism
SRA	sequence read archive
sRNA	small RNA
ST	sequence type
TAP	tobacco acid pyrophosphatase
TE	Tris-EDTA
Tris	tris(hydroxymethyl)aminomethane
TZP	piperacillin-tazobactam
UBP	universal biotinylated primer
VFDB	virulence factors database
vs.	versus
v/v	volume per volume
w/v	weight per volume

Units as well as nucleotides and amino acids are abbreviated according to the International System of Units and the International Union of Pure and Applied Chemistry nucleotide/amino acid code, respectively.

1 Introduction

Adaption of bacteria to complex and changing environments is well reflected by global changes in gene expression profiles, which may become fixed by adaptive mutations to facilitate survival in challenging habitats [1]. Thus, to study microbial pathogenesis and to fully understand bacterial adaptation strategies it is crucial to explore the genomic make-up of a pathogen and to analyze how this influences the transcriptional landscape. One of the most crucial adaptations a bacterial pathogen has to accomplish is the adaptation to the activity of antimicrobial compounds. In the last decade multidrug-resistant bacterial pathogens have been isolated from patients material at constantly increasing rates [2]. This poses a serious threat to human health and leads to alarming limitations of treatment options especially against Gram-negative pathogens like *Pseudomonas aeruginosa* and *Klebsiella pneumoniae* [3].

1.1 *Pseudomonas aeruginosa* is a versatile, opportunistic human pathogen

Pseudomonas aeruginosa, the most prominent and best-studied member of the genus *Pseudomonas,* belonging to the class of γ-Proteobacteria [4], is a highly versatile and adaptable bacterium, able to thrive in a vast number of terrestrial and aquatic habitats [5-7]. This variability is achieved by a versatile metabolic capacity which allows the utilization of over 80 organic compounds as energy and carbon sources [8,9]. Usually, *P. aeruginosa* generates energy based on oxidative metabolism; however, it can also survive and persist under anaerobic conditions using nitrate or nitrite as an alternative electron acceptor [10] or the fermentation of arginine and pyruvate [11]. This high ecological versatility is facilitated by the large and complex genome which contains almost 10 % transcriptional regulators and two-component regulatory systems, which allows a high metabolic flexibility [6]. One major contributor to the successful spreading of *P. aeruginosa* in a variety of ecological niches is its ability to forms biofilms on surfaces such as those of rocks and soil but also implant material, catheter and other medical devices [12]. Biofilms are surface attached communities of bacteria embedded in an extracellular polysaccharide matrix which facilitates survival in hostile environments [12].

As a result of this genomic and metabolic versatility, *P. aeruginosa* has the potential to cause severe infections in a wide range of diverse hosts, from plants to amoeba, insects and vertebrates. While healthy humans become rarely infected, *P. aeruginosa* accounts for up to 15 % of all hospital-acquired infections, ranking second to third among Gram-negative pathogens [13-17]. Nearly all acute infections caused by *P. aeruginosa* occur in immunocompromised patients such as patients

with AIDS [18] or neutropenia patients undergoing chemotherapy [19], patients with a damaged epithelial barrier caused by severe burn wounds [20] or patients undergoing urinary catheterization or ventilation [21,22].

Besides these acute, health-care associated infections, *P. aeruginosa* can chronically colonize the lung of patients suffering from chronic obstructive pulmonary disease (COPD) or cystic fibrosis (CF) which causes severely compromised lung functions. In CF patients infections of *P. aeruginosa* account for the majority of the morbidity and mortality [22]. The autosomal recessive disorder CF, also known as mucoviscidosis, is caused by mutations of a chloride ion channel named cystic fibrosis transmembrane conductance regulator (CFTR), leading to pathological changes in multiple organs and tissues [23]. The most severe implications occur in the lung, where a non-functional CFTR disturbs the sodium and chloride ion transport across the epithelium [24] that leads to an inefficient mucociliary clearance and/or hyperosmolarity of airway surface liquid which promotes bacterial colonization [21].

1.2 *Klebsiella pneumoniae* causes outbreaks throughout the world

Another bacterium with a high potential of threatening public health is *Klebsiella pneumoniae*, like *P. aeruginosa* a member of the group of ESKAPE pathogens (*Enterococcus faecium*, *Staphylococcus aureus*, *Klebsiella pneumoniae*, *Acinetobacter baumannii*, *Pseudomonas aeruginosa* and *Enterobacter* species) [25] - bugs with limited remaining treatment options. Although several, diverse mechanisms are leading to antimicrobial resistance (AMR) [26-28], the occurrence of the *Klebsiella pneumoniae* carbapenemase (KPC) [29] and the New Delhi metallo-beta-lactamase (NDM) [30] are of serious concern and have become a severe threat especially in nosocomial infections [31-33].

K. pneumoniae is a ubiquitous Gram-negative human pathogen of the family Enterobacteriaceae, and therefore closely related to *Escherichia coli*. While *E. coli* is primarily a commensal organism, *K. pneumoniae* is capable of surviving in various natural habitats as well as colonizing mucosal surfaces of humans and livestock [34]. In humans, *K. pneumoniae* is able to cause community- and hospital-acquired infections of the urinary and respiratory tract. Together with *E. coli* it is the leading cause of bacteremia in the UK [35] and causes diseases like liver abscess, pneumonia, meningitis and endophthalmitis with mortality rates exceeding 50 % for severe systemic infections [34]. The majority of infections caused by *K. pneumoniae* occurs mainly in hospitalized, immunocompromised patients suffering from diseases such as diabetes mellitus or chronic pulmonary obstruction [34] and are associated with high rates of morbidity and mortality [36]. However, since the end of the 1980s, *K. pneumoniae* infections causing pyogenic liver abscess (PLA) in otherwise healthy individuals emerged in Taiwan and other Asian countries, and cases are increasingly reported [37-40].

Pathogenicity of *K. pneumoniae* depends on various, different virulence factors including the capsular serotype, lipopolysaccharide, iron-scavenging systems (siderophores), and adhesins [34]. Among these virulence factors, the capsule is thought to be the most important one [40]. It is composed of complex acidic polysaccharides and protects the bacterium during the course of an infection from phagocytosis [41] and antimicrobial peptides [42]. *K. pneumoniae* capsules can be classified into 77 different capsular (K) serotypes. Among these, types K1, K2, K4, and K5 are highly virulent and often associated with severe infections [40], noteworthy are K1 and K2 serotypes as the main cause of PLA [43].

Due to the remarkable collection of virulence factors and an accompanying multidrug resistance phenotype, many *K. pneumoniae* strains are able to spread extensively among patients, leading to nosocomial outbreaks, especially in neonatal units [34,44]. Clinical *K. pneumoniae* outbreaks have been described since the 1950s [45] and are becoming a major concern of clinicians. *K. pneumoniae* is responsible for approximately 15 % of Gram-negative infections in hospital intensive care units in the United States [46,47] and a PubMed search for the entry “outbreak” in combination with “Klebsiella” yielded almost 600 reports (as of March 2015). This enormous potential to threaten human health due to very limited treatment options has recently led to the classification of carbapenem resistant Enterobacteriaceae as an “urgent threat to human health” by the U.S. Centers for Disease Control and Prevention (CDC) [48].

1.3 The antibiotic era and its current global crisis

The term antibiotic was first introduced and defined by Selman A. Waksman in a 1947 paper:

> [The term ‘antibiotic’ or ‘antibiotic substance’] *"should be used to designate the action of the chemical agents, produced by micro-organisms and possibly other living bodies, which were responsible for these antimicrobial effects."* [49]

Antibiotics are undoubtedly one of the most successful forms of chemotherapy in the history of medicine and contributed greatly to the control of bacterial infectious diseases which were the leading causes of morbidity and mortality for most of human existence [50]. The ‘antibiotic era’ started at the beginning of the 20th century with the work of Noble laureates Paul Ehrlich, Alexander Fleming and Selman Waksman. Ehrlich’s work led to the discovery of compound 606 in 1911 (later named Salvarsan) against the spirochete *Treponema pallidium,* the causative agent of syphilis [51]. And only a few years after Fleming’s famous observation of a fungus with antimicrobial activity on the September 3 in 1928, the first antibacterial drug, Penicillin, was purified and clinically tested by

Nobel laureates Howard W. Florey and Ernst B. Chain in 1941, shortly followed by the discovery of Streptomycin, the first anti-tuberculosis drug, in 1943 by Waksman and colleagues [50,52,53]. Between 1940 and 1962 extensive research and elaborated screening methods led to the discovery and development of more than 20 novel classes of antibiotics that have reached the market [54]. The vast majority of all classes of antibiotics is based on natural products. Estimates of the origin of natural product antibiotics range from 40 million years up to 2 billion years ago and studies suggest that resistance mechanism might be similarly old [55,56]. A recent study identified a highly diverse collection of resistance conferring genes in 30,000-year-old permafrost samples and could therefore demonstrate antibiotic resistance was present long before antibiotics were used in human medicine [57]. Therefore, it is of little surprise, that resistance to certain antibiotics occurred only a few years after they were introduced as a therapeutic (see Figure 1.1). Interestingly, the first beta-lactamase was already identified by the group of Florey and Chain several years before Penicillin was marketed [58,59] and Alexander Fleming stated already in 1946:

> *"There is probably no chemotherapeutic drug to which in suitable circumstances the bacteria cannot react by in some way acquiring 'fastness'* [resistance]*."* [60]

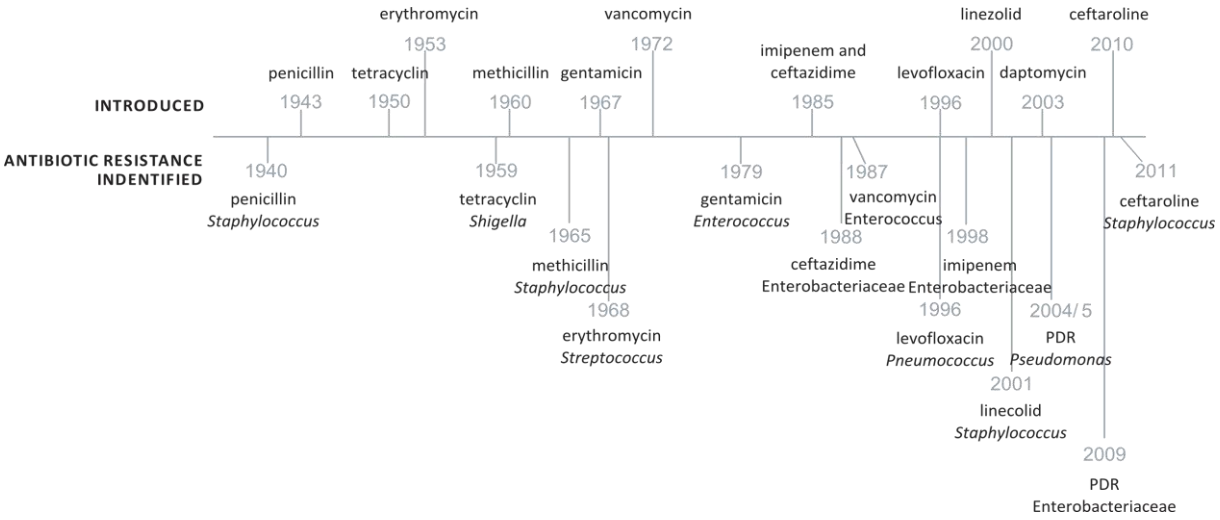

Figure 1.1: Brief history of antibiotics

The timeline shows the introduction of important antimicrobial drugs and the occurrence of the first resistant microbes. Figure adapted from [48]. PDR, pandrug resistant

More dramatically, the often inappropriate usage of these drugs in humans, livestock and poultry has been accompanied by a rapid emergence of resistant or even multidrug-resistant strains. Along with this spread of (multi-) drug resistance, a constant decline in the discovery of novel antimicrobial agents has potentially drastic consequences for human health around the world [61]. Only two new

classes of systemic drugs have reached the market: the oxazolidinone drug linezolid in 2000 by Pfizer and the cyclic lipopeptide daptomycin in 2003 by Cubist, both active against Gram-positive bacteria [54,62]. Moreover, the total number of new systemic antibacterial agents approved by the U.S. Food and Drug Administration (FDA) has significantly decreased over the past decades (see Figure 1.1) as several large pharmaceutical companies have exited the space. In particular there are almost no agents in the clinical pipeline for the treatment of infections caused by resistant Gram-negative bacterial pathogens [63].

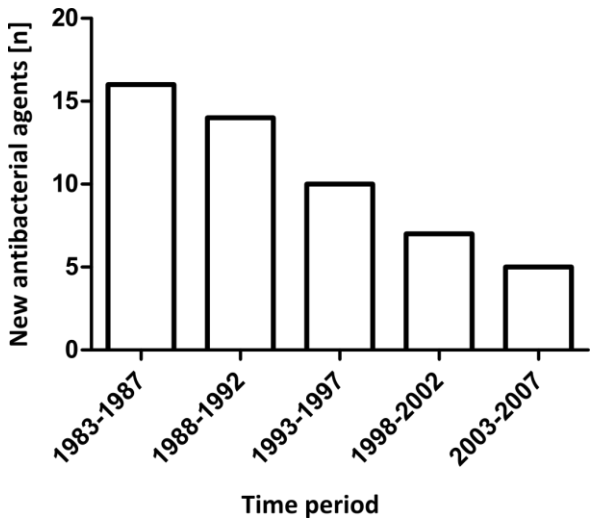

Figure 1.2: New antibacterial agents approved by the U.S. FDA

Graph shows the total number of novel systemic antimicrobial agents in 5 year intervals from 1983 to 2007. Figure adapted from [64].

The current rise of antimicrobial resistance (AMR) reaches an alarming rate and poses a growing, serious threat to human health [65,66], since infections with MDR isolates are associated with severe adverse clinical outcomes, increases in the hospital length of stay, morbidity and mortality, and greater overall cost of treating the infection [67-69].

Not only is the frequency of AMR increasing, but also the spectrum of antibiotic resistant infections is widening world-wide [70]. Figure 1.3 depicts the dramatic increase in the rate of *K. pneumoniae* isolates being non-susceptible to one of the following antibiotics: aminoglycosides, fluoroquinolones, third-generation cephalosporins and carbapenems, which are the most important classes of antimicrobial agents used to treat infections with this pathogen. Probably most concerning is the rise in carbapenem resistant *K. pneumoniae* isolates, since these drugs are considered to be used as "last-line agents" or "antibiotics of last resort" when treating resistant bacteria [71].

The AMR crisis bears tremendous consequences on human health, the global economy and on society in general [68,72,73]. The Infectious Diseases Society of America considers antimicrobial resistance as "one of the greatest threats to human health worldwide" [74,75]. Each year, at least 2

million people acquire serious infections with bacteria that are resistant to one or more antimicrobials in the United States with an estimation of 23,000 deaths per year attributable to these antibiotic-resistant infections. Leaving all those neglected, which die from other conditions that were complicated by an antibiotic-resistant infection [48]. In Europe, approximately 25,000 people die annually from antibiotic-resistant bacteria and added costs and loss of productivity as a result of antibiotic resistance conservatively amount to 1.5 billion euro [76,77]. A recent report from the British Review on Antimicrobial Resistance presented a scenario of 10 million deaths attributed to drug resistant bacteria per year and accumulated costs for the world economy of up to 100 trillion U.S. dollar, if antibiotic resistance is not tackled in a concentrated manner [78]. The combination of an increase in drug resistant microbes and a steady decrease in novel systemic antimicrobial agents resulted in the warning to enter a 'post antibiotic era', where these invaluable drugs are no longer useful in the treatment of bacterial infections [79].

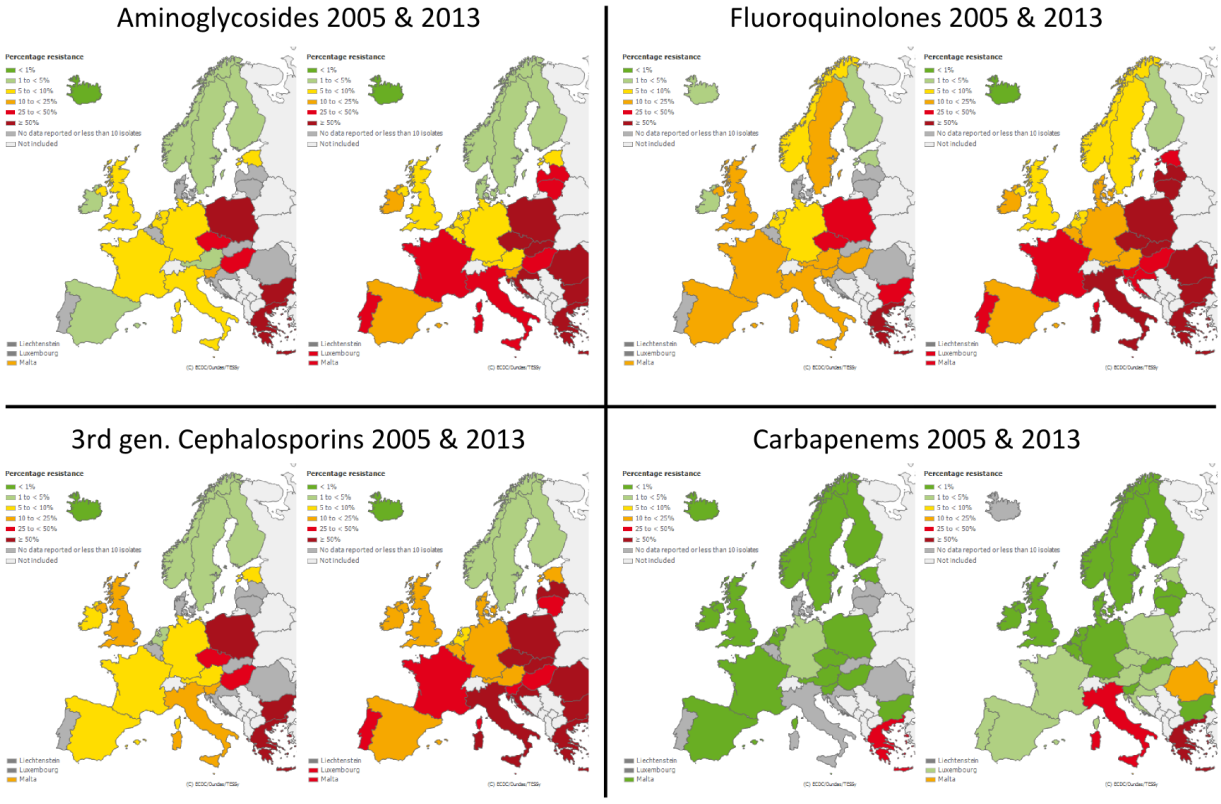

Figure 1.3: Development of AMR in *K. pneumoniae* in Europe between 2005 and 2013

Maps showing the development of aminoglycoside-, fluoroquinolone-, third-generation cephalosporin- and carbapenem non-susceptibility of *K. pneumoniae* in Europe between 2005 and 2013. Colors indicate percentage of resistance: green < 1 %; light green 1 - 5 %; yellow 5 - 10 %; orange 10 - 25 %; red 25 - 50 %; dark red ≥ 50 %; dark gray no data; light gray not included. These graphs have been generated from data submitted to TESSy, The European Surveillance System.

1.4 Antimicrobial resistance in Gram-negative bacteria: intrinsic, acquired, and adaptive

Since antibiotics have been introduced in clinical therapy, bacteria have developed sophisticated resistance strategies leading to an arms race of clinicians with potential deadly human pathogens [80]. The development of antibiotic resistance can thereby be separated into three principal types of antibiotic resistance, namely: intrinsic, acquired, and adaptive resistance (see Table 1.1) [81-83]. The best studied mechanisms and classical examples of antibiotic resistance are intrinsic and acquired resistance, both are irreversible mechanisms and therefore independent of the presence of the antibiotic. Adaptive resistance however, is defined as the reversible bacterial response to the presence of an antimicrobial agent in the surrounding environment [82]. Therefore, acquired resistance might be transmitted vertically to subsequent generations, whereas adaptive resistance is transient and usually reverts upon removal of the antimicrobial agent [82].

Table 1.1: Overview of the different types of resistance

Resistance	Shaped by changes of		Exemplary mechanisms
	genome	environment	
Intrinsic	+	−	Low outer membrane permeability Beta-lactamase production Efflux pump expression Horizontal gene transfer
Acquired	+	−	Mutations leading to reduced uptake and/or Efflux pump overexpression Target mutations
Adaptive	−	+	High beta-lactamase production Efflux pump overexpression

Table adapted from [81].

P. aeruginosa is one of the best studied examples of bacteria with an already high intrinsic resistance towards a broad spectrum of antibiotics. This natural low susceptibility is mainly depended on two mechanisms: An outer membrane with very low permeability and the presence of several efflux systems [84]. The permeability of the outer membrane of *P. aeruginosa* is approximately 100 times lower as compared to the one of *E. coli*, which is achieved by a lack of high-permeability porins that are usually present in most Gram-negative bacteria [84,85]. Additional to this low membrane permeability, *P. aeruginosa*, like most Gram-negative bacteria, contains several efflux pumps which reduce the intracellular drug concentration by extruding the antimicrobial agent and provide

resistance towards a broad spectrum of antibiotics [86]. Bacterial efflux pumps are highly diverse and can be separated into five different classes: the major facilitator superfamily (MFS), the ATP-binding cassette (ABC) family, the resistance-nodulation-division (RND) family, the small multidrug resistance (SMR), and the multidrug and toxic compound extrusion (MATE) family [87]. The probably best studied efflux pumps are those of the RND family, which typically operate as a tripartite system composed of a periplasmic membrane fusion protein, an cytoplasmic efflux transporter and an outer-membrane protein [88]. *P. aeruginosa* possesses at least 11 RND efflux systems which are able to extrude a wide variety of (antimicrobial) compounds (see Figure 1.4). In most cases, all three structural genes of RND-pumps are under the control of a single promoter, which is tightly regulated by a downstream located negative transcriptional regulator. The strong expression of efflux pumps usually occurs due to mutations in these negative regulators, which therefore depicts an example of acquired resistance. In some cases, e.g. *mexAB-oprM* or *mexXY*, transcriptional regulation is controlled by a complex system of regulators [89-91], which allows the expression of these efflux pumps upon environmental signals like antibiotic- or peroxide-stress [92-94], therefore representing an example for adaptive resistance.

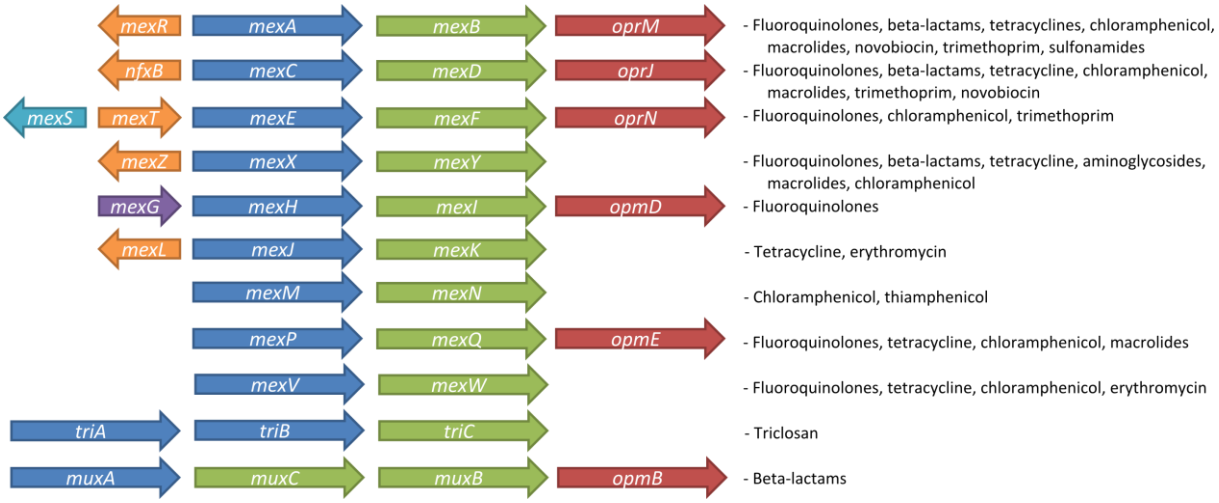

Figure 1.4: RND efflux systems in *P. aeruginosa* and their substrate specificity

Genes are illustrated according to their product as indicated by the following color scheme: Orange, transcriptional regulator; light blue, oxidoreductase; blue, membrane fusion protein; green, RND efflux transporter; red outer membrane protein and purple, protein with unknown function. Exemplary substrates of each RND pumps are listed on the right. Adapted from [69] and [95] with additional information from [96] and [97].

1.4.1 Fluoroquinolone resistance in Gram-negative bacteria is defined by target modifications

Fluoroquinolones are very potent antimicrobial agents with excellent oral bioavailability, reaching concentrations in serum equivalent to those for intravenous administration. They are broad-spectrum antibiotics with antibacterial activity against Gram-positive as well as Gram-negative bacteria [98,99]. As a consequence, fluoroquinolones are widely and increasingly used for the treatment of bacterial infections not only in the hospital setting but also for outpatients. The broad, frequent, and worldwide use of the fluoroquinolones, as well as the frequently inappropriate application of these antibiotics, is an important factor driving resistance, which has reached clinically relevant levels in the last decade [66,100,101].

Fluoroquinolones act by directly inhibiting DNA replication, transcription, and recombination via an interaction of the drug with complexes composed of DNA and either of the two target enzymes, DNA gyrase and topoisomerase IV [98,102]. These enzymes unwind the double stranded DNA molecule by binding the DNA, opening the circular molecule, passing another strand through the break and resealing the DNA. Fluoroquinolone bind to these enzymes and thereby stabilize the DNA-enzyme complex which results in an accumulation of unrepaired double strand breaks [103].

The molecular mechanisms of fluoroquinolone resistance include two dominant mechanistic categories for all bacterial species studied so far [104,105]. The activity of multidrug resistance (MDR) efflux pumps decreases intracellular fluoroquinolone concentrations [86], and alterations of the drug target by mutations at key sites in the so called quinolone resistance-determining regions (QRDRs) of the genes encoding DNA gyrase (*gyrA* and *gyrB*) and/or topoisomerase IV (*parC* and *parE*) lead to decreased binding affinity of the quinolones for their respective drug targets [106,107]. More recently, mobile genetic elements carrying the *qnr* [108], *qepA* [109], or *aac(6')-Ib-cr* [110] gene, which confer reduced susceptibility to quinolones in members of the *Enterobacteriaceae* family, have also been described. These plasmid-mediated resistance determinants exert their activity by either reducing the intracellular drug concentration through efflux (*qepA*), structural modification of the drug (*aac(6')-Ib-cr)* or by binding to gyrase or topoisomerase IV and thereby inhibiting quinolone binding (*qnr*) [111,112].

1.4.2 Beta-lactam resistance through an interplay of enzymes, efflux and porins

Beta-lactam antibiotics, one of the first drugs used in antimicrobial therapy, represent over 65 % of the world's antibiotic market and are one of the most largest antibiotic classes with more than 50 different drugs [113,114]. Furthermore, they are one of the largest and most important classes of antimicrobial agents against Gram-positive and Gram-negative pathogens [115]. Beta-lactams are

characterized by a for-membered beta-lactam ring and exert their antimicrobial activity by interfering with the final stage of the bacterial cell wall synthesis [116,117]. They inhibit the peptidoglycan biosynthesis which is essential for growth, viability, shape, division and integrity of bacterial cells [118-120]. Beta-lactams can be subdivided into several classes including the four most prominent ones: penicillins, cephalosporins, carbapenems, and monobactams [113]. Examples of beta-lactams of high clinical importance are the third generation cephalosporin ceftazidime and the carbapenem meropenem which have a high activity against Pseudomonads [121]. Furthermore, carbapenems such as imipenem and meropenem are recommended as first-line therapy for severe infections caused by Enterobacteriaceae producing extended spectrum beta-lactamases (ESBLs) [122]. Therefore, carbapenems are often 'last resort'-drugs in infections of Gram-negative bacteria [123,124] and the emergence of carbapenem resistance is an tremendous threat since only very few treatment options remain [75].

Although diminished membrane permeability, enhanced efflux or the modification of drug targets in the cell wall contribute to beta-lactam resistance [113], production of carbapenemases, especially in Enterobacteriaceae, is the most widespread cause of carbapenem resistance [71]. Carbapenemases can be either metal-beta-lactamases (e.g. Ambler class B enzymes of VIM, IMP or NDM type) or serine-beta-lactamases (e.g. class A enzymes of KPC type or class D enzymes like OXA-48) [33,125,126]. The wide spectrum of hydrolyzed antibiotics by KPC and NDM enzymes and their location on promiscuous plasmids are major contributors to the rapid and global spread of these enzymes, making them a “health nightmare” for clinicians [127].

1.4.3 Aminoglycoside resistance via drug modifications

Aminoglycoside antibiotics, first described in 1944 by the group of Selman Waksman [52], are highly potent broad-spectrum antibiotics with bactericidal efficacy against Gram-negative and Gram-positive bacteria. Aminoglycoside exert their antimicrobial activity through binding to the 30S subunit of prokaryotic ribosomes and thereby hinder bacterial protein synthesis [128]. This binding perturbs the elongation of the nascent protein chain by impairing the proofreading process which leads to misread, truncated or incorrectly folded proteins [128]. Bacterial cell death after aminoglycoside uptake occurs due to i) insertion of misread proteins into the inner membrane resulting in membrane destabilization [129] and/or ii) accumulation of aminoglycosides to a concentration that leads to complete inhibition of ribosomal activity [130,131].

Like almost all antibiotics, resistance to aminoglycoside antibiotics in Gram-negative bacteria is multifactorial and includes different mechanisms like target mutations, methylation of 16S rRNA, altered intracellular drug concentration due to changed uptake and efflux, and enzymatic

modification of the drug [131]. The latter one is the most prevalent mechanism in Enterobacteriaceae in the clinical setting [132]. Aminoglycoside modifying enzymes (AMEs) are usually located on mobile elements like introns or plasmids and can be divided into the three different classes of acetyltransferases (AACs), nucleotidyltranferases (ANTs), or phosphotransferases (APHs). [132]

Apart from these classical and well-studied mechanisms of antimicrobial resistance, many other factors of Gram-negative bacteria might be influential on the susceptibility profile. Large mutant library screens in *P. aeruginosa* have been published which have analyzed the resistance development against ciprofloxacin [133], tobramycin [134] or a collection of six [135] and 19 [136] different antibiotics, respectively. Although these studies identified between 112 and 233 gene knock-outs which altered the minimal inhibitory concentration (MIC) of the studied antibiotics, including many known resistance determinants like *mexR* (transcriptional repressor of *mexAB-oprM*) or *oprF* (encoding the most common outer membrane protein of *P. aeruginosa*), the impact of the majority of these identified genes on antibiotic non-susceptibility in a clinical setting remains unclear.

1.5 Aims of the thesis

The battle against failure of antibiotic therapy requires a multipronged strategy that includes implementation of effective infection control principles, rational use of antimicrobial agents, and development of new antimicrobial compounds. Furthermore, investigations on the epidemiology of new highly virulent multidrug-resistant strains and detailed knowledge about the molecular mechanisms leading to antimicrobial resistance are crucial for designing specific treatment and infection control strategies [137].

Pseudomonas aeruginosa and *Klebsiella pneumoniae* are both striking examples of highly successful nosocomial and community-acquired Gram-negative pathogens. Both are pathogens with an extensive repertoire of virulence traits and are prone to acquire resistance to a broad variety of antimicrobial agents. The interplay of intrinsic, acquired and adaptive resistance mechanisms on antimicrobial resistance is still not completely understood and large parts of the resistome of these organisms remains unexplored [138].

One aim of this thesis is to evaluate the quantitative contributions of quinolone target alterations and efflux pump expression to fluoroquinolone resistance in *Pseudomonas aeruginosa* and to ascertain if further, yet unknown resistance determinants exist. We will explore the complex molecular ciprofloxacin resistance mechanisms by applying different resequencing technologies to describe the nature and frequency of quinolone resistance determinants. Furthermore, we will use deep transcriptome sequencing (RNA-Seq) on a large collection of clinical isolates to perform unbiased transcriptome-wide association studies to uncover novel resistance determinants.

A further aim is the description of the transcriptomic landscape of *K. pneumoniae* and the association of transcriptional profiles to the important clinical phenotypes of biofilm formation, virulence and antibiotic resistance. We will combine deep transcriptome sequencing data with biological experiments to perform global phenotype-genotype associations which have the power to reveal novel determinants of these clinically highly important phenotypes.

2 Materials and Methods

2.1 Bacterial isolates and growth conditions

Bacterial strains used in this thesis are listed in Table 2.1. All strains were maintained at -70 °C as 25 % (v/v) glycerol stocks. *Escherichia coli* strain DH5α was used for all cloning procedures, and *E. coli* strain S17-1 for conjugative DNA transfer. The completely sequenced *Pseudomonas aeruginosa* strain PA14 [139] was used as reference strain.

Unless indicated otherwise, all *P. aeruginosa* and *E. coli* strains were cultured at 37 °C in Luria-Bertani broth (LB; 1 5 g/l yeast extract, 7.5 g/l NaCl, 10 g/l tryptone) with vigorous shaking at 180 rpm. For cultivation on agar plates, LB medium with 1.6 % (w/v) agar or Columbia agar supplemented with 5 % sheep blood (bioMérieux) was used. When required for selection, 100 µg/ml tetracycline and 400 µg/ml carbenicillin were used for *P. aeruginosa* PA14 and 12.5 µg/ml tetracycline and 100 µg/ml ampicillin for *E. coli* DH5α or S17.1, respectively.

Table 2.1: Bacterial strains used in this thesis (without clinical isolates)

Strain	Relevant genotype	Reference
E. coli		
DH5α	F– Φ80lacZ ΔM15 Δ(lacZYA-argF) U169 recA1 endA1 hsdR17 (rK–, mK+) phoA supE44 λ– thi-1 gyrA96 relA1	[140]
S17.1	recA thi pro hsdR RP4-2-Tc::Mu-Km::Tn7	[141]
P. aeruginosa		
PA14		[139]

2.1.1 Collection of clinical *P. aeruginosa* isolates

In total, 172 clinical *P. aeruginosa* isolates, sampled at several locations in Germany and Europe, were included in this study. 100 isolates were collected at the Hannover Medical School (MHH) between 2005 and 2007, obtained from 90 individuals, 31 of whom were cystic fibrosis (CF) patients, with clinical infections at various sites. Two isolates per patient were analyzed in this study when the isolates clearly differed in their antibiotic resistance profiles; otherwise, one isolate per patient was analyzed. Furthermore, 40 isolates, sampled in Germany, Rumania, Hungary and Italy, were provided from the University of Freiburg. 14 isolates were received from the Robert-Koch-Institute in Wernigerode, 10 isolates from the Charité Berlin and 8 isolates from the German National Reference Laboratory for Multidrug-Resistant Gram-negative Bacteria in Bochum. The ciprofloxacin susceptibility data of each isolate, as shown in Table 2.2, was either derived from the contributing

institution or determined in house using the Vitek2 system (bioMérieux) according to guidelines from the Clinical and Laboratory Standards Institute (CLSI) [142].

Table 2.2: Clinical *P. aeruginosa* isolates and resistance profiles

Origin	Isolate	CF[§]	Material	Sample origin	CIP MIC*	RNA-seq	Sanger / Pyroseq.
National Reference Laboratory, Bochum, Germany	B197	n.d.	n.d.	n.d.	S ≤ 0.125	yes	no
	B214	n.d.	n.d.	n.d.	S 0.5	yes	no
	B266	n.d.	n.d.	n.d.	S 1	yes	no
	B271	n.d.	n.d.	n.d.	S ≤ 0.125	yes	no
	B337	n.d.	n.d.	n.d.	S ≤ 0.125	yes	no
	B34	n.d.	n.d.	n.d.	S 0.5	yes	no
	B428	n.d.	n.d.	n.d.	S 0.5	yes	no
	B445	n.d.	n.d.	n.d.	S ≤ 0.25	yes	no
Hannover Medical School, Germany	MHH6827	no	midstream urine	Hannover, Germany	R > 8	yes	yes
	MHH6829	no	midstream urine	Hannover, Germany	R > 8	yes	yes
	MHH6870	no	midstream urine	Hannover, Germany	R > 8	yes	yes
	MHH6887	no	tracheal secrete	Hannover, Germany	I 2	yes	yes
	MHH6938	no	bronchoalveolar lavage	Hannover, Germany	R > 8	yes	yes
	MHH6964	no	wound swab abdomen	Hannover, Germany	R 8	yes	yes
	MHH7032	no	venous catheter	Hannover, Germany	R > 8	yes	yes
	MHH7055	no	bronchoalveolar lavage	Hannover, Germany	R 8	yes	yes
	MHH7084	no	permanent catheter urine	Hannover, Germany	R > 8	yes	yes
	MHH7091	yes	lung transplant recipient	Hannover, Germany	S 1	yes	yes
	MHH7125	no	tonsil swab	Hannover, Germany	R > 8	yes	yes
	MHH7135	no	bronchial secrete	Hannover, Germany	R 8	yes	yes
	MHH7176	no	midstream urine	Hannover, Germany	R > 8	yes	yes
	MHH7200	yes	tonsil swab	Hannover, Germany	R > 8	yes	yes
	MHH7252	no	tracheal secrete	Hannover, Germany	I 2	yes	yes
	MHH7261	no	permanent catheter urine	Hannover, Germany	R > 8	yes	yes
	MHH7313	no	tracheal secrete	Hannover, Germany	R 4	yes	yes
	MHH7321	no	tracheal secrete	Hannover, Germany	R 4	no	yes
	MHH7368	no	nasal swab	Hannover, Germany	R > 8	yes	yes
	MHH7444	yes	bronchoalveolar lavage	Hannover, Germany	I 2	yes	yes
	MHH7508	yes	bronchial secrete	Hannover, Germany	S 1	yes	yes
	MHH7509	yes	bronchial secrete	Hannover, Germany	S 1	no	yes
	MHH7624	yes	tonsil swab	Hannover, Germany	S 1	no	yes
	MHH7807	yes	bronchoalveolar lavage	Hannover, Germany	S 1	no	yes
	MHH7818	yes	tracheal secrete	Hannover, Germany	S 1	yes	yes
	MHH7823	no	tonsil swab	Hannover, Germany	R > 8	yes	yes
	MHH7863	no	bronchial secrete	Hannover, Germany	R > 8	yes	yes
	MHH8044	yes	tracheal secrete	Hannover, Germany	I 2	yes	yes
	MHH8349	no	midstream urine	Hannover, Germany	R > 8	yes	yes
	MHH8478	no	midstream urine	Hannover, Germany	R > 8	yes	yes

MHH8481	yes	bronchial secrete	Hannover, Germany	I	2	yes	yes
MHH8482	yes	bronchial secrete	Hannover, Germany	I	2	yes	yes
MHH8607	no	sputum	Hannover, Germany	I	2	yes	yes
MHH8613	no	ear swab	Hannover, Germany	R	> 8	yes	yes
MHH8614	no	midstream urine	Hannover, Germany	R	> 8	yes	yes
MHH8627	no	drainage bile duct	Hannover, Germany	S	0.25	yes	yes
MHH8694	no	midstream urine	Hannover, Germany	R	> 8	no	yes
MHH8697	no	rectal swab	Hannover, Germany	R	> 8	yes	yes
MHH9100	yes	lung transplant recipient	Hannover, Germany	I	2	no	yes
MHH9144	no	tracheal secrete	Hannover, Germany	S	1	no	yes
MHH8931	yes	lung transplant donor	Hannover, Germany	R	4	yes	yes
MHH9157	no	wound swab abdomen	Hannover, Germany	S	0.5	yes	yes
MHH9229	no	tonsil swab	Hannover, Germany	S	1	yes	yes
MHH9460	n.d.	tracheal secrete	Hannover, Germany	I	2	yes	yes
MHH9466	no	bronchial secrete	Hannover, Germany	S	1	no	yes
MHH9481	no	bronchial rinsing	Hannover, Germany	R	4	yes	yes
MHH9484	no	tonsil swab	Hannover, Germany	S	1	yes	yes
MHH9509	n.d.	tracheal secrete	Hannover, Germany	I	2	yes	yes
MHH9534	no	bronchial secrete	Hannover, Germany	I	2	yes	yes
MHH9536	n.d.	tracheal secrete	Hannover, Germany	I	2	yes	yes
MHH9561	n.d.	tonsil swab	Hannover, Germany	S	1	yes	yes
MHH9604	n.d.	bronchial secrete	Hannover, Germany	S	1	yes	yes
MHH9619	n.d.	tonsil swab	Hannover, Germany	I	2	yes	yes
MHH9639	n.d.	tonsil swab	Hannover, Germany	S	1	yes	yes
MHH9652	no	drainage liquid	Hannover, Germany	R	> 8	yes	yes
MHH9674	no	bronchoalveolar lavage	Hannover, Germany	R	8	yes	yes
MHH9678	n.d.	tonsil swab	Hannover, Germany	S	1	yes	yes
MHH9709	n.d.	tonsil swab	Hannover, Germany	I	2	yes	yes
MHH9717	no	tracheal secrete	Hannover, Germany	R	> 8	yes	yes
MHH9748	no	tonsil swab	Hannover, Germany	I	2	yes	yes
MHH9830	no	tracheal secrete	Hannover, Germany	I	2	yes	yes
MHH9847	n.d.	tracheal secrete	Hannover, Germany	S	1	yes	yes
MHH9854	yes	nasal swab	Hannover, Germany	S	1	yes	yes
MHH9923	n.d.	tracheal secrete	Hannover, Germany	I	2	yes	yes
MHH9924	n.d.	swab intraoperative	Hannover, Germany	I	2	yes	yes
MHH10047	no	tonsil swab	Hannover, Germany	S	1	yes	yes
MHH10049	yes	nasal swab	Hannover, Germany	S	0.5	yes	yes
MHH10660	yes	lung transplant donor	Hannover, Germany	I	2	yes	yes
MHH10728	no	tracheal secrete	Hannover, Germany	I	2	no	yes
MHH10978	yes	tonsil swab	Hannover, Germany	R	8	yes	yes
MHH10983	yes	lung transplant recipient	Hannover, Germany	I	2	no	yes
MHH11148	no	tonsil swab	Hannover, Germany	R	4	yes	yes
MHH11444	yes	tonsil swab	Hannover, Germany	S	1	yes	yes
MHH11445	yes	tonsil swab	Hannover, Germany	S	1	yes	yes
MHH11540	no	midstream urine	Hannover, Germany	R	> 8	yes	yes

	MHH11572	no	midstream urine	Hannover, Germany	R -	yes	yes
	MHH11785	yes	lung transplant donor	Hannover, Germany	R > 8	yes	yes
	MHH11935	no	bronchoalveolar lavage	Hannover, Germany	S 1	yes	yes
	MHH11989	yes	tonsil swab	Hannover, Germany	R 4	yes	yes
	MHH12178	no	catheter swab abdomen	Hannover, Germany	S 0.5	yes	yes
	MHH12207	yes	bronchoalveolar lavage	Hannover, Germany	I 2	yes	yes
	MHH12269	yes	sputum	Hannover, Germany	S 1	yes	yes
	MHH12274	no	bronchoalveolar lavage	Hannover, Germany	R 4	yes	yes
	MHH13062	no	permanent catheter urine	Hannover, Germany	R 8	yes	yes
	MHH13224	no	bronchial rinsing	Hannover, Germany	I 2	yes	yes
	MHH13281	yes	lung transplant recipient	Hannover, Germany	I 2	no	yes
	MHH13305	yes	bronchial secrete	Hannover, Germany	R 4	yes	yes
	MHH13395	no	bronchoalveolar lavage	Hannover, Germany	S 0.5	yes	yes
	MHH13428	no	swab intraop. abdomen	Hannover, Germany	I 2	yes	yes
	MHH13633	no	tracheal secrete	Hannover, Germany	R > 8	yes	yes
	MHH13682	yes	lung transplant donor	Hannover, Germany	R > 8	yes	yes
	MHH13684	yes	lung transplant recipient	Hannover, Germany	R 8	yes	yes
	MHH13714	no	permanent catheter urine	Hannover, Germany	R 4	yes	yes
	MHH14039	yes	nasal swab	Hannover, Germany	S 1	no	yes
	MHH14088	no	perfusate	Hannover, Germany	I 2	yes	yes
	MHH14103	no	swab heel	Hannover, Germany	R > 8	yes	yes
	MHH14322	no	bronchial rinsing	Hannover, Germany	R 8	yes	yes
	MHH14387	yes	lung transplant recipient	Hannover, Germany	I 2	yes	yes
	MHH14449	no	bronchial secrete	Hannover, Germany	S 0.5	yes	yes
	MHH14865	yes	lung transplant recipient	Hannover, Germany	R > 4	no	yes
University of Freiburg, Germany	Psae0613	n.d.	n.d.	n.d.	R 128	yes	no
	Psae1152	n.d.	drainage catheter	Stuttgart, Germany	R 32	yes	no
	Psae1471	n.d.	respiratory tract	Berlin, Germany	R ≥ 4	yes	no
	Psae1640	n.d.	urine	Munich, Germany	R 64	yes	no
	Psae1646	n.d.	urine	Munich, Germany	I 2	yes	no
	Psae1655	n.d.	respiratory tract	Munich, Germany	I 2	yes	no
	Psae1657	n.d.	respiratory tract	Munich, Germany	I 2	yes	no
	Psae1659	n.d.	respiratory tract	Munich, Germany	I 2	yes	no
	Psae1660	n.d.	respiratory tract	Munich, Germany	I 2	yes	no
	Psae1661	n.d.	respiratory tract	Freiburg, Germany	R 8	yes	no
	Psae1688	n.d.	urine	Limburg, Germany	S 0.5	yes	no
	Psae1695	n.d.	respiratory tract	Bremen, Germany	R 64	yes	no
	Psae1711	n.d.	n.d.	Regensburg, Germany	R 128	yes	no
	Psae1715	n.d.	respiratory tract	Freiburg, Germany	S 1	yes	no
	Psae1716	n.d.	blood	Freiburg, Germany	R 32	yes	no
	Psae1747	n.d.	respiratory tract	Freiburg, Germany	R 16	yes	no
	Psae1758	n.d.	respiratory tract	Limburg, Germany	R ≥ 4	yes	no
	Psae1766	n.d.	respiratory tract	Bremen, Germany	S 1	yes	no
	Psae1775	n.d.	respiratory tract	Ruedesheim, Germany	S 0.5	yes	no
	Psae1793	n.d.	respiratory tract	n.d.	R 8	yes	no

	Psae1807	n.d.	respiratory tract	Berlin, Germany	S	0.25	yes	no
	Psae1829	n.d.	respiratory tract	Regensburg, Germany	I	2	yes	no
	Psae1875	n.d.	respiratory tract	Berlin, Germany	S	0.5	yes	no
	Psae1892	n.d.	respiratory tract	Gera, Germany	R	32	yes	no
	Psae1910	n.d.	respiratory tract	Regensburg, Germany	R	4	yes	no
	Psae1928	n.d.	respiratory tract	Bremen, Germany	R	32	yes	no
	Psae1950	n.d.	respiratory tract	Bremen, Germany	R	8	yes	no
	Psae2134	n.d.	respiratory tract	Timisoara, Rumania	R	16	yes	no
	Psae2136	n.d.	respiratory tract	Timisoara, Rumania	R	16	yes	no
	Psae2162	n.d.	n.d.	Catania, Italy	R	≥ 4	yes	no
	Psae2180	n.d.	urine	n.d.	R	4	yes	no
	Psae2302	n.d.	respiratory tract	Rozzano, Italy	R	4	yes	no
	Psae2305	n.d.	respiratory tract	Sassari, Italy	R	4	yes	no
	Psae2307	n.d.	respiratory tract	Sassari, Italy	R	64	yes	no
	Psae2319	n.d.	n.d.	Palermo, Italy	R	128	yes	no
	Psae2324	n.d.	respiratory tract	Neubrandenburg, Germany	S	0.125	yes	no
	Psae2326	n.d.	urine	Neubrandenburg, Germany	R	16	yes	no
	Psae2328	n.d.	urine	Neubrandenburg, Germany	S	0.125	yes	no
	Psae2335	n.d.	urine	Trencin, Hungary	R	16	yes	no
	Psae2338	n.d.	respiratory tract	Bari, Italy	R	64	yes	no
Robert Koch Institute, Wernigerode, Germany	RKI_100_12	n.d.	n.d.	n.d.	S	0.25	yes	no
	RKI_12_11	n.d.	n.d.	n.d.	R	> 64	yes	no
	RKI_24_11	n.d.	n.d.	n.d.	R	16	yes	no
	RKI_339_12	n.d.	n.d.	n.d.	S	0.25	yes	no
	RKI_359_11	n.d.	n.d.	n.d.	R	64	yes	no
	RKI_360_11	n.d.	n.d.	n.d.	R	64	yes	no
	RKI_37_11	n.d.	n.d.	n.d.	I	2	yes	no
	RKI_392_11	n.d.	n.d.	n.d.	S	0.125	yes	no
	RKI_395_11	n.d.	n.d.	n.d.	R	64	yes	no
	RKI_53_11	n.d.	n.d.	n.d.	R	> 64	yes	no
	RKI_82_10	n.d.	n.d.	n.d.	R	32	yes	no
	RKI_96_12	n.d.	n.d.	n.d.	S	0.5	yes	no
	RKI_98_12	n.d.	n.d.	n.d.	R	8	yes	no
	RKI_99_12	n.d.	n.d.	n.d.	R	8	yes	no
Charité- Universitätsmedizin, Berlin, Germany	Ch2671	n.d.	tracheal-bronchial secrete	Berlin, Germany	S	1	yes	no
	Ch2672	n.d.	n.d.	Berlin, Germany	R	≥ 4	yes	no
	Ch2674	n.d.	tracheal-bronchial secrete	Berlin, Germany	R	≥ 4	yes	no
	Ch2675	n.d.	tracheal-bronchial secrete	Berlin, Germany	R	≥ 4	yes	no
	Ch2677	n.d.	permanent catheter urine	Berlin, Germany	R	≥ 4	yes	no
	Ch2678	n.d.	sputum	Berlin, Germany	R	≥ 4	yes	no
	Ch2680	n.d.	drainage secrete	Berlin, Germany	S	1	yes	no
	Ch2682	n.d.	n.d.	Berlin, Germany	S	≤ 0.25	yes	no
	Ch2706	n.d.	rectal swab	Berlin, Germany	R	≥ 4	yes	no
	Ch2734	n.d.	tracheal-bronchial secrete	Berlin, Germany	I	2	yes	no

CIP, ciprofloxacin; n.d., not determined

[§]CF, patients diagnosed with cystic fibrosis

*The ciprofloxacin MIC values are given in µg/ml, the classification into resistance (R), intermediate (I) and susceptible (S) isolates is according to CLSI guidelines [142].

2.1.2 Collection of clinical *K. pneumoniae* isolates

A total of 37 clinical *K. pneumoniae* isolates was included in this study (see Table 2.3). 19 isolates, collected at several hospitals in Saxony, were provided by a diagnostic laboratory (Medizinisches Labor Ostsachsen, Görlitz, Germany), 12 isolates were sampled at the Charité-Universitätsmedizin, Berlin, Germany and three isolates were collected at a medical practice (Dr. Schanz, Salzgitter, Germany). Furthermore, three already published *K. pneumoniae* isolates (MGH 78578 (http://www.ncbi.nlm.nih.gov/nuccore/NC_009648.1), JH1 and 1162281 [143]) were included. The antibiotic susceptibility profile of each isolate, as shown in Table 2.4, was evaluated using the Vitek2 system (bioMérieux). Breakpoints of antibiotic resistance were determined according to CLSI guidelines [142].

Table 2.3: Clinical *K. pneumoniae* isolates and patient information

Origin	Isolate	Material	Patient age	Patient sex	Sample origin
Medizinisches Labor Ostsachsen, Goerlitz, Germany	isolate 1_1	rectal swab	65	female	Bennewitz, Germany
	isolate 1_2	tracheal secretion	n.d.	n.d.	Riesa, Germany
	isolate 1_3	rectal swab	71	female	Bennewitz, Germany
	isolate 1_4	rectal swab	44	male	Bennewitz, Germany
	isolate 1_6	wound swab	65	female	Bennewitz, Germany
	isolate 1_8	katheter	n.d.	n.d.	Riesa, Germany
	isolate 1_9	midstream urine	89	female	Leipzig, Germany
	isolate 1_10	wound swab	81	female	Grimma, Germany
	isolate 1_11	rectal swab	61	female	Wurzen, Germany
	isolate 1_12	nasal swab	53	female	Bennewitz, Germany
	isolate 1_13	rectal swab	81	female	Bennewitz, Germany
	isolate 1_15	rectal swab	42	male	Bennewitz, Germany
	isolate 1_16	bronchea	68	male	Dresden, Germany
	isolate 2_2	wound swab	71	female	Dresden, Germany
	isolate 2_4	wound swab	58	male	Thalheim, Germany
	isolate 2_8	sputum	71	male	Erfurt, Germany
	isolate 2_9	midstream urine	91	female	Leipzig, Germany
	isolate 2_10	wound swab	71	male	Leipzig, Germany
	isolate 2_14	midstream urine	45	male	Weinböhla, Germany
Charite-Universitätsmedizin, Berlin, Germany	isolate 3_3	tracheal secretion	71	male	Berlin, Germany
	isolate 3_4	rectal swab	20	male	Berlin, Germany
	isolate 3_5	rectal swab	25	male	Berlin, Germany

	isolate 3_6	blood culture	34	female	Berlin, Germany
	isolate 3_7	rectal swab	72	female	Berlin, Germany
	isolate 3_8	rectal swab	61	male	Berlin, Germany
	isolate 3_10	blood culture	58	male	Berlin, Germany
	isolate 3_11	rectal swab	26	male	Berlin, Germany
	isolate 3_12	rectal swab	57	male	Berlin, Germany
	isolate 3_13	eye swab	85	female	Berlin, Germany
	isolate 3_14	pharyngeal swab	69	male	Berlin, Germany
	isolate 3_17	rectal swab	71	female	Berlin, Germany
private practice, Salzgitter, Germany	isolate 1_14	midstream urine	77	male	Salzgitter, Germany
	isolate 2_7	midstream urine	90	female	Salzgitter, Germany
	isolate 2_11	midstream urine	67	female	Salzgitter, Germany
previously published	MGH 78578	-	-	-	-
	JH1	-	-	-	-
	1162281	-	-	-	-

n.d., not determined

Table 2.4: Antibiotic resistance profiles of *K. pneumoniae* isolates

Origin	Isolate	AMP*	SAM*	TZP*	CXM*	CAZ*	IPM*	MEM*	CIP*	LVX*	GEN*
Medizinisches Labor Ostsachsen, Goerlitz, Germany	isolate 1_1	R ≥ 32	R ≥ 32	R ≥ 128	R ≥ 64	R ≥ 64	R ≥ 16	R ≥ 16	R ≥ 4	R ≥ 8	S ≤ 1
	isolate 1_2	R ≥ 32	R ≥ 32	S 16	R ≥ 64	I 8	S ≤ 0.25	S ≤ 0.25	I 2	S 1	R ≥ 16
	isolate 1_3	R ≥ 32	R ≥ 32	R ≥ 128	R ≥ 64	R ≥ 64	R ≥ 16	R ≥ 16	R ≥ 4	R ≥ 8	S 4
	isolate 1_4	R ≥ 32	R ≥ 32	R ≥ 128	R ≥ 64	R ≥ 64	R ≥ 16	R ≥ 16	R ≥ 4	R ≥ 8	S 4
	isolate 1_6	R ≥ 32	R ≥ 32	R ≥ 128	R ≥ 64	R ≥ 64	R >32	R >32	R ≥ 4	n.d.	S 4
	isolate 1_8	R ≥ 32	R ≥ 32	S 16	R ≥ 64	n.d.	S ≤ 0.25	S ≤ 0.25	R ≥ 4	n.d.	S ≤ 1
	isolate 1_9	R ≥ 32	R ≥ 32	R ≥ 64	R ≥ 64	R ≥ 64	R 8	R ≥ 16	R ≥ 4	R ≥ 8	S 4
	isolate 1_10	R ≥ 32	R ≥ 32	R ≥ 128	R ≥ 64	n.d.	R ≥ 16	R ≥ 16	R ≥ 4	R ≥ 8	S ≤ 1
	isolate 1_11	R ≥ 32	R ≥ 32	R ≥ 64	R ≥ 64	R ≥ 64	R ≥ 16	R 4	R ≥ 4	R ≥ 8	S 4
	isolate 1_12	R ≥ 32	R ≥ 32	R ≥ 128	R ≥ 64	R ≥ 64	R ≥ 16	R 8	R ≥ 4	R ≥ 8	S 4
	isolate 1_13	R ≥ 32	R ≥ 32	R ≥ 128	R ≥ 64	R ≥ 64	I 2	R ≥ 16	R ≥ 4	R ≥ 8	S 4
	isolate 1_15	R ≥ 32	R ≥ 32	R ≥ 128	R ≥ 64	R ≥ 64	R 8	I 2	R ≥ 4	R ≥ 8	S 4
	isolate 1_16	R ≥ 32	R ≥ 32	R ≥ 128	R ≥ 64	R ≥ 64	S 0.5	I 2	R ≥ 4	n.d.	R ≥ 16
	isolate 2_2	R ≥ 32	R ≥ 32	R ≥ 64	R ≥ 64	R ≥ 64	S ≤ 1	S ≤ 0.25	R ≥ 4	I 4	R ≥ 16
	isolate 2_4	R ≥ 32	R ≥ 32	n.d.	R ≥ 64	n.d.	R 32	R 16	R ≥ 4	R ≥ 8	S 4
	isolate 2_8	R ≥ 32	R ≥ 32	S 8	R ≥ 64	S 4	S ≤ 1	S ≤ 0.25	S ≤ 0.25	n.d.	S ≤ 1
	isolate 2_9	R ≥ 32	R ≥ 32	R ≥ 64	R ≥ 64	R ≥ 64	R 8	R 8	R ≥ 4	R ≥ 8	S 4
	isolate 2_10	R ≥ 32	R ≥ 32	R ≥ 128	R ≥ 64	I 8	S ≤ 1	S ≤ 0.25	R ≥ 4	R 4	S ≤ 1
	isolate 2_14	R ≥ 32	R ≥ 32	R ≥ 128	R ≥ 64	R ≥ 64	S ≤ 1	S 1	R ≥ 4	R ≥ 8	R ≥ 16
Charite-Universitätsmedizin, Berlin, Germany	isolate 3_3	R ≥ 32	R ≥ 32	R ≥ 64	R ≥ 64	R 16	R 8	R ≥ 16	R ≥ 4	R ≥ 8	R ≥ 16
	isolate 3_4	R ≥ 32	R ≥ 32	R ≥ 64	R ≥ 64	R 16	R 4	R ≥ 16	R ≥ 4	R ≥ 8	S ≤ 1
	isolate 3_5	R ≥ 32	R ≥ 32	R ≥ 64	R ≥ 64	S 4	R 4	R ≥ 16	R ≥ 4	R ≥ 8	S ≤ 1
	isolate 3_6	R ≥ 32	R ≥ 32	R ≥ 64	R ≥ 64	R 16	R 8	R ≥ 16	R ≥ 4	R ≥ 8	R ≥ 16
	isolate 3_7	R ≥ 32	R ≥ 32	R ≥ 64	R ≥ 64	S 4	R 8	R ≥ 16	R ≥ 4	R ≥ 8	R ≥ 16
	isolate 3_8	R ≥ 32	R ≥ 32	R ≥ 64	R ≥ 64	R 64	R 4	R 8	R ≥ 4	R ≥ 8	R ≥ 16
	isolate 3_10	R ≥ 32	R ≥ 32	R ≥ 64	R ≥ 64	R 16	R 8	R ≥ 16	R ≥ 4	R ≥ 8	R ≥ 16

	isolate 3_11	R	≥ 32	R	≥ 32	R	≥ 64	R	≥ 64	R	16	R	8	R	≥ 16	R	≥ 4	R	≥ 8	R	≥ 16
	isolate 3_12	R	≥ 32	R	≥ 32	R	≥ 64	R	≥ 64	S	4	R	4	R	8	R	≥ 4	R	≥ 8	R	≥ 16
	isolate 3_13	R	≥ 32	R	≥ 32	R	≥ 64	R	≥ 64	R	16	R	4	R	8	R	≥ 4	R	≥ 8	S	≤ 1
	isolate 3_14	R	≥ 32	R	≥ 32	R	≥ 64	R	≥ 64	R	16	R	4	R	16	R	≥ 4	R	≥ 8	S	≤ 1
	isolate 3_17	R	≥ 32	R	≥ 32	R	≥ 64	R	≥ 64	S	4	R	4	R	8	R	≥ 4	R	≥ 8	R	≥ 16
private practice, Salzgitter, Germany	isolate 1_14	R	≥ 32	R	≥ 32	R	≥ 64	R	≥ 64	R	≥ 64	S	≤ 1	S	≤ 0.25	R	≥ 4	I	4	S	≤ 1
	isolate 2_7	R	≥ 32	S	≤ 2	S	4	S	4	S	≤ 1	S	≤ 1	S	≤ 0.25	S	≤ 0.25	S	≤ 0.125	S	≤ 1
	isolate 2_11	R	≥ 32	R	16	S	4	S	≤ 1	S	≤ 1	S	≤ 1	S	≤ 0.25	I	2	I	4		n.d.
previously published	MGH 78578	R	≥ 32	R	≥ 32	R	≥ 128	R	≥ 64	R	≥ 64	S	≤ 1	S	≤ 0.25	S	1	S	1	R	≥ 16
	JH1	R	≥ 32	S	≤ 2	S	≤ 2	S	2	S	≤ 1	S	≤ 1	S	≤ 0.25	S	≤ 0.25	S	≤ 0.125	S	≤ 1
	1162281	R	≥ 32	R	≥ 32	R	≥ 64	I	16	R	≥ 64	S	≤ 1	S	≤ 0.25	R	≥ 4	R	≥ 8	R	8

AMP, ampicillin; SAM, ampicillin-sulbactam; TZP, piperacillin-tazobactam; CXM, cefuroxime-axetil; CAZ, ceftazidime; IPM, imipenem; MEM, meropenem; CIP, ciprofloxacin; LVX, levofloxacin; GEN, gentamicin; n.d., not determined

*MIC values are given in µg/ml, the classification into resistance (R), intermediate (I) and susceptible (S) isolates is according to CLSI guidelines [142].

2.2 Plasmids and Oligomers

All plasmids and primers used for sequencing, cloning, and mutagenesis are listed in Table 2.5 and Table 2.6, respectively. Primers were adopted from previous publications or designed with Primer3 [144] based on the sequence of the PA14 genome and ordered from Eurofins MWG Operon. Unless indicated otherwise, sequencing of PCR products and plasmids was performed at Eurofins MWG Operon.

Isolation and manipulation of recombinant DNA molecules was performed in accordance with standard molecular cloning techniques or as indicated by the product manufacturers' instructions.

Table 2.5: Plasmids used in this thesis

Plasmid	Relevant characteristics	Reference
pME6032	pVS1-p15A *E. coli-Pseudomonas* shuttle vector, *lacI*^{q}*-Ptac* expression vector, Tc^r	[145]
pEX18Ap	Gene replacement vector; oriT+ sacB+, Apr/Cbr	[146]

Table 2.6: Primers used in this thesis

Name	Sequence 5' - 3'*	Function	Reference
gyrAfp5	GATGCACGTGACGGCCTGAA	pyrosequencing	[147]
gyrArp5UBP	AGCATGTAGCGCAGCGAGAAGTCGTGACTGGGAAAACCCTGGCG	pyrosequencing	[147]
parCfp3	GGCTGGATGCCGATTCCAAG	pyrosequencing	[147]
parCrp3UBP	CGCCAGGGTTTTCCCAGTCACGACTAACGCATGGCGGCGAAGGACTT	pyrosequencing	[147]
UBP	5'-biotin-CGCCAGGGTTTTCCCAGTCACGAC	pyrosequencing	[147]
gyrAs246	CCACCCGCACGGCGA	pyrosequencing	[147]
parCs256	AAGTTCCACCCGCACGGC	pyrosequencing	[147]
gyrBfp4	GAACTGTACATCGTGGAGGGTGA	Sanger sequencing	[147]

gyrBrp4	ACCCCGCGATACTCGTTGAC	Sanger sequencing	[147]
parEfp3	AGGACGCCTTCAGCCTGTG	Sanger sequencing	[147]
parErp3	GGAAATGGCGGACGAACAG	Sanger sequencing	[147]
rpoD For	CGCAACAGCAATCTCGTCTGAAA	qRT-PCR	[148]
rpoD Rev	GCGGATGATGTCTTCCACCTGTT	qRT-PCR	[148]
mexA For	GGCGACAACGCGGCGAAGG	qRT-PCR	[148]
mexA Rev	CCTTCTGCTTGACGCCTTCCTGC	qRT-PCR	[148]
mexC For	GCAATAGGAAGGATCGGGGCGTTGG	qRT-PCR	[148]
mexC Rev	CCTCCACCGGCAACACCATTTCG	qRT-PCR	[148]
mexE For	TCATCCCACTTCTCCTGGCGCTACC	qRT-PCR	[148]
mexE Rev	CGTCCCACTCGTTCAGCGGTTGTTCGATG	qRT-PCR	[148]
mexX For	AATCGAGGGACACCCATGCACATCC	qRT-PCR	[148]
mexX Rev	CCCAGCAGGAATAGGGCGACCAG	qRT-PCR	[148]
gyrAfp6XbaI	ACATCATCTAGACGCAAGCGCCTGCATTGAAC	mutagenesis	[147]
gyrAD87Nr	ATGGTGT**T**GTAGACCGCGGTGTCGCCG	mutagenesis	[147]
gyrAT83Ir	TGGTGTCGTAGACCGCG**A**TGTCGCC	mutagenesis	[147]
gyrAT83ID87Nr	TGGTGT**T**GTAGACCGCG**A**TGTCGCC	mutagenesis	[147]
gyrArp6HindIII	ACATCA*AAGCTT*CGATCAACCGCGCCTTGTTC	mutagenesis	[147]
gyrAD87Nf	CGGCGACACCGCGGTCTAC**A**ACACCAT	mutagenesis	[147]
gyrAT83If	GGCGACA**T**CGCGGTCTACGACACCA	mutagenesis	[147]
gyrAT83ID87Nf	GGCGACA**T**CGCGGTCTAC**A**ACACCA	mutagenesis	[147]
gyrBFP5XbaI	ACATCA*TCTAGA*ACCACGACCATCGGGAGTGA	mutagenesis	[147]
gyrBE468Dr	CCGAC**G**TCCTGGGAGGAGAGC	mutagenesis	[147]
gyrBS466Fr	CCGACCTCCTGG**A**AGGAGAGC	mutagenesis	[147]
gyrBS466Yr	CCGACCTCCTGG**T**AGGAGAGC	mutagenesis	[147]
gyrBE468Df	GCTCTCCTCCCAGGA**C**GTCGG	mutagenesis	[147]
gyrBS466Ff	GCTCTCCT**T**CCAGGAGGTCGG	mutagenesis	[147]
gyrBS466Yf	GCTCTCCT**A**CCAGGAGGTCGG	mutagenesis	[147]
gyrBRP5HindIII	ACATCA*AAGCTT*AGGCCGGGGTTTCCATGAG	mutagenesis	[147]
parCfp4XbaI	AACTAC*TCTAGA*ACCTTCCTGCTCGATACCGG	mutagenesis	[147]
parCS87Lr	GCCTCGTAGCAGGCC**A**AGTCGCCGTGCGGG	mutagenesis	[147]
parCS87Wr	GCCTCGTAGCAGGCC**C**AGTCGCCGTGCGGG	mutagenesis	[147]
parCrp4HindIII	AACTGG*AAGCTT*ACCATCGGCAGCTTCTTGG	mutagenesis	[147]
parCS87Lf	CCCGCACGGCGACT**T**GGCCTGCTACGAGGC	mutagenesis	[147]
parCS87Wf	CCCGCACGGCGACT**G**GGCCTGCTACGAGGC	mutagenesis	[147]
nfxBFP1XbaI	ACATCA*TCTAGA*CGACACCGCAGCCTTCAG	mutagenesis	[147]
nfxBRP1	GGATTGGAGGCGCCATGGAGCGATGGGTCCCGGTTGGT	mutagenesis	[147]
nfxBFP2	AAACCAACCGGGACCCATCGCTCCATGGCGCCTCCAAT	mutagenesis	[147]
nfxBRP2HindIII	ACATCA*AAGCTT*CGGTCGTTGAGACGATCGAG	mutagenesis	[147]
mexRFP1XbaI	ACATCA*TCTAGA*ACTTCGACGGCAGCTTCAC	mutagenesis	[147]
mexRRP1	AGGTTTACTCGGCCAAACCAGAACATTCTTTTCGAAGCACAAT	mutagenesis	[147]
mexRFP2	GTGCTTCGAAAAGAATGTTCTGGTTTGGCCGAGTAAACCT	mutagenesis	[147]
mexRRP2HindIII	ACATCA*AAGCTT*GTCGCTGCCTTCCTTGAACA	mutagenesis	[147]
mexSFP1XbaI	ACATCA*TCTAGA*AGCACAACCCAAGCGATCAA	mutagenesis	[147]
mexSRP1	ATGCACTGCAGAGGTTTGCGCGGGTATTCGAGTTCGACCAG	mutagenesis	[147]
mexSFP2	TGGTCGAACTCGAATACCCGCGCAAACCTCTGCAGTGCATC	mutagenesis	[147]
mexSRP2HindIII	ACATCA*AAGCTT*AGGTGGGCGAAGATTTCCTG	mutagenesis	[147]

mexZFP1XbaI	ACATCA***TCTAGA***GGGTCGATCTGGAACAGCAC	mutagenesis	[147]
mexZRP1	GGACGATTGACGCCCTCAGGTGAACGTCCTCACAAGGG	mutagenesis	[147]
mexZFP2	TTCCCTTGTGAGGACGTTCACCTGAGGGCGTCAATCGTC	mutagenesis	[147]
mexZRP2HindIII	ACATCA***AAGCTT***GCACCTGGTTGCCCATCTC	mutagenesis	[147]
gyrARPSacI	GATC***GAGCTC***CCCCGAGCCTTACTCTTCGTT	cloning of *gyrA*	[147]
gyrAFPSacI	GATCC***GAGCTC***AAAGGAACCAGGCTTCTCATGG	cloning of *gyrA*	[147]
gyrAseqF	ATGCAGTACATCCCCGGTC	sequencing of pME::gyrA	[147]
gyrAseqR	CTGAACTGCACCAGCGG	sequencing of pME::gyrA	[147]
pMEseqF	ACCCTCACTGATCCGCTAGTCC	sequencing of pME::gyrA	[147]
pMEseqR	TTGCACCATTCGATGGTGTCAA	sequencing of pME::gyrA	[147]
phoE:F:604.1:oF	GTTTTCCCAGTCACGACGTTGTAACCTACCGCAACACCGACTTCTTCGG	MLST *Klebsiella*	[40]
phoE:R:604.2:oR	TTGTGAGCGGATAACAATTTCTGATCAGAACTGGTAGGTGAT	MLST *Klebsiella*	[40]
tonB:1F:oF	GTTTTCCCAGTCACGACGTTGTACTTTATACCTCGGTACATCAGGTT	MLST *Klebsiella*	[40]
tonB:2R:oR	TTGTGAGCGGATAACAATTTCATTCGCCGGCTGRGCRGAGAG	MLST *Klebsiella*	[40]
ForwardSeq:oF	GTTTTCCCAGTCACGACGTTGTA	MLST *Klebsiella*	[40]
ReverseSeq:oR	TTGTGAGCGGATAACAATTTC	MLST *Klebsiella*	[40]
wzi_for2	GTGCCGCGAGCGCTTTCTATCTTGGTATTCC	*wzi* typing	[149]
wzi_rev	GAGAGCCACTGGTTCCAGAAYTTSACCGC	*wzi* typing	[149]
KPC_FP	ATGTCACTGTATCGCCGTCT	bla_{KPC} detection	[150]
KPC_RP	TTGACGCCCAATCCCTCG	bla_{KPC} detection	[150]

*Mutated nucleotides are bold and underlined; restriction sites are italicized and underlined

2.3 DNA manipulation techniques

2.3.1 Transformation of chemically competent *E. coli*

Chemically competent *E. coli* Dh5α and S17-1 were prepared following standard laboratory protocols. Briefly, 50 ml LB culture of an OD_{600} of 0.4 - 0.6 were chilled on ice for 10 min and centrifuged at 4 °C at 3,200 × g for 15 min. After resuspending the pellet in 10 ml 0.1 M $CaCl_2$ and a second incubation on ice for 5 min, the cells were centrifuged and the pellet was resuspended in 1 ml 0.1 M $CaCl_2$ including 15 % (v/v) glycerol. 100 µl aliquots were stored at -70 °C.

For transformation, competent cells were gently thawed on ice for 10 min, mixed with the respective DNA and further incubated on ice for 30 min. After a heat shock of 42 °C for 30 s, cells were chilled on ice, 800 µl LB were added and the cells were incubated with vigorous shaking at 37 °C for 1 h. Appropriate dilutions were plated on LB agar plates containing antibiotics for selection of transformants and incubated overnight at 37 °C.

2.3.2 Electroporation of *P. aeruginosa*

To prepare electrocompetent *P. aeruginosa* cells, a bacterial lawn was scraped with an inoculation loop from an overnight grown Columbia agar plate and resuspended in 0.5 ml 300 mM sucrose solution. The suspension was centrifuged at 10,000 × g for 2 min and washed twice with sucrose solution. The pellet was resuspended in 100 µl sucrose solution und directly used for electroporation using 100 ng of plasmid DNA. Electroporation was carried out using electroporation cuvettes (2 mm electrode gap) in a Gene Pulser II (Bio-Rad) with following settings: 2.45 kV voltage, 25 µF capacitance and 200 Ω resistance. Immediately after discharge, 1 ml pre-warmed LB was added and the cells were incubated for 1.5 h at 37 °C. Appropriate dilutions were plated on LB agar plates containing antibiotics for selection of transformants and incubated overnight at 37 °C.

2.3.3 Plasmid transfer by biparental mating

pEX18Ap mutagenesis constructs (see chapter 2.3.4) were introduced into *P. aeruginosa* PA14 by conjugation with *E. coli* S17-1 as the donor strain. Therefore, PA14 was grown in 10 ml LB broth for 24 h at 42 °C, while *E. coli* S17.1 carrying the respective pEX18Ap plasmid construct was grown in 10 ml LB broth supplemented with 100 µg/ml ampicillin for 6 - 8 h at 37 °C. Bacterial cells were harvested by centrifugation at 6,000 × g for 5 min, washed twice with LB, mixed in a 1 : 4 ratio (*P. aeruginosa* : *E. coli*) and applied as a single drop on an LB agar plate. After incubation at 37 °C overnight, cells were thoroughly washed off with 2 ml PBS. Different dilutions of the suspension were plated on LB agar plates supplemented with 400 µg/ml carbenicillin and 10 µg/ml nalidixic acid to select the *P. aeruginosa* transconjugants. To promote plasmid counterselection, single colonies were picked, cultivated overnight in 10 ml LB broth containing 10 % sucrose and passaged in this medium three times with 50 µl inoculum and an incubation time of 8 - 16 h for each passage. After the final passage appropriate dilutions were plated on LB agar supplemented with 10 % sucrose to obtain single colonies. Integration of the desired mutation into the PA14 genome was confirmed using Sanger sequencing.

2.3.4 Construction of knock-out and single-nucleotide polymorphism mutants

Single nucleotide polymorphisms (SNPs) in *gyrA*, *gyrB*, and *parC*, as well as knockouts of *nfxB*, *mexR*, *mexS*, and *mexZ* in an isogenic *P. aeruginosa* PA14 background were carried out by homologous recombination using the suicide vector pEX18Ap [146]. Therefore, approximately 1,000 bp long mutagenic fragments were created by overlap extension PCR as described previously [151]. To

generate knockout mutants, the 500 bp long flanking regions upstream and downstream of the gene or SNP of interest were amplified using overlapping primers listed in
Table 2.6 and cloned into the *Bam*HI and *Xba*I restriction sites of plasmid pEX18Ap. The resulting constructs were transferred into PA14 by biparental mating using *E. coli* S17-1 as the donor strain (see chapter 2.3.3). The antibiotic resistance profiles of all mutants were determined in Mueller-Hinton (MH) broth (Roth) microdilution as described previously [152] (see chapter 2.4.1).

2.3.5 Cloning of *gyrA* and complementation of clinical isolates

To complement *gyrA* mutations in clinical isolates with the wild-type PA14 allele, *gyrA* was amplified from the PA14 chromosome with primers gyrAFPSacI and gyrARPSacI and was cloned into the *Sac*I restriction site of plasmid pME6032 [145], yielding plasmid pME::gyrA. The correct insertion and sequence were verified by Sanger sequencing using primers gyrAseqF, gyrAseqR, pMEseqF, and pMEseqR. Complementation was performed via electroporation as described in chapter 2.3.2. The cells were plated on LB agar plates supplemented with 100 µg/ml tetracycline. The ciprofloxacin MICs for isolates containing pME::gyrA with and without the addition of 1 mM isopropyl-β-d-thiogalactopyranoside (IPTG) were determined using E-test strips (bioMérieux) (see chapter 2.4.2).

2.4 Antibiotic susceptibility testing

2.4.1 Broth microdilution

Bacterial overnight cultures were adjusted to an OD_{600} of 0.1 in MH broth and diluted 1:100 in fresh MH broth. 100 µl of this cell suspension was mixed with 100 µl MH broth supplemented with ciprofloxacin in increasing concentrations of a twofold dilution series in 96-well plates. Bacterial growth was monitored in triplicates after 18 h incubation at 37 °C without shaking and the lowest concentration where no cell growth could be observed was recorded.

2.4.2 E-test

Ciprofloxacin susceptibility of clinical *P. aeruginosa* isolates complemented with the PA14 *gyrA* allele was determined using E-test strips with gradient antimicrobial concentrations (bioMérieux). Isolates were grown overnight at 37 °C and 180 rpm in MH broth and diluted with phosphate buffered saline (PBS, 137 mM NaCl; 2.7 mM KCl; 10 mM Na_2HPO_4; 2 mM KH_2PO_4; pH 7.4) to a final OD_{600} of 0.15. The suspension was applied to LB agar plates supplemented with 100 µg/ml tetracycline, with and without IPTG, respectively, by streaking with a cotton swab. Once the remaining liquid was absorbed

by the agar, the E-test stripe was applied to the plate. Results were recorded after 24 h of growth at 37 °C.

2.5 Phenotypic characterization assays of *K. pneumoniae* isolates

2.5.1 *Galleria mellonella* virulence assay

Protocols for the *Galleria mellonella* virulence assay were adjusted from previous publications [150,153]. Bacterial isolates were grown in LB until mid-exponential growth phase. Cells were harvested at 8.000 rpm for 5 min and washed with sterile phosphate-buffered saline (10 mM PBS, pH 7.5). Cultures were adjusted to an OD_{600} of 0.5 and 10-fold serially diluted in PBS. For each isolate, ten randomly chosen, healthy *Galleria mellonella* larvae (fauna topics GmbH) were inoculated with 20 µl of a 1:10 dilution containing approximately 8×10^5 colony forming units (CFU) by injection into the haemocoel of the rear left proleg with a 100 µl Hamilton syringe and a 30-G needle. The larvae were placed in sterile Petri dishes and incubated in the dark at 37 °C. Mortality was monitored for 72 h. Larval death was assessed by the lack of movement of larvae in response to physical stimulation with a sterile inoculating loop. 10 larvae inoculated with 20 µl PBS and ten larvae without any treatment were used as negative controls. Each experiment was performed in duplicates on different days. Experiments were repeated if more than one larva died in the controls. Colony forming units were enumerated by plating appropriate 10-fold dilutions on LB agar plates in triplicates.

2.5.2 Measurement of bacterial growth

Planktonic growth of *K. pneumoniae* isolates was monitored in LB, BM2 minimal medium [154] (62 mM potassium phosphate buffer, pH 7, 7 mM $(NH_4)_2SO_4$, 2 mM $MgSO_4$, 10 µM $FeSO_4$) supplemented with 50 mM glucose, and BM2 supplemented with 50 mM mannose, respectively using an automated growth analysis system (Bioscreen C MBR, Oy Growth Curves Ab Ltd). Cells of overnight cultures grown in LB at 37 °C were harvested at 8.000 rpm for 5 min and washed twice with the desired medium. Cultures were diluted to an OD_{600} of 0.02 and 200 µl were transferred into a 100-well honeycomb plate (four replicates per isolate). The plates were incubated at 37 °C with continuous shaking and 15 min measurement intervals for a period of 24 h. Maximal optical density and doubling time were determined using GrowthRates [155].

2.5.3 Crystal violet biofilm assay

Protocols to measure biofilm formation were adapted from previous publications [156,157]. An overnight culture grown in LB at 37 °C and 180 rpm was washed and diluted to an OD_{600} of 0.02 in fresh LB. 8 wells of a 96-well microtiter plate (BD biosciences) were inoculated with 100 µl and the plate was incubated at 37 °C in a humid atmosphere. After 24 h wells were washed three times with 200 µl sterile water and stained with 150 µl crystal violet staining solution (0.1 % m/v in water) for 30 min. Wells were washed tree times with 200 µl water, crystal violet was extracted with 200 µl 95% ethanol for 30 min and absorbance was measured at 590 nm in an EnSpire Multimode Plate Reader (PerkinElmer). All experiments were performed with 8 individual repeats per measurement. Isolates were regarded as high biofilm producers if their OD_{590} value was three times the OD_{590} value of the negative control [158].

2.6 DNA sequencing

2.6.1 Identification of mutations in *gyrA* and *parC* using pyrosequencing

To extract DNA for pyrosequencing, 500 µl of an overnight culture of *P. aeruginosa* clinical isolates was harvested and was lysed for 15 min at 95 °C in 100 µl lysis buffer (0.25% m/v sodium dodecyl sulfate, 50 mM NaOH). After the addition of 900 µl dH_2O, 2 µl were used as a PCR template.

To identify mutations at amino acid positions 83 and 87 in *gyrA* and position 87 in *parC*, a pyrosequencing assay was established. Amplification was performed as described by Doostzadeh *et al.* [159] using a 24-mer universal biotinylated primer (UBP) adapted from the work of Royo *et al.* [160] (shown in

Table 2.6). Sequencing primers gyrAs246 and parCs256 were designed with Primer3 [144] to anneal 3 bp upstream (*gyrA*) and 5 bp upstream (*parC*) of the SNP, respectively. Pyrosequencing was performed on a PSQ 96MA pyrosequencer (Pyrosequencing AB) with PyroMark Gold chemistry (Qiagen) as described by Royo *et al.* [160] at the Genome Analytics Group of the HZI.

2.6.2 Identification of mutations in *gyrB* and *parE* using Sanger sequencing

To identify mutations in *gyrB* and *parE* of *P. aeruginosa*, the QRDRs of both genes were amplified with primers gyrBfp4, gyrBrp4, parEfp3, and parErp3 (see

Table 2.6). PCR products were sequenced using the same sets of primers on a 3730xl DNA analyzer (Applied Biosystems) at the Genome Analytics Group of the HZI.

2.6.3 Capsular typing of *K. pneumoniae*

To determine the *K. pneumoniae* capsular type, a fragment of the *wzi* gene was amplified by primers wzi_for2 and wzi_rev adopted from [149] and Sanger sequenced with primer wzi_for2 (see Table 2.6). The gene *wzi* encodes an outer membrane protein involved in capsule attachment to the cell surface and is conserved in all capsular types of *Klebsiella pneumoniae*. Sequences were analyzed and compared to published results via http://bigsdb.web.pasteur.fr/klebsiella/klebsiella.html.

2.6.4 Determination of the *Klebsiella pneumoniae* carbapenemase types

An 872 bp long fragment from the *Klebsiella pneumoniae* carbapenemase coding gene bla_{KPC} was amplified with primers KPC_FP and KPC_RP from [150] (see Table 2.6) with an annealing temperature of 51 °C. Nucleotide sequences were obtained by Sanger sequencing (Eurofins MWG Operon) using both primers and compared to known bla_{KPC} alleles in MEGA 6.0 [161].

2.7 Quantitative real-time reverse transcription-PCR

The expression levels of the *P. aeruginosa* genes *mexA*, *mexC*, *mexE*, *mexX*, and the house-keeping gene *rpoD* were determined by quantitative real-time reverse transcription-PCR (qRT-PCR). RNA was isolated at the late-logarithmic growth phase (OD_{600} of 1.5 to 2.0) from 3 ml MH liquid culture by using the RNeasy kit (Qiagen), as described by the manufacturer. RNA was eluted from the RNeasy columns in a volume of 50 µl water and was treated with a DNA-*free* kit (Ambion). cDNA was synthesized by using random hexamer primers (Invitrogen) and SuperScript II reverse transcriptase (Invitrogen) according to the manufacturer's instructions. qRT-PCRs were performed in duplicate in a 20-µl volume with 25 ng cDNA and a primer concentration of 500 nmol/l on a LightCycler 480 system (Roche Diagnostics) using the SYBR green I master mix. The primers were adopted from the work of Tomás *et al.* [148] and sequences are listed in Table 2.6. Gene expression was calculated using the LightCycler 480 software version 1.5 by the $\Delta\Delta C_T$ method [162] and a standard curve to measure PCR efficiency. All results were normalized to the expression of the house-keeping gene *rpoD* of the same clinical isolate and were calibrated relative to expression in *P. aeruginosa* PA14. According to Cabot *et al.* [163], isolates with ≥ 3-fold *mexA* overexpression were regarded as positive, whereas values between 2- and 3-fold were regarded as borderline expression. For *mexC*, *mexE*, and *mexX*, ≥ 10-fold overexpression was regarded as positive and 5- to 10-fold overexpression was regarded as borderline expression.

2.8 Deep transcriptome sequencing

2.8.1 Bacterial culture conditions and RNA extraction

Bacteria were cultured in LB at 37 °C and vigorous shaking with 180 rpm until late exponential growth phase at OD_{600} of 2.0. Three independent bacterial cultures were pooled and 4 ml thereof were mixed with the same amount of RNAprotect (Qiagen). Followed by 10 min incubation at room temperature, cells were harvested by centrifugation at 6000 rpm for 5 min. Pellets were stored up to two weeks at -70 °C prior to RNA extraction. After thawing on ice, the pellet was thoroughly resuspended in 100 µl TE buffer (10 mM Tris-HCl; 1 mM EDTA, pH 8) supplemented with lysozyme (800 µg/ml) and incubated for 10 min at room temperature. Total RNA was extracted using Qiashredder columns (Qiagen) and the RNeasy plus kit (Qiagen) according to the manufacturer's instructions. Residual DNA was removed by a DNase (Ambion) treatment for 30 min at 37 °C using 1 µl DNase per 50 µl of total RNA.

2.8.2 mRNA enrichment, library preparation and Illumina-based RNA sequencing

Messenger RNAs were enriched using 7 µg of total RNA using the MICROBExpress™ bacterial mRNA enrichment kit (Ambion) according to the manufacturer's instructions. RNA-seq library preparation was performed according to [164] with an additional step of tobacco acid pyrophosphatase (TAP, epicenter) treatment to convert 5'-triphosphate RNA into 5'-monophosphate RNA before adapter ligation according to the manufacturer. The custom-made protocol from Dötsch *et al.* uses 5'-barcoded RNA-libraries, which enables a pooled sequencing of several samples. Up to 18 libraries were pooled to equal amounts (total 100 ng) and treated with duplex-specific nuclease (DSN, Evrogen) for additional rRNA removal according to Illumina's "DSN Normalization Sample Preparation Guide". Prior to sequencing, libraries were checked for quality and size distribution on an Agilent 2100 Bioanalyzer Pico Chip (Agilent). Sequencing was performed on an Illumina HiSeq 2500 at the Genome Analytics Group of the HZI generating paired-end reads each of 100 base pairs length. Several pools of clinical *P. aeruginosa* samples were also sequenced on a Illumina Genome Analyzer IIx.

The establishment of the cDNA library protocol as well as sample preparation, sequencing and raw data analysis of the 159 clinical *P. aeruginosa* isolates was performed in equal amounts by Monika Schniederjans and Ariane Khaledi (Helmholtz Centre for Infection Research) [164].

2.9 Generation of the *K. pneumoniae* pan-genome

11 fully sequenced and annotated *K. pneumoniae* strains whose sequence information is publicly available in GenBank/EMBL were used to generate a non-redundant *K. pneumoniae* pan-genome. Strain 342 was omitted since it is more likely to belong to *K. variicola* [165]. These 11 *K. pneumoniae* genomes contain 57,312 genes in total, with an average of 5,210 genes per strain (for more detailed information see Table 2.7).

With the aim to generate a non-redundant gene set, all gene sequences were blasted against each other using BLASTN, discarding hits having < 90 % length and 90 % sequence identity. Only genes having reciprocal homologs in all 11 genomes were considered as "core"; otherwise, they were classified as "accessory". Accessory genes having homologs in 8 to 10 out of the 11 *K. pneumoniae* genomes were manually re-evaluated. The set of core genes detected in the reciprocal blast search comprised 3,270 genes with additional 41 genes assigned to the core-genome after re-evaluation. Furthermore, small RNAs in *K. pneumoniae* subsp. MGH 78578 were predicted by using sRNAscanner [166] with default parameters. A total of 30 sRNAs were included in the final gene set. To generate a single reference sequence file, the pan-genome was concatenated by adding the 50 bp long genomic sequence upstream- and downstream of each gene and a separator of 100 "N"s between all genes.

The generation of the *K. pneumoniae* pan-genome has been performed together with Uthayakumar Muthukumarasamy and Klaus Hornischer (Helmholtz Centre for Infection Research).

Table 2.7: List of completely sequenced *K. pneumoniae* genomes used to generate the pan-genome

GenBank Accession ID	*K. pneumoniae* strain	Locus tag / format used	Number of genes	MLST sequence type
AP006725	NTUH-K2044 [167]	KP1_0001	5123	23
CP000647	MGH 78578	KPN_00001	4887	38
CP002910	KCTC 2242 [168]	KPN2242_r25078	5035	375
CP003200	HS11286 [169]	KPHS_00010	5404	11
CP003785	1084 [170]	A79E_0001	5067	23
CP003999	Kp13 [171]	KP13_00049	5299	442
CP006648	CG43	D364_00005	4897	86
CP006656	JM45	N559_0001	4980	11
CP006918	30684/NJST258_2 [172]	KPNJ2_00001	5545	258
CP006923	30660/NJST258_1 [172]	KPNJ1_00001	5577	258
CP006659	ATCC BAA-2146 [173]	KPN2146_0001	5498	11
Total genes (including 30 predicted small RNAs):			57342	
pan-genome:			7859	
unique genes (singletons):			1598	
core-genome:			3336	
accessory genes:			2925	

2.10 Bioinformatic analyses of RNA-sequencing data

2.10.1 Mapping and gene expression profiling

Raw sequencing reads were de-multiplexed by a custom Perl script, adapter and barcode sequences as well as low quality sequences were removed using the fastq-mcf script included in the ea-utils package (https://code.google.com/p/ea-utils/). Reads with more than one mismatch in the adapter sequence were discarded. Processed reads of *K. pneumoniae* isolates were mapped against the *K. pneumoniae* pan-genome, reads of *P. aeruginosa* isolates were mapped against the reference strain PA14 [139], both with stampy using bwaoptions -q10 [174].

Absolute quantification of *K. pneumoniae* gene expression was performed as described by Dötsch *et al*. [164]. Read counts were extracted from the SAM output files and normalized to generate normalized reads per kilobase of gene sequence (nRPK [164]) values according to the following equation:

$$\mathrm{nRPK} = log2\left(\frac{1000}{li} * \frac{RPG}{Fj} + 1\right)$$

where l_i is the length in bp of gene *i*, *RPG* is the absolute count of reads of gene *i* and F_j is the size factor calculated by DESeq [175] of isolate *j*. This normalization method delivers more robust data as e.g. RPKM when analyzing highly expressed genes [164].

A gene was considered as expressed, when the corresponding nRPK value was higher than the threshold nRPK_0 (Dötsch *et al.*, submitted for publication), whereby nRPK_0 is defined as:

$$\mathrm{nRPK0} = log2\left(\frac{1000}{lmed} * \frac{1}{Fmin} + 1\right) = log2\left(\frac{1000}{700} * \frac{1}{0.398} + 1\right) \approx 2.20$$

where l_{med} is the median length in bp of all genes in the pan-genome and F_{min} is the smallest size factor of all RNA-seq libraries (i.e. the lowest sequencing depth) as determined in DESeq. Gene expression profiles were further analyzed in R using the packages scatterplot3D and gplots.

Differential gene expression for *P. aeruginosa* genes was calculated against the PA14 reference strain using the R software package DESeq [175] based on the read counts calculated from the SAM output files. For whole transcriptome association studies, nRPK values were calculated based on the formula shown above.

2.10.2 Variance in *K. pneumoniae* gene expression

The variation in gene expression was analyzed in R with DESeq using pairwise comparisons of each gene in all possible combinations of two isolates, resulting in 666 comparisons:

$$(\sum_{K=1}^{n} k \text{, with n} = 36, \text{the number of comparisons for one isolate})$$

In these pairwise comparisons, a gene was regarded as differentially expressed when the absolute value of log2 fold change was above one. The value of variation is expressed as the fraction of comparisons in which the gene is differentially regulated vs. all comparisons for that specific gene. Genes lower as the 10th percentile or higher as the 90th percentile were regarded as very stable and highly variable expressed, respectively.

2.10.3 *De novo* assembly of accessory genes

All reads not mapping to the *K. pneumoniae* pan-genome were mapped with stampy against the virulence factors database (VFDB) [176] and also against a manually curated antibiotic resistance database, consisting of data from the Antibiotic Resistance Genes Database (ARDB) [177], http://www.lahey.org/qnrstudies/, and http://www.lahey.org/Studies/ containing 1365 entries in total. The complete resistance database is attached to this thesis as supplementary file S1 in FASTA format (resistance_genes.fasta). The coverage of each gene was assessed using a custom Perl script. Additionally, these unmapped reads were used as input for a *de novo* transcriptome assembly with OASES [178]. After testing k-mers from 17 to 41, the assembly was performed with k-mer 33 and a minimal transcript length of 250 bp. The assembled transcripts were blasted against the microbial genome database [179,180] using a minimal hit length of 100 bp and a minimum sequence similarity of 70 %. To generate a non-redundant list, the sequences of all positive hits were extracted and blasted against each other, discarding hits having less than 80 % length and 80 % sequence identity. All reads not mapping to the pan-genome were mapped against this list using stampy. Only genes with coverage of at least 70 % were regarded as true positive hits resulting in a dataset of 1482 genes.

2.10.4 Nucleotide sequence accession number

The RNA-seq data of *K. pneumoniae* has been deposited at the National Center for Biotechnology Information sequence read archive (SRA; http://www.ncbi.nlm.nih.gov/sra) under the accession no. SRP051240.

2.11 Phylogenetic analyses

2.11.1 Phylogenetic relationship of *K. pneumoniae* isolates based on commonly transcribed genes

To construct the phylogenetic relationship, a consensus sequence of 404 commonly transcribed genes was generated for each *K. pneumoniae* isolate using the *mpileup* option in the SAMtools package [181]. Only protein coding sequences from the core-genome which are transcribed in every isolate with minimal coverage of 5 reads per position were used. The coverage was determined with the "depth" command in SAMtools and the sequences of 404 genes fulfilling the criteria were extracted using a Perl script. The corresponding orthologous gene sequences from 11 publicly available *K. pneumoniae* genomes were extracted and included in the alignment generation. All sequences were aligned with Clustal Omega [182,183] to generate an alignment of 314,561 bp length. The consensus Neighbor Joining tree was drawn with MEGA 6.0 [161] using the maximum composite likelihood model and 1000 bootstrapping replications.

2.11.2 Phylogenetic relationship of *P. aeruginosa* isolates based on core-genome genes

The phylogenetic relationship was studied using a total of 148 genes that were at least 90 % covered with sequencing reads in all clinical isolates and had orthologs in the five *Pseudomonas aeruginosa* reference strains PA14, PAO1, LESB58, PACS2, and PA7. The ortholog information was obtained from a pre-computed *Pseudomonas* genome alignment with the Mauve multiple genome alignment tool [184]. The respective gene sequences were extracted using the SAMtools package.

Phylogenetic distances between the isolates were calculated using a k-mer based approach developed by Ole Lund and Rolf Kaas (Technical University of Denmark, personal communication). The sequences were split into 17-mers and compared pair-wise between tall isolates. The resulting distance matrix (generated by Monika Schniederjans, Helmholtz Centre for Infection Research) was used to build a neighbor-joining tree in MEGA 6 [161]. Information about ciprofloxacin resistances was added and visualized using iTOL (http://itol.embl.de [185]).

2.11.3 Multilocus sequence typing (MLST)

To perform MLST [186], sequences from *gapA*, *infB*, *mdh*, *pgi* and *rpoB* were extracted by SAMtools' *mpileup* option [181]. Due to low read coverage, sequencing of *phoE* and *tonB* was performed by

classical Sanger sequencing according to [40] using universal sequence primers (see **Table** 2.6) and an annealing temperature of 50 °C. Nucleotide sequences were analyzed via http://bigsdb.web.pasteur.fr/klebsiella/klebsiella.html.

2.12 Gene Ontology term enrichment

The current UniProt Gene Ontology (GO) knowledge database was downloaded on 07/09/14 [187]. Using custom Perl scripts, the gene locus IDs (in KEGG format) were mapped to their UniProt identifiers and extracted the relevant GO IDs from the flat files. Significantly enriched or depleted categories were tested by one-sided hypergeometric tests in R and the retrieved P-values were adjusted by the Benjamini-Hochberg correction to control the false-discovery rate.

2.13 Transcriptome-wide association of differentially expressed genes and accumulation of SNPs for infection relevant phenotypes

Bacterial isolates were classified according to a particular phenotype (biofilm or virulence) and compared to identify i) differentially expressed genes in one group vs. the other group using Wilcoxon's rank-sum test and ii) group specific accumulations of mutations using Fisher's exact test. In both cases, P-values were adjusted by the Benjamini-Hochberg correction to control the false-discovery rate. Genes were regarded as differentially expressed, when their median expression differed by at least two-fold, the standard deviation was not higher than the median and their adjusted P-value was smaller than 0.05. SNPs and short insertions and deletions (indels) were detected using SAMtools [181]. SNPs with a Phred quality score above 30 and indels with a score above 150 were regarded as positive and further manually verified using the Integrative Genomics Viewer [188]. The Phred quality score Q is defined as

$$Q = -10\ log10(P) \text{ or } P = 10^{\frac{(-Q)}{10}},$$

with P representing the P-value as estimated by SAMtools. Thus, a Phred score of 30 corresponds to a P-value of 0.001 [189,190].

3 Results

3.1 Quantitative contributions of target alteration and decreased drug accumulation to *Pseudomonas aeruginosa* fluoroquinolone resistance

In this present study, Sanger sequencing and pyrosequencing was used to determine the nature and frequency of hot spot SNP mutations in the quinolone resistance-determining regions (QRDRs) of the *gyrA* and *gyrB* genes, encoding DNA gyrase, as well as in those of *parC* and *parE*, encoding topoisomerase IV. A panel of 100 clinical *P. aeruginosa* isolates obtained from patients of the Hannover Medical School, collected over a period of 2 years (2005 to 2007) was analyzed here. The isolates were recovered from various clinical sites, and most of them exhibited resistance not only to fluoroquinolones (see Table 2.2) but also to various other antimicrobial compounds (data not shown). Pyrosequencing technology has been proven to be time and cost competitive and to allow efficient detection of SNPs in localized regions where the nucleotide variants are known [191]. Two different pyrosequencing assays were designed for sequencing analysis of the most prominent mutation hot spots in the QRDR of the A subunit of the DNA gyrase, encoded by *gyrA*, which spans amino acid positions 83 to 87, and in the QRDR of the A subunit of topoisomerase IV, encoded by *parC*, which spans amino acid positions 82 to 84.

The QRDRs of the B subunits of DNA gyrase (encoded by *gyrB*) and topoisomerase IV (encoded by *parE*) are larger, spanning amino acid positions 429 to 585 in the GyrB protein and 357 to 503 in the ParE protein. Therefore, Sanger sequencing was performed for the identification of relevant mutations in the QRDRs of *gyrB* and *parE*.

3.1.1 Frequency and nature of mutations in the QRDRs of *gyrA*, *gyrB*, *parC*, and *parE* in clinical *P. aeruginosa* isolates

Sequencing confirmed the presence of mutations in the QRDRs in most of the clinical isolates. The relative frequencies of the specific mutations are shown in Figure 3.1A. In accordance with the findings of several previous studies [192-198], the most frequently observed mutation, T83I, was encoded in the QRDR of *gyrA*, whereas mutations in *gyrB* were less frequent [197,199,200]. Here, the majority of mutations were found at amino acid positions 466 to 468; however, two isolates exhibited an I529V mutation, which has not been described previously. Two mutations within the QRDR of *parC* were detected in the panel of 100 clinical isolates (S87W and S87L), and only three mutations were present in *parE* (one M437I and two A473V mutations). The majority of clinical

isolates harbored either a single mutation in *gyrA* or *gyrB* or a combination of mutations in *gyrA* and *parC* (Figure 3.1B). Fewer isolates exhibited mutations in *gyrB* in combination with *parE* or in *gyrA* in combination with *gyrB*, with or without additional mutations in the QRDR of *parC*. As in previous studies [195,200], no single *parC* mutations were found in the panel of clinical *P. aeruginosa* isolates. Two of the isolates harbored a single mutation in *parE*, and for 14 isolates, no mutations in the QRDRs were detected.

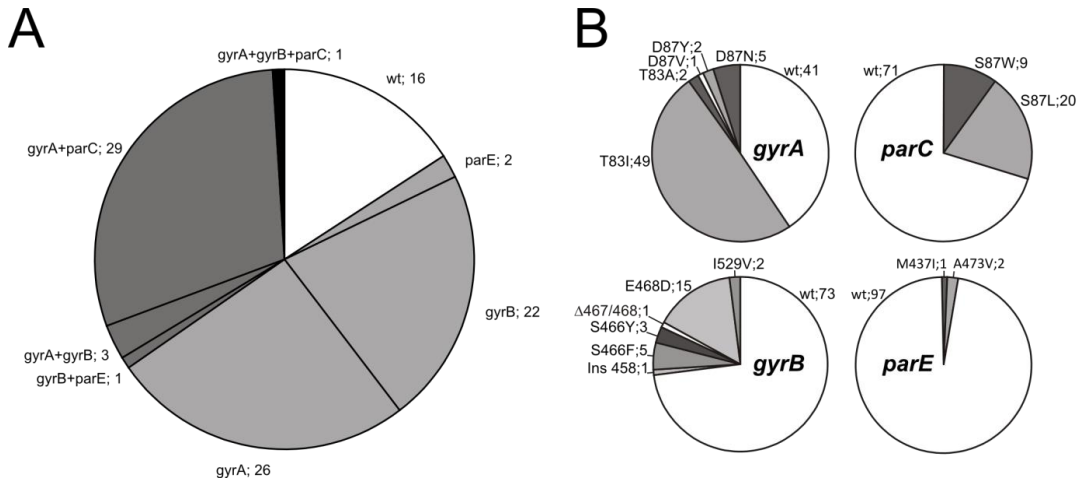

Figure 3.1: Mutations identified in the *gyrA*, *gyrB*, *parC*, and *parE* genes of 100 clinical isolates.

(A) Co-occurrence of mutations in the QRDRs of *gyrA*, *gyrB*, *parC*, and *parE* in individual clinical *P. aeruginosa* isolates. The proportions of isolates with a single (light shaded sectors), double (dark shaded sectors), or triple (filled sectors) mutation, or with no identified QRDR mutation (open sectors), are shown.

(B) Frequency and nature of mutations found in the QRDRs of *gyrA*, *gyrB*, *parC*, and *parE* in 100 clinical Pseudomonas aeruginosa isolates. Each mutation (given as the wild-type allele, amino acid position, and mutant allele) is followed by a semicolon and the number of isolates harboring the mutation. Δ, deletion at the specified position; wt, wild-type allele or silent mutation. Figure published in [147].

3.1.2 Correlation of the presence of SNPs in the QRDRs of *gyrA*, *gyrB*, *parC* and *parE* with the ciprofloxacin resistance phenotype in clinical *P. aeruginosa* isolates.

The presence of SNPs within the QRDRs of *gyrA*, *gyrB*, *parC* and *parE* was correlated with phenotypic resistance to fluoroquinolones in the clinical *P. aeruginosa* isolates. Figure 3.2 shows the relationship of the ciprofloxacin MIC values for all 100 clinical *P. aeruginosa* isolates to the presence of mutations in the QRDRs. The majority of clinical isolates harbored single mutations in *parE*, *gyrA*, or *gyrB*; however, those mutations did not necessarily lead to ciprofloxacin MIC values exceeding 2 µg/ml (noteworthy, resistance according to the Clinical and Laboratory Standards Institute [CLSI] breakpoints is categorized by MIC values exceeding 2 µg/ml). In contrast, combinations of mutations

in the QRDRs of *gyrA* and *parC* always resulted in a ciprofloxacin-resistant phenotype, with MIC values of ≥8 µg/ml. The two isolates that harbored single *parE* mutations and the 14 isolates without mutations in the QRDRs exhibited MIC values that did not exceed 2 µg/ml and thus were categorized as susceptible or intermediate according to CLSI breakpoints.

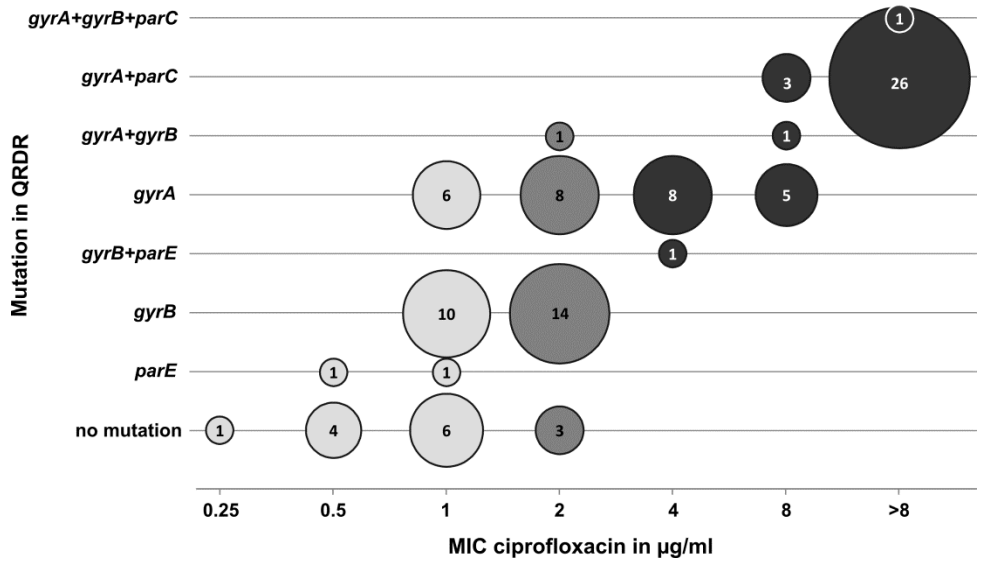

Figure 3.2: Correlation of ciprofloxacin MIC values with the presence of mutations in the QRDRs of *gyrA*, *gyrB*, *parC*, and *parE* (and combinations thereof) for 100 *P. aeruginosa* clinical isolates.

The number of isolates with the same combination of MIC and genotype is given inside each circle. Light, medium, and dark shaded circles represent sensitive, intermediate, and resistant isolates, respectively, according to the CLSI clinical breakpoints [142]. Figure published in [147].

3.1.3 Introduction of dominant SNPs in the QRDRs of *gyrA*, *gyrB* and *parC* into the susceptible *P. aeruginosa* reference strain PA14

In order to pinpoint the contributions of the most frequent mutations in the QRDRs of *gyrA*, *gyrB*, and *parC* to fluoroquinolone resistance, the respective SNPs were introduced into the fluoroquinolone-susceptible reference strain PA14 and the resistance profile were measured. Plasmid constructs for allelic exchange were generated for two SNPs in *gyrA* (resulting in amino acid exchanges T83I and D87N), three SNPs in *gyrB* (S466F, S466Y, and E468D), and two SNPs in *parC* (S87L and S87W). These SNPs were introduced into the reference strain singly and in various combinations.

As shown in Table 3.1, the introduction of *parC* mutations alone had no impact on susceptibility to ciprofloxacin, whereas mutations in the QRDR of *gyrB* or *gyrA* increased the MIC of ciprofloxacin 8- to 16-fold. Similarly, as already reported, the introduction of a single *parC* mutation did not alter the

susceptibility of *Escherichia coli* to fluoroquinolone [201]. The simultaneous introduction of two SNPs into the QRDR of *gyrA* (T83I and D87N) did not increase ciprofloxacin resistance over that with T83I alone. However, the simultaneous introduction of SNPs in *gyrA* (T83I) and *parC* (either S87L or S87W) increased the ciprofloxacin MIC 256-fold over that for the reference PA14 strain. None of the mutations in the QRDRs had any impact on the resistance of the parental strain to beta-lactam antibiotics, carbapenems, or aminoglycosides (data not shown).

Table 3.1: MICs of in vitro generated PA14 mutants

	PA14 mutant	**CIP MIC**
wild type	PA14	0.125
mutations in QRDR	*gyrA* T83I	2
	gyrA D87N	1
	gyrA T83I-D87N	2
	gyrB S466F	1
	gyrB S466Y	1
	gyrB E468D	1
	parC S87L	0.125
	parC S87W	0.125
efflux mutations	Δ*nfxB*	2
	Δ*mexR*	0.5
	Δ*mexS*	2
	Δ*mexZ*	0.25
	Δ*nfxB* + Δ*mexZ*	2
	Δ*mexR* + Δ*mexS*	2
	Δ*mexR* + Δ*mexZ*	0.5
	Δ*mexS* + Δ*mexZ*	2
combination of efflux and QRDR mutations	*gyrA* T83I + Δ*nfxB*	32
	gyrA T83I + Δ*mexR*	8
	gyrA T83I + Δ*mexS*	32
	gyrA T83I + Δ*mexZ*	2
	gyrB E468D + Δ*nfxB*	8
	gyrB E468D + Δ*mexR*	2
	gyrB E468D + Δ*mexS*	8
	gyrB E468D + Δ*mexZ*	1
	gyrA T83I + *parC* S87L	32
	gyrA T83I + *parC* S87W	32
	gyrA T83I + *parC* S87L + Δ*nfxB*	256
	gyrA T83I + *parC* S87L + Δ*mexR*	64
	gyrA T83I + *parC* S87L + Δ*mexS*	256
	gyrA T83I + *parC* S87L + Δ*mexZ*	32

CIP, ciprofloxacin; MIC in µg/ml

3.1.4 Most clinical *P. aeruginosa* isolates harboring mutations in the QRDR additionally express efflux pumps

Mutations in genes encoding the two subunits of DNA gyrase raised the ciprofloxacin MIC 8- to 16-fold over that for the *P. aeruginosa* reference strain. Those *gyrA* mutants, as well as the majority of the clinical isolates harboring relevant mutations in the QRDRs of *gyrA* and/or *gyrB*, exhibited MIC values of ≤ 2 μg/ml. However, clinical isolates with a single mutation in *gyrA* which reached corresponding MIC values of 8 μg/ml were identified. The broad MIC range for clinical *P. aeruginosa gyrA* mutants has been observed in several studies previously [202,203], and although it is tempting to speculate that this can be explained by differential expression of efflux pumps [199,204], no clear association between increased MICs for the *gyrA* mutants and increased expression of efflux pumps could be demonstrated in previous studies [203,205,206]. Along the same lines, it has been demonstrated for some individual clinical *P. aeruginosa* isolates that elevated meropenem MIC levels could not be explained by decreased levels of OprD and/or overexpression of the MexAB-OprM and MexEF-OprN efflux pumps [207,208], and it was thought that other resistance mechanisms yet to be identified might account for the resistance phenotype. Therefore, to test whether differential expression of efflux pumps in those isolates could account for the high MIC values, the expression of four efflux pumps—MexAB-OprM, MexCD-OprJ, MexEF-OprN and MexXY-OprM— was monitored in 29 selected clinical isolates. Nine of these isolates did not harbor mutations in any of the QRDRs; ten isolates harbored a single *gyrA* mutation; and ten isolates had mutations in *gyrA* in combination with *parC*. The transcription of the genes encoding the membrane fusion proteins of the pumps (*mexA*, *mexC*, *mexE*, and *mexX*) was quantified using qRT-PCR, and the results are shown in Table 3.2.

Table 3.2: Expression of *mexA*, *mexC*, *mexE* and *mexX* in 29 clinical isolates and in four in vitro generated PA14 knock-out mutants compared to PA14 wild type strain.

	Fold change in expression of[a)]					
Isolate	*mexA*	*mexC*	*mexE*	*mexX*	CIP MIC*	QRDR mutation
MHH10049	0.99	**11.6**	n.d.	**50.57**	0.5	wt
MHH12178	1.72	3.22	3.50	**11.87**	0.5	wt
MHH7624	0.93	2.10	1.88	**17.25**	1	wt
MHH9229	1.19	**18.24**	1.82	*6.45*	1	wt
MHH9639	0.22	*8.52*	3.18	**93.65**	1	wt
MHH10047	*2.48*	3.01	*5.63*	**21.86**	1	wt
MHH11935	*2.01*	*5.43*	**13.05**	**21.27**	1	wt
MHH9748	0.95	1.24	**43.69**	4.47	2	wt
MHH9830	*2.87*	**10.60**	**33.72**	**76.38**	2	wt
MHH7508	0.38	3.03	**10.75**	*7.16*	1	*gyrA* D87N
MHH7807	1.18	1.42	4.94	**45.14**	1	*gyrA* D87Y
MHH7091	0.87	0.80	1.58	**63.14**	1	*gyrA* T83I
MHH11445	1.47	2.00	3.87	**110.02**	1	*gyrA* T83I
MHH7252	1.16	1.93	2.39	*6.34*	2	*gyrA* T83I
MHH14088	0.62	**14.94**	2.83	**74.33**	2	*gyrA* T83I
MHH7313	1.31	3.04	*5.66*	**15.72**	4	*gyrA* T83I
MHH11148	0.73	0.67	0.74	**27.32**	4	*gyrA* T83I
MHH12274	0.85	1.25	1.92	**55.25**	4	*gyrA* T83I
MHH7055	**4.38**	1.88	2.69	**38.43**	8	*gyrA* T83I
MHH6964	0.87	1.13	4.02	**42.34**	8	*gyrA* T83I + *parC* S87L
MHH6829	1.01	0.9	**13.53**	*6.71*	>8	*gyrA* T83I + *parC* S87L
MHH6870	0.92	1.27	*5.55*	**53.41**	>8	*gyrA* T83I + *parC* S87L
MHH7176	1.11	1.39	*5.36*	**54.14**	>8	*gyrA* T83I + *parC* S87L
MHH7823	0.95	0.73	3.23	**37.57**	>8	*gyrA* T83I + *parC* S87L
MHH7863	1.17	0.75	4.92	**31.39**	>8	*gyrA* T83I + *parC* S87L
MHH8349	1.22	1.25	4.46	**45.60**	>8	*gyrA* T83I + *parC* S87L
MHH8478	1.13	1.83	*6.00*	**56.84**	>8	*gyrA* T83I + *parC* S87L
MHH8614	1,00	1.69	*6.13*	**49.78**	>8	*gyrA* T83I + *parC* S87L
MHH9652	1.19	1.08	4.43	**41.37**	>8	*gyrA* T83I + *parC* S87L
Δ*nfxB*	0.59	**16.08**	0.70	0.58	2	knockout of *nfxB* in PA14
Δ*mexR*	1.58	0.64	0.81	0.73	0.5	knockout of *mexR* in PA14
Δ*mexS*	0.65	0.33	**318.2**	0.67	2	knockout of *mexS* in PA14
Δ*mexZ*	0.81	0.75	2.30	*6.17*	0.25	knockout of *mexZ* in PA14

CIP, ciprofloxacin; n.d., not determined; wt, wild type or silent mutation

a) Overexpression is indicated by boldface values and borderline expression values are underlined and italicized (according to the work of Cabot *et al*.[163]).

*The ciprofloxacin MIC values are given in µg/ml, the classification into resistance (R), intermediate (I) and susceptible (S) isolates is according to CLSI guidelines [142].

According to work done by Cabot *et al.* [163], ≥ 3-fold overexpression of *mexA* was regarded as positive, whereas values between 2- and 3-fold were regarded as borderline expression. For *mexC*, *mexE*, and *mexX*, ≥ 10-fold overexpression was regarded as positive, and 5- to 10-fold overexpression was regarded as borderline expression. The majority of clinical isolates exhibited increased expression of at least one efflux pump; MexXY-OprM expression was increased the most. This result has also been observed previously [209]. However, no clear association between the expression of efflux pumps and increased fluoroquinolone MIC values for isolates harboring mutations in the QRDRs could be observed (see Figure 3.3).

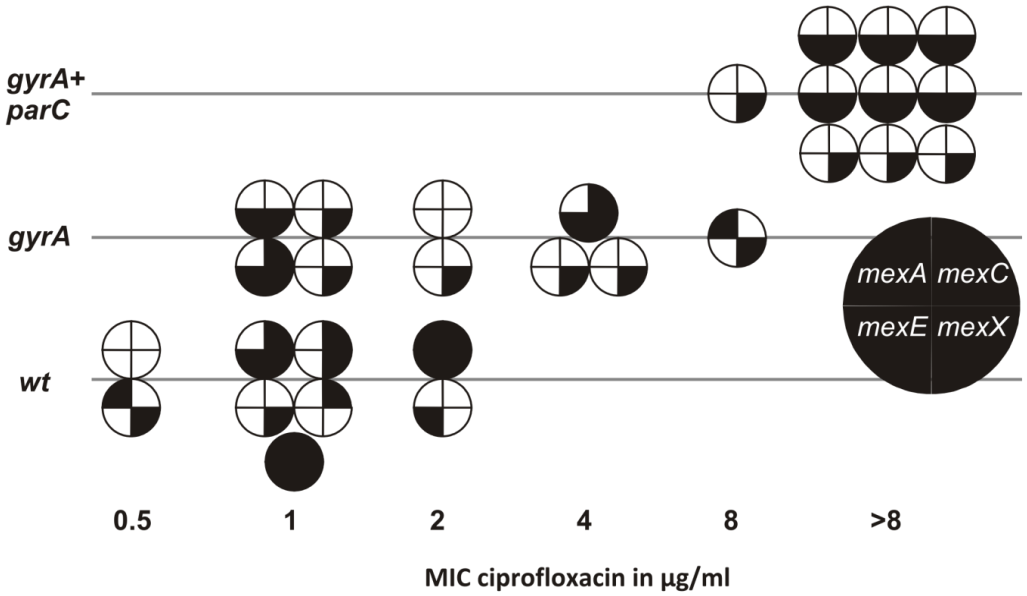

Figure 3.3: Influence of multidrug efflux (MEX) pump overexpression and QRDR mutation on ciprofloxacin MIC.

The variations of MIC values for a particular genotype cannot be explained by the additional expression of MEX pumps. The figure shows the expression of four MEX pumps in 29 selected clinical *P. aeruginosa* isolates. Each circle represents one clinical isolate while each quarter represents one efflux pump (top left: MexAB-OprM, top right: MexCD-OprJ, bottom left: MexEF-OprN and bottom right: MexXY-OprM) with black quarters representing an overexpression of a pump, gray quarters representing borderline expression and white quarter representing wild -type expression levels (according to Cabot *et al.* 2011 [163]). The isolates were arranged according to their QRDR genotype (wild type, single mutation in *gyrA* or simultaneous mutation in *gyrA* and *parC*) and their ciprofloxacin MIC. Figure published in [147].

3.1.5 Inactivation of the efflux regulator-encoding genes *mexR*, *nfxB*, *mexS*, and *mexZ* in the susceptible *P. aeruginosa* reference strain

In order to pinpoint the contributions of overexpression of the MexAB-OprM, MexCD-OprJ, MexEF-OprN, and MexXY-OprM efflux pumps to fluoroquinolone resistance, the respective efflux regulator-encoding genes in the fluoroquinolone-susceptible reference strain PA14 were inactivated and the

resistance profile measured suing the Vitek2 system (bioMérieux, Nürtingen, Germany). Deletion of the efflux regulator-encoding gene *mexR*, *nfxB*, or *mexZ* or of the oxidoreductase-encoding gene *mexS* led to overexpression of the efflux pump MexAB-OprM by 1.6-fold, MexCD-OprJ by 16-fold, MexXY-OprM by 6-fold, or MexEF-OprN by 320-fold, respectively (Table 3.2). Additionally, the efflux regulator-encoding genes were inactivated in the PA14 strain background in various combinations (Δ*nfxB* + Δ*mexZ*, Δ*mexR* + Δ*mexS*, Δ*mexR* + Δ*mexZ*, and Δ*mexS* + Δ*mexZ*) and also combined with mutations in the QRDRs (*gyrA*, *gyrB*, and *gyrA* in combination with *parC,* respectively). As shown in Table 3.1, overexpression of the efflux pumps clearly increased the ciprofloxacin MIC values for the susceptible *P. aeruginosa* reference strain 2- to 16-fold. Inactivation of *nfxB* or *mexS* had the most pronounced phenotype. The combined inactivation of various efflux regulator-encoding genes (Δ*nfxB* + Δ*mexZ*, Δ*mexR* + Δ*mexS*, Δ*mexR* + Δ*mexZ*, and Δ*mexS* + Δ*mexZ*) did not lead to further increases in MIC levels. This absence of an additive effect might be explained by antagonistic interactions of efflux pumps during planktonic growth, which have been found to occur in *nfxB* mutants [210]. However, the inactivation of efflux regulator-encoding genes in the PA14 *gyrA*, *gyrB*, and *gyrA/parC* mutant backgrounds clearly enhanced the fluoroquinolone resistance level further in an additive manner. In agreement with these results, the deletion of efflux pumps in resistant *P. aeruginosa* strains with multiple target alterations has been demonstrated previously to lead to a reduced fluoroquinolone MIC [211]. It might thus be surprising that a clear correlation between increased fluoroquinolone MIC values for clinical isolates harboring a particular QRDR genotype and the expression of major efflux pumps could not be identified.

3.1.6 Mutation in the QRDR of *gyrA* adds to preexisting isolate-specific resistance levels

Although overexpression of efflux pumps further enhanced fluoroquinolone resistance in a QRDR mutant background, a clear association between the expression of efflux pumps and increased fluoroquinolone MIC values in the set of clinical isolates could not be identified. Therefore we wondered whether the contribution of a *gyrA* mutation to the fluoroquinolone resistance level could differ for different isolates. To address this question, the wild-type *gyrA* was cloned gene into the pME6032 vector, resulting in vector pME::gyrA, and introduced into various clinical isolates in *trans*. All of those clinical isolates exhibited *gyrA* mutations, but the MIC values ranged from 0.25 µg/ml to 2 µg/ml (see Table 3.3).

Table 3.3: Complementation of clinical isolates with plasmid pME::gyrA

Isolate	CIP MIC in µg/ml -IPTG	+IPTG	Dif[a] log2	Mutation in *gyrA*
7252	2	0.5	2	T83I
7444	4	0.5	3	T83I
7807	0.25	0.25	0	D87Y
8044	1	0.25	2	T83A
8931	1	0.25	2	D87N
9481	1	0.25	2	T83I
9674	8	2	2	D87Y
12207	1	0.5	1	T83I
13224	1	0.5	1	D87N
13428	0.5	0.125	2	D87N
14088	0.5	0.125	2	T83I
PA14 *gyrA* T83I	1	0.125	3	T83I
PA14 wt	0.125	0.125	0	wt

a) Dif, difference in log2 of ciprofloxacin MIC

In all but one cases, complementation with the wild-type *gyrA* gene led to a 2- to 8-fold reduction in fluoroquinolone resistance irrespective of the original resistance level. These results indicate that mutations within the *gyrA* QRDR add to preexisting isolate-specific resistance levels of unknown origin. Two comprehensive screenings of a *P. aeruginosa* PA14 mutant library have shown that approximately 100 to 200 genes are involved in the ciprofloxacin resistome [133,136] It thus will be interesting to determine which of the identified gene inactivations, if any, play a role in fluoroquinolone resistance in clinical settings.

3.2 Antibiotic resistance profiling in clinical *Pseudomonas aeruginosa* isolates using global transcriptomics

To gain deeper insights into the ciprofloxacin resistome of *P. aeruginosa*, the complete transcriptome of a collection of 159 clinical isolates from diverse origins, sampled from several hospitals across Europe, was studied. The majority of these isolates was collected at the Hannover Medical School [n=87]. A further set of a 72 clinical isolates from the Charité Berlin [n=10] and three strains collections, containing isolates from several hospitals, were included (Robert Koch Institute, Wernigerode [n=14]; University of Freiburg [n=40]; National Reference Laboratory, Bochum [n=8]).
Here, this collection of clinical isolates was used to explore the molecular mechanisms contributing to ciprofloxacin resistance in *P. aeruginosa.*

3.2.1 Phylogenetic distribution of clinical *P. aeruginosa* isolates

The 159 clinical strains exhibited a broad taxonomical distribution as depicted in the phylogenetic tree, which was constructed on the basis of the sequence of 148 commonly expressed genes (Figure 3.4). The tree is separated into three clusters of isolates being closely related to the reference strains PAO1, PA14 and PA7, respectively. The largest cluster, highlighted in light gray in Figure 3.4, contained 92 clinical isolates and the strains PAO1, PACS2, and LESB58. Another big cluster included 64 clinical isolates and the PA14 reference strain, highlighted in dark gray in Figure 3.4. Three isolates (MHH6887, MHH13682, MHH13684) were taxonomically distant from all others and closer related to the known outlier PA7 [212].
When analyzing the phylogenetic relationship of all isolates in greater detail, a cluster of 15 isolates showed very high sequence similarities in the 148 genes used to construct the phylogenetic tree. These 15 isolates originated all from the Hannover Medical School and were furthermore isolated within a short period of just a few months. These isolates were all part of the PAO1 cluster, as indicated by an arrow in Figure 3.4. Because of this close phylogenetic relationship and the short temporal distance these isolates were collected, they are very likely to resemble a clonal spread of a single successful strain within one hospital. Since this possible clonal outbreak might influence follow-up analyses, these 15 isolates were excluded from all subsequent transcriptome-wide association studies.

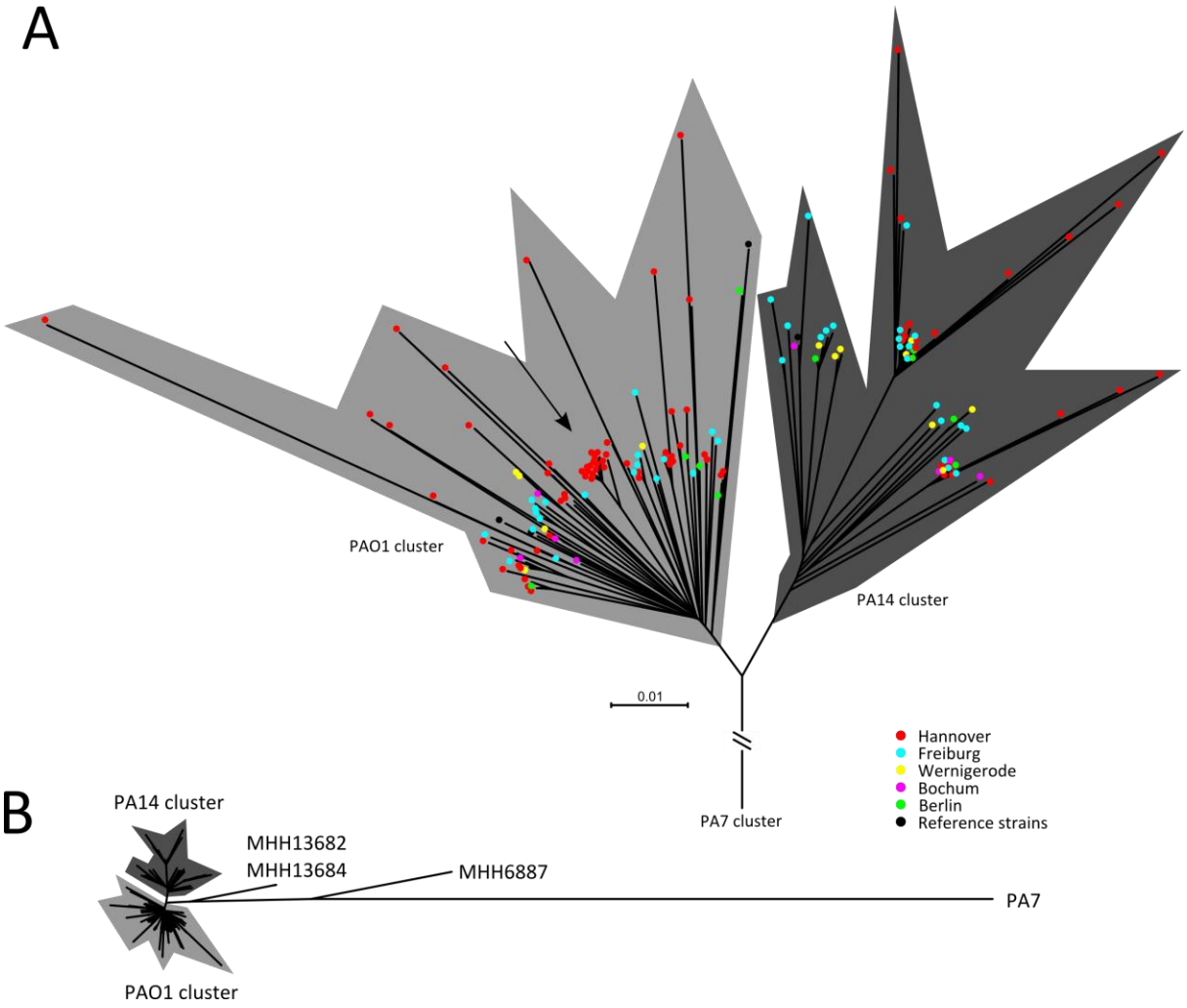

Figure 3.4: Phylogenetic relationship of clinical *P. aeruginosa* isolates based on 148 genes.

A: The unrooted neighbor-joining tree includes all 159 clinical isolates and additionally five reference strains (PA14, PAO1, LESB58, PACS2 and PA7). The phylogenetic relationship is based on a distance matrix calculated from k-mers (17-mers) of all genes that were covered by reads to at least 90 % in all isolates and had a respective ortholog in all reference strains (in total 148 genes) in MEGA 6 [161]. The scale indicates the number of base substitutions per site. Isolates clustering together with the PAO1 reference strain are highlighted in light gray and all isolates in the PA14 cluster in dark gray. Isolates are colored according to their origin as indicated in the legend. Arrow indicates possible clonal outbreak at Hannover Medical School.

B: The true phylogenetic distance between the PAO1 and the PA14 clusters towards the PA7 cluster is indicated here.

The antibiotic susceptibility profiles of all 159 isolates (see Table 2.2) were determined using the automated Vitek2 system (bioMérieux). According to CLSI antibiotic resistance breakpoints [142], most of the isolates were categorized as multidrug-resistant with non-susceptibility to three or more antimicrobial classes [213] (data not shown). Antibiotic resistance profiling demonstrated that 82 isolates (51.6 %) were resistant to ciprofloxacin with MIC values exceeding 2 µg/ml. 31 isolates (19.5 %) showed an intermediate resistance phenotype with an MIC value of 2 µg/ml and 46 isolates (28.9

%) were classified as susceptible with MIC values below 2 µg/ml. Figure 3.5 shows the ciprofloxacin resistance profile in association with the phylogenetic relationship and reveals a broad distribution of ciprofloxacin non-susceptibility with only a weak association of resistance to phylogenetic distance.

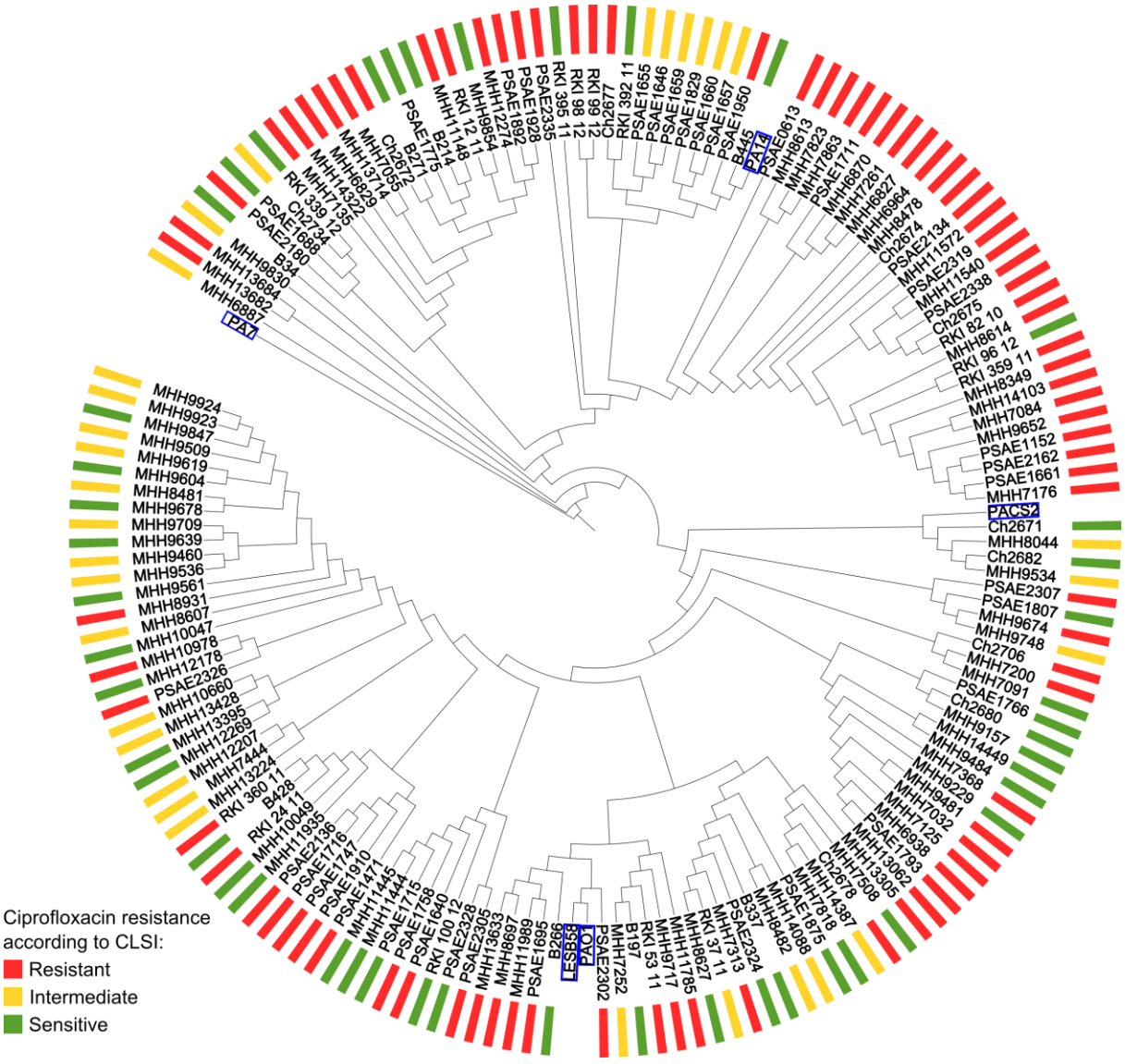

Figure 3.5: Phylogenetic association of ciprofloxacin susceptibility within 159 clinical isolates.

The phylogenetic tree includes all 159 clinical isolates and additionally five reference strains (PA14, PAO1, LESB58, PACS2 and PA7). The phylogenetic relationship is based on a distance matrix calculated from k-mers (17-mers) of all genes that were covered by reads to at least 90 % in all isolates and had a respective ortholog in all reference strains (in total 148 genes). The tree was built using the neighbor-joining algorithm and PA7 as a outgroup in MEGA 6 [161] and is shown irrespective of the tree branch length. Reference strains are framed in blue. The ciprofloxacin resistance profile (according to CLSI [142]) is indicated by colored bars (see legend) and was integrated using iTOL [185].

3.2.2 Nature and dimension of chromosomal ciprofloxacin resistance conferring mutations in *P. aeruginosa*

In order to provide a detailed analysis of ciprofloxacin resistance conferring mechanisms, the transcriptomic data of the 159 clinical isolates were used to extract genomic information about sequence variations within the QRDRs of the of *gyrA*, *gyrB*, *parC* and *parE.* Therefore, SNPs and short indels were extracted using SAMtools [181] and further verified using the Integrative Genomics Viewer [188]. In 13 isolates, where the coverage of cDNA sequencing reads was not satisfying, the respective sequence information was taken, if possible, from the analyses in chapter 3.1. Sequence coverage was below the threshold of three sequencing reads per position for *parC* (n=9), *gyrB* (n=1) and *parE* (n=7) of 13 isolates in total. In the case of a single isolate the sequence information of *parE* could not be added, since this isolate was not included in the previous analyses.

A total of 123 isolates (77.4 %) harbored at least one mutation within the QRDRs with the majority of these showing either a single mutation in *gyrA* (n=45) or a combination of a *gyrA* mutation with a mutation in *parC* (n=47), *parE* (n=5) and *gyrB* (n=2), respectively. 20 isolates harbored a single mutation in *gyrB* (n=18) or *parE* (n=2), four isolates had a triple mutation in *gyrA*, *gyrB* and *parC* and 36 isolates had no amino acid alterations within the QRDRs (see Figure 3.6).

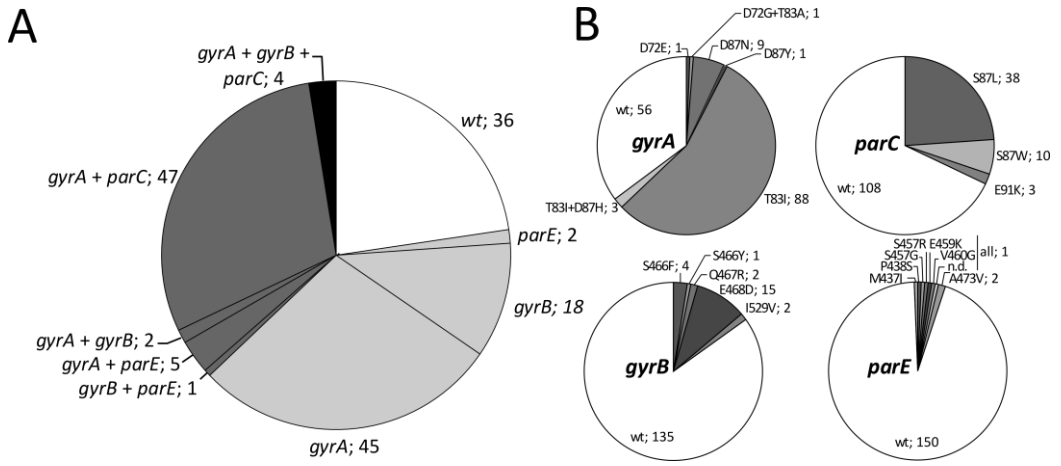

Figure 3.6: Mutations identified by RNA-seq in *gyrA*, *gyrB*, *parC*, and *parE* of 159 clinical isolates.

A: Co-occurrence of mutations in the QRDRs of *gyrA*, *gyrB*, *parC*, and *parE* in individual clinical *P. aeruginosa* isolates. The proportions of isolates with a single (light shaded sectors), double (dark shaded sectors), or triple (filled sectors) mutation, or with no identified QRDR mutation (open sectors), are shown.

B: Frequency and nature of mutations found in the QRDRs of *gyrA*, *gyrB*, *parC*, and *parE* in 159 clinical Pseudomonas aeruginosa isolates. Each mutation (given as the wild-type allele, amino acid position, and mutant allele) is followed by a semicolon and the number of isolates harboring the mutation. wt, wild-type allele or silent mutation.

The association of mutations within the QRDRs of *gyrA*, *gyrB*, *parC*, and *parE* with the ciprofloxacin MIC is depicted in Table 3.4. It shows that a singular mutation in *gyrA* raised the median ciprofloxacin

MIC from 0.5 to 4 µg/ml in the panel of clinical isolates. In combination with a mutation in *parC* (47 isolates) the median MIC increased to more than 8 µg/ml. Thus, there was a high correlation (r=0.766; Spearman nonparametric correlation) between the presence of a particular SNP in *gyrA* (T83I) and *parC* (either S87L, S87W or E91K) and ciprofloxacin MICs above 8 µg/ml. A minor fraction of isolates showed mutations in *parE* and *gyrB*, which had a less pronounced effect on the median ciprofloxacin MIC with values of 0.75 µg/ml and 2 µg/ml, respectively. With just two exceptions, any MIC of more than 4 µg/ml required a mutation in *gyrA*, rendering the detection of *gyrA* target mutations as suitable resistance markers.

Table 3.4: Association of single and multiple QRDR mutations with ciprofloxacin MIC.

QRDR mutation	Isolates [n]	MIC ciprofloxacin in µg/ml								
		0.125	0.25	0.5	1	2	4	8	>8	Median
no mutation	36	8	4	9	9	4		1	1	0.5
parE	2			1	1					0.75
gyrB	17				6	11				2
gyrA	45				5	15	10	10	5	4
gyrB + *parE*	1						1			4
gyrA + *gyrB*	2					1		1		5
gyrA + *parE*	5						1	1	3	> 8
gyrA + *parC*	47							10	37	> 8
gyrA + *gyrB* + *parC*	4							1	3	> 8

The table shows the association of mutations within the QRDRs with the ciprofloxacin minimal inhibitory concentration. Isolates having MIC values above 8 µg/ml were merged and listed as >8. See supplementary table S2 for a detailed list of mutations.

3.2.3 Expression of multidrug efflux pumps in clinical isolates

Besides target mutations of gyrase and topoisomerase IV, up-regulation of multidrug efflux pumps has been shown to be an initial and very common event that contributes to the development of low-level resistance in the clinical setting [214,215]. To further investigate the involvement of an enhanced efflux in clinical isolates on a broader and unbiased basis, the whole panel of 159 isolates was screened for the expression of eleven known RND efflux pumps.

Figure 3.7 visualizes the expression of all known RND efflux systems in *P. aeruginosa*, which typically consist of genes encoding a membrane fusion protein, an efflux transporter and an outer membrane protein. Since the cognate outer membrane protein of MexXY (OprA) is not present in PA14 [216], the plot also includes the genes encoding the outer membrane proteins OpmG, Omph and OmpI which do not belong to RND efflux pump operons and are known to be possible MexXY interaction partners [217,218]. The normalized reads per kilobase of gene sequence (nRPK) values of each gene

are plotted with red indicating a high expression (maximal value of 18) and blue indication low expression. The plot shows that in terms of absolute expression *mexAB-oprM* is expressed at highest and *mexMN* and *mexPQ-opmE* are expressed at lowest levels. Furthermore it indicates that efflux pump expression varies largely between the isolates and this variation is independent from the phylogenetic background.

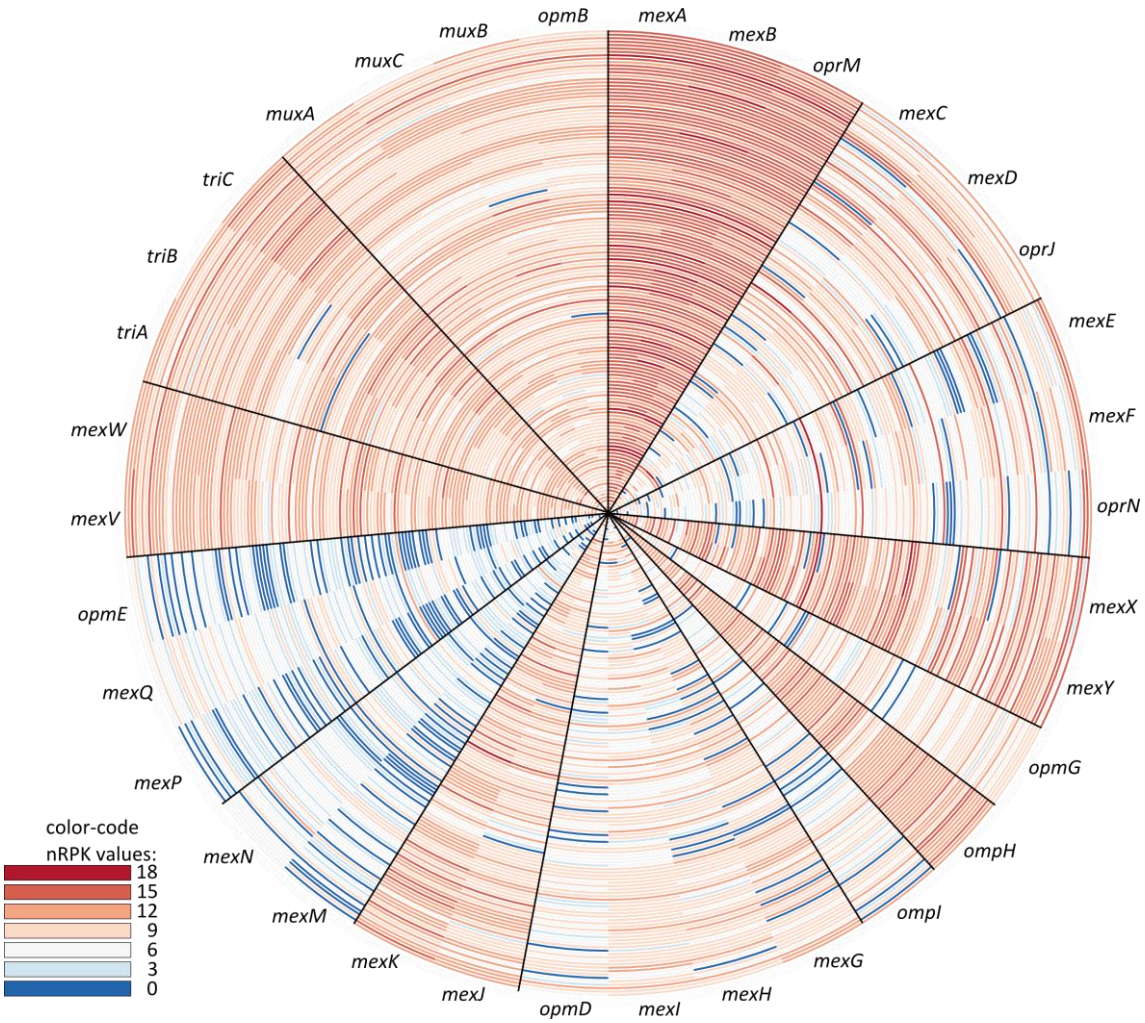

Figure 3.7: Absolute expression of eleven RND efflux pump in *P. aeruginosa* clinical isolates.

The Circos [219] plot shows the normalized read counts in nRPK of 11 RND efflux pumps and three outer membrane proteins. Expression varies from 18 nRPK (red) to 0 nRPK (blue) according to the legend on the left. Genes are arranged in segments representing the 11 RND efflux pumps operons and are separated by black lines. The names of all genes are indicated outside of the rings. Isolates are arranged according to their phylogenetic relationship shown in Figure 3.5 starting with MHH6887 as the outermost ring. With the exception of MHH8607 (shown as the innermost ring), isolates involved in the possible clinical outbreak are not shown.

An efflux pump was regarded as overexpressed, in comparison to the PA14 reference strain, when both membrane fusion protein and efflux transporter showed at least a two-fold increase in expression as determined by DESeq as well as a P-value of less than 0.05 (after Benjamini-Hochberg

correction). Using these thresholds, 122 out of the panel of 159 clinical isolates overexpressed *mexXY*, which was therefore by far the most frequently overexpressed efflux pump. Besides *mexXY*, *mexAB* (48 isolates), *mexCD* (38 isolates) and *mexEF* (38 isolates) were also commonly overexpressed in comparison to PA14 (see Table 3.5). Out of the remaining seven efflux systems, only *muxACB* (18 isolates), *mexJK* (9 isolates) and *mexMN* (2 isolates) were overexpressed to some extent, the remaining four efflux pumps were never overexpressed.

Table 3.5: Overexpression of RND efflux pumps in 159 clinical isolates as compared to PA14

Hypothetical protein	Membrane fusion protein	Secondary Membrane fusion protein	Efflux transporter	Secondary Efflux transporter	Outer membrane protein	Over-expressing isolates [n]
	mexA		*mexB*		*oprM*	48
	mexC		*mexD*		*oprJ*	38
	mexE		*mexF*		*oprN*	38
	mexX		*mexY*			122
mexG	*mexH*		*mexI*		*opmD*	0
	mexJ		*mexK*			9
	mexM		*mexN*			2
	mexP		*mexQ*		*opmE*	0
	mexV		*mexW*			0
	triA	*triB*	*triC*			0
	muxA		*muxC*	*muxB*	*opmB*	18

The table shows the number of isolates overexpressing one or more of the 11 RND efflux pumps from *P. aeruginosa.*

3.2.4 Sequence analysis of efflux pump regulatory genes

To evaluate how mutations in regulatory genes correlated to efflux pump overexpression, the genetic alterations in the negative regulators *mexR*, *nfxB* and *mexZ* as well as in the oxidoreductase *mexS* were examined. SNPs were called using SAMtools with a Phred quality score above 30 and indels with a score above 150. Mutations were further manually verified using the Integrative Genomics Viewer [188]. Figure 3.8 shows that overexpression of efflux pumps can be explained in most isolates by mutations within the respective negative regulatory protein encoding genes. Only *mexAB* and *mexXY* seem to be in many cases overexpressed without showing mutations within their adjacent regulatory gene *mexR* and *mexZ*, respectively. This might be explained by the highly complex regulatory structure of these two operons and the involvement of several transcriptional regulators in the expression of these two efflux pumps [89-91].

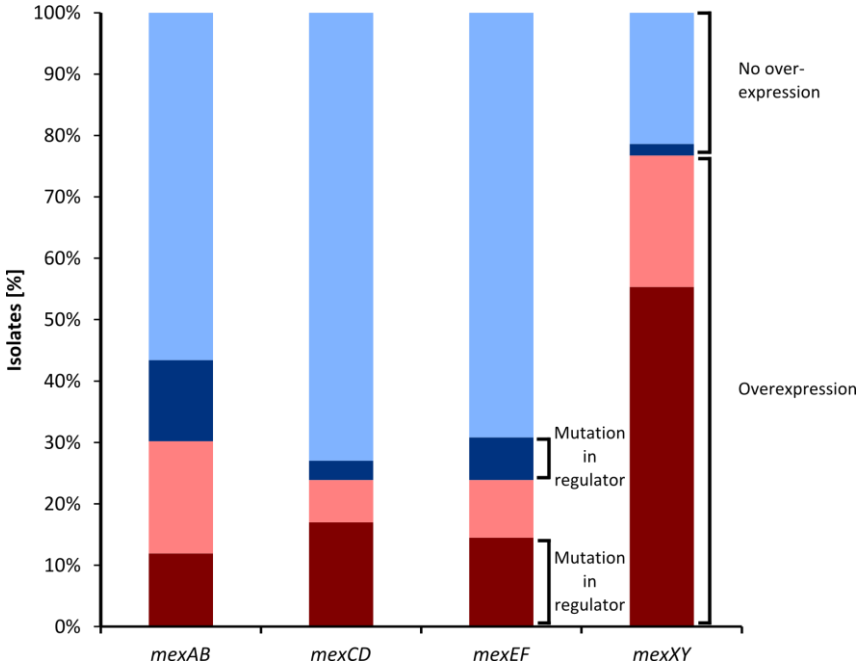

Figure 3.8: Correlation of efflux pumps expression and mutations in regulatory genes.
The percentage of isolates showing overexpression of one of the four efflux pumps (*mexAB*, *mexCD*, *mexEF* and *mexXY*, respectively) is depicted in red, the rate of isolates without overexpression is shown in blue. Additionally, the percentage of isolates that harbor at least one mutation (either non-synonymous SNP or indel) in the corresponding negative regulatory gene (*mexR*, *nfxB*, *mexS and mexZ*, respectively) is indicated as dark colors, whereas light colors indicate regulatory genes with wildtype nucleotide sequence. SNPs occurring between PA14 and PAO1 reference strains were excluded from the analysis.

3.2.5 Correlation of enhanced efflux and fluoroquinolone resistance

We next correlated efflux pump expression to the ciprofloxacin resistance phenotype of these isolates. Although the specific influence of the four main efflux systems (*mexAB*, *mexCD*, *mexEF* and *mexXY*) on ciprofloxacin susceptibility could be clearly shown in isogenic mutants, here, a high number of susceptible isolates exhibited strong overexpression of these four efflux pumps. Out of 46 ciprofloxacin susceptible isolates only six showed no overexpression of these four efflux pumps, whereas 21, 11 and eight isolates overexpressed one, two and three efflux pumps, respectively. Furthermore, we found large variations of the ciprofloxacin MIC within isolates of the same genotype. For example, both isolates Ch2680 and Ch2682 do not have mutations in the QRDRs and furthermore overexpress *mexAB* at similar levels (nRPK of *mexA* in Ch2680 12.97 and in Ch2682 13.11), whereas the ciprofloxacin MIC varies from 1 µg/ml (Ch2680) to ≤ 0.25 µg/ml (Ch2682). One possible explanation could be the presence of mutations within the structural genes rendering the efflux pump nonfunctional. But neither non-synonymous mutations nor indels could be detected in these two isolates in the sequence of *mexA* and *mexB*, respectively. Another reason could be the

presence of other, still unknown, resistance mechanisms that influence the ciprofloxacin resistance phenotype.

3.2.6 Whole transcriptome association studies

In order to identify possible chromosomally encoded resistance mechanisms, in addition to the already identified QRDR mutations, we performed unbiased phenotype-genotype correlations. Therefore, whole transcriptome association studies were used to search for the enrichment of SNPs, and differentially expressed genes in the non-susceptible isolates vs. the susceptible isolates. The 159 clinical isolates were classified as non-susceptible, intermediate and susceptible towards ciprofloxacin according to current CLSI standards [142]. 82 isolates were categorized as non-susceptible and 46 isolates as susceptible to ciprofloxacin. 31 isolates showed a MIC of 2 µg/ml and were therefore classified as intermediate; these isolates and additionally the isolates which are possibly involved in the clonal outbreak were not included in the following studies; summing to 123 isolates (82 resistant and 41 susceptible) which could be used for whole transcriptome comparisons. To test for a group specific accumulation of SNPs, Fisher's exact test was used and differentially expressed genes were identified using Wilcoxon's rank-sum test. In both cases, retrieved P-values were adjusted by the Benjamini-Hochberg correction to control the false-discovery rate.

This transcriptome-wide association study of ciprofloxacin resistant and susceptible isolates for the enrichment of adaptive SNPs revealed four non-synonymous mutations to be significantly enriched in the ciprofloxacin resistant isolates. Besides these four SNPs causing amino acid alterations, 11 synonymous SNPs, which do not change the protein sequence, were also significantly enriched (see Table 3.6 and Figure 3.9). The two non-synonymous mutations which showed the highest significance were located at nucleotide position 2,015,011 in the PA14 reference genome, which corresponds to amino acid position 83 within the DNA-gyrase GyrA (T83I), and nucleotide position 5,845,617 which corresponds to amino acid position 87 within the topoisomerase IV ParC (either S87L or S87W). Out of the 82 resistant isolates, 76 harbored *gyrA* T83I, whereas only five out of the 42 susceptible isolates showed this mutation. The *parC* mutations S87L and S87W were identified in 38 resistant isolates and no susceptible isolate harbored these mutations.

The other two genes with significantly enriched non-synonymous mutations were *kynU* (E115D) and *glmU* (H288R). Both, the kynureninase encoded by *kynU* and *glmU*, encoding a bifunctional uridyltransferase, as well as all genes with synonymous substitutions have not been associated with ciprofloxacin resistance in three previous genome-wide mutagenesis screens of antibiotic resistance determinants in *P. aeruginosa* [133,135,136].

When comparing only highly resistant isolates, which showed a MIC of 8 µg/ml or more, with the susceptible ones, only the mutations of *gyrA* and *parC* were significantly enriched with P-values of 5.59E-13 and 1.51E-5, respectively.

Table 3.6: Significantly enriched SNPs when comparing resistant vs. susceptible isolates

Gene locus	Gene name	Genomic position in PA14	Mutation	P-value
PA14_23260	*gyrA*	2,015,001	C/T (non-syn)	6.62E-05
PA14_59910	-	5,334,364	A/G (syn)	0.0021
PA14_65605	*parC*	5,845,617	G/C,A (non-syn)	0.0024
PA14_37610	*kynU*	3,346,395	A/C (non-syn)	0.0034
PA14_59910	-	5,334,353	T/C (syn)	0.0057
PA14_73220	*glmU*	6,519,825	A/G (syn)	0.0103
PA14_39330	*rbsA*	3,501,621	G/A,C (syn)	0.0117
PA14_50460	*flgD*	4,484,406	C/G,A (syn)	0.0118
PA14_35500	*bkdB*	3,156,528	C/T (syn)	0.0141
intergenic	-	3,621,954	A/G (syn)	00199
PA14_66400	*aefA*	5,924,077	C/T (syn)	0.0330
PA14_07680	*prkA*	661,363	G/A (syn)	0.0359
PA14_39330	*rbsA*	3,501,606	A/G (syn)	0.0362
PA14_73220	*glmU*	6,520,084	T/C (non-syn)	0.0373
PA14_66820	*phaC1*	5,967,799	C/T (syn)	0.0431

syn, synonymous; non-syn, non-synonymous

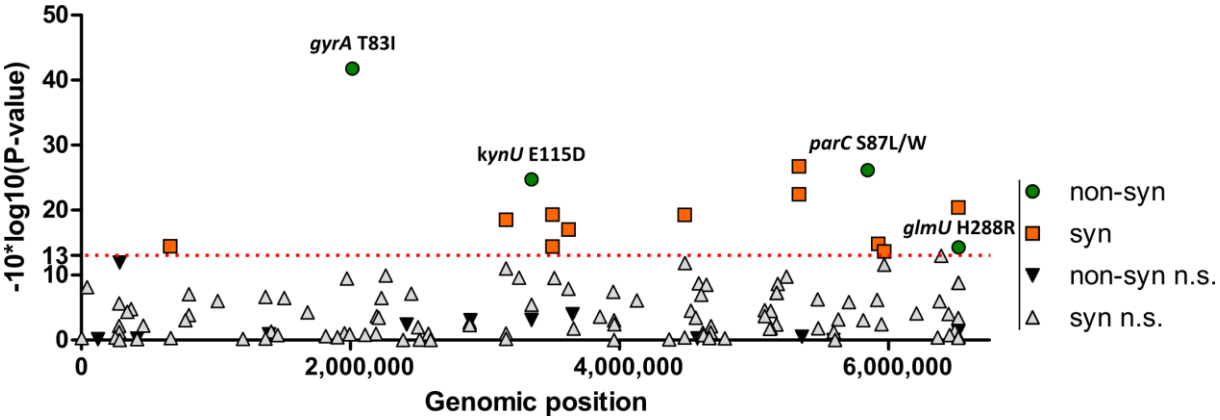

Figure 3.9: Manhattan plot of SNPs associated with ciprofloxacin resistance.

The plot shows the genomic position of the PA14 chromosome on the x-axis and the corresponding P-value of each SNP on the y-axis (indicated as -10*log10[P-value]) when comparing ciprofloxacin resistant (n=82) versus susceptible isolates (n=41). The red dotted line indicates P = 0.05, with genes above having P-values < 0.05. Significantly enriched SNPs are colored according to the legend given on the right.

non-syn, non-synonymous; syn, synonymous; n.s., not significant.

Whereas the transcriptome-wide association study of mutations involved in ciprofloxacin resistance revealed the presence of SNPs in *gyrA* and *parC* as highly significant resistance markers, no differentially expressed genes could be identified in the resistance isolates compared to the susceptible ones (data not shown). Although numerous genes were enriched after using Wilcoxon's rank-sum test to compare the expression of all genes within these two groups, no hits remained significant after applying the Benjamini-Hochberg correction and thus all were regarded as false positive hits.

These findings further highlight the previous results, that ciprofloxacin resistance is predominantly determined by mutations in *gyrA*, especially by the amino acid substitution of threonine to isoleucine at position 83, and the occurrence of secondary mutations at amino acid position 87 in ParC, which further increases the level of resistance.

3.2.7 Comparative analysis of RNA-seq accuracy

To assess the accuracy of RNA-seq concerning gene expression levels and sequence variations, we compared the results obtained here with our previous analyses described in chapter 3.1. 87 out of the 159 clinical isolates which have been studied by RNA-seq were also analyzed previously by Sanger- and pyrosequencing to identify mutations within the QRDRs of *gyrA*, *gyrB*, *parC* and *parE*. The comparison of both results showed a perfect agreement and no inconsistencies between Sanger-/pyrosequencing and RNA-seq were found, revealing a high accuracy of the transcriptomic approach (see supplementary table S2). The only exceptions were the sequences of 17 genes in a total of 13 isolates; in which the sequence coverage of three reads per position could not be achieved and therefore mutations could not be identified. Since samples were pooled for sequencing, a reduction of analyzed samples in a single sequencing run is expected to result in an enhanced sequencing coverage and improved SNP detection.

Additionally to the mutations identified by Sanger- or pyrosequencing, the RNA-seq based approach led to the identification of further amino acid substitutions in *gyrA* (D72E and D87H), *gyrB* (Q467) and *parC* (E91K). The amino acid substitutions D87H in *gyrA* and E91K in *parC* have already been described in previous publications and could be linked to fluoroquinolone resistance in *E. coli* [220] and *P. aeruginosa* [221].

We next examined the accuracy of differential gene expression analysis by RNA-seq by comparing the results with our previous results obtained by qRT-PCRs. The expression of the four membrane fusion protein encoding genes *mexA*, *mexC*, *mexE* and *mexX* has been studied previously in 27 out of these 159 clinical isolates (see chapter 3.1.4) and therefore it was possible to compare the results of RNA-seq and qRT-PCRs. The correlation of fold change values from both methods is depicted in

Figure 3.10. The graph illustrates that determination of gene expression highly correlates between both methods, with a Pearson correlation coefficient of 0.77 over all genes and samples. In addition to the high quantitative correlation, the qualitative comparison of both methods whether an efflux pump was regarded as overexpressed or not, was concordant in 90 out of 107 (> 84 %) possible comparisons (the expression of *mexE* could not be measured in one isolate using qRT-PCR). Both values of quantitative and qualitative correlation are therefore in the same ranges, which have been reported in the literature and this data furthermore indicates the power and accuracy of RNA-seq [222].

However, the graph displays some minor discrepancies between RNA-seq and qRT-PCR in some samples. These discrepancies might be assigned to technical differences between both methods: For instance, qRT-PCR primers were designed based on the PA14 reference sequence and therefore might not bind efficiently when analyzing clinical samples containing possible mismatches in the binding sequence, whereas RNA-seq allows up to one mismatch per sequencing read. A further influencing factor might be a different normalization of these datasets; while qRT-PCRs are analyzed in comparison to the expression of the house-keeping gene *rpoD* using the $\Delta\Delta C_T$ method [162], RNA-seq data is analyzed using DESeq, a method which is based on the negative binomial distribution and therefore does not rely on a single reference gene [175].

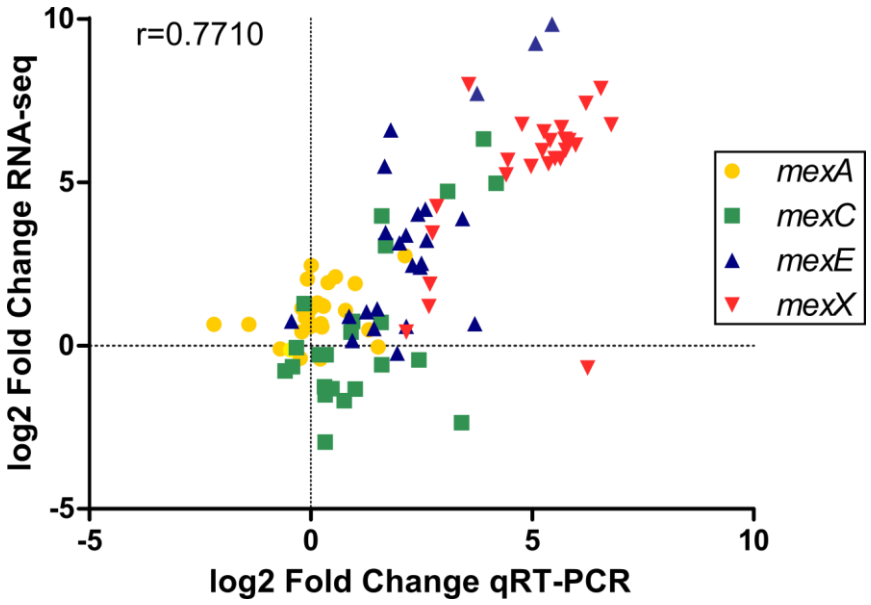

Figure 3.10: Comparison of RNA-seq with qRT-PCR for the expression of the membrane fusion protein encoding genes of the four major RND-efflux pumps

The graph shows the comparison of retrieved RNA-seq expression values versus qRT-PCR values for the four genes *mexA* (yellow), *mexC* (green), *mexE* (blue) and *mexX* (red) in 27 clinical isolates. Fold change expression values are given in comparison to the reference strain PA14. The Pearson correlation coefficient *r* was determined using GraphPad Prism 5.0.

3.3 Transcriptome analysis of clinical *Klebsiella pneumoniae* isolates

In the last years, numerous studies focused on the epidemiology, phylogeny and the genomic structure of *K. pneumoniae* [223], yet little is known about the global transcriptome profile of this important bacterial pathogen. Only a limited number of transcriptional studies on *K. pneumoniae* have been performed so far. However, they deliver valuable and important insights into the transcriptional architecture and regulatory aspects of *K. pneumoniae* [224,225], its adaptation to changing environments [226] and the development colistin resistance [227].

3.3.1 Phylogenetic distribution of *K. pneumoniae* clinical isolates

With the aim to gain detailed insights into the variation of the *K. pneumoniae* transcriptional landscape, we performed deep transcriptome sequencing on 34 clinical isolates. These isolates were sampled from various infection sites like blood, urine, wound- and rectal swabs (see Table 2.3) from out-patients as well as in-patients of ten German hospitals. The median patient's age was 65 years with a range from 20 to 90 years. Additionally to these 34 clinical isolates, the three previously completely sequenced *K. pneumoniae* clinical strains (MGH 78578 [228], JH1 and 1162281 [143]) were also included in this RNA-seq study.

The *K. pneumoniae* isolates were grown under standard laboratory conditions in rich medium at 37 °C until late logarithmic growth phase. After RNA extraction and ribosomal RNA depletion, strand-specific, barcoded transcriptome sequencing [164] was performed on an Illumina HiSeq 2500. This generated a total of 787 million paired-end reads, each with a length of 100 base pairs. Up to 99 % of the reads (13.1 to 36.6 million reads per isolate with a median of 20 million reads, see Table 3.7) could be mapped to a non-redundant *K. pneumoniae* pan-genome. This pan-genome was generated on the basis of publicly available DNA sequence data of 11 *K. pneumoniae* isolates (see chapter 2.9) to gain comprehensive and unbiased insights into the transcriptional landscape of this pathogen.

Since deep transcriptome sequencing delivers not only quantitative data on the gene expression profile but also high quality sequence data of transcribed coding sequences [222], we used the information on cDNA sequence variations among the strains to analyze their phylogenetic relationship. Figure 3.11 depicts the phylogenetic distribution of our set of 37 clinical isolates as well as of the 11 previously completely sequenced reference strains. The tree is based on the complete sequence of 404 genes corresponding to 314,561 nucleotide positions, all of which were covered by at least five sequencing reads in our pool of clinical isolates. Overall 35,796 variable sites were detected among the strains. In addition to this cDNA based phylogenetic reconstruction, we performed multilocus sequence typing (MLST) [186] and *wzi* typing [149] for all isolates (the results are also shown in Figure 3.11). The *Klebsiella* MLST scheme consists of the partial sequences of eight

house-keeping genes: *gapA*, *infB*, *mdh*, *pgi*, *phoE*, *rpoB* and *tonB.* The nucleotide sequences of *gapA*, *infB*, *mdh*, *pgi*, and *rpoB* were extracted from the RNA-seq data. Since the coverage of *phoE* and *tonB* did not match our strict quality criteria, Sanger sequencing was performed for these two genes as already described [186]. The full sequence of the *wzi* gene, encoding the outer membrane protein Wzi, which is involved in cell surface capsule attachment and highly conserved in distinct capsular (K) types [149,229,230], was also sequenced by Sanger sequencing.

Table 3.7: Mapping statistics of *Klebsiella pneumoniae* clinical isolates

isolate	total reads	mapped reads[a)]	isolate	total reads	Mapped reads[a)]
isolate_1_1	19,774,122	98.37 %	isolate_2_10	16,771,836	98.37 %
isolate_1_2	19,997,876	98.40 %	isolate_2_11	25,988,654	98.07 %
isolate_1_3	19,805,660	97.86 %	isolate_2_14	24,699,566	98.26 %
isolate_1_4	19,050,880	98.90 %	isolate_3_3	32,203,450	93.18 %
isolate_1_6	20,013,850	98.94 %	isolate_3_4	36,613,354	94.41 %
isolate_1_8	17,296,248	98.75 %	isolate_3_5	13,488,566	94.35 %
isolate_1_9	21,941,834	98.69 %	isolate_3_6	22,986,806	93.94 %
isolate_1_10	21,271,760	97.63 %	isolate_3_7	20,621,076	95.74 %
isolate_1_11	21,707,348	98.86 %	isolate_3_8	15,656,488	94.32 %
isolate_1_12	24,019,352	98.58 %	isolate_3_10	18,126,752	93.46 %
isolate_1_13	17,915,984	98.70 %	isolate_3_11	20,594,442	92.68 %
isolate_1_14	21,448,234	98.11 %	isolate_3_12	15,275,544	95.81 %
isolate_1_15	19,660,480	98.16 %	isolate_3_13	20,154,768	95.07 %
isolate_1_16	26,170,286	98.21 %	isolate_3_14	13,119,036	97.53 %
isolate_2_2	18,681,538	98.55 %	isolate_3_17	28,967,092	93.52 %
isolate_2_4	23,040,802	98.99 %	MGH 78578	17,899,166	98.05 %
isolate_2_7	15,252,086	98.98 %	JH1	30,738,730	96.55 %
isolate_2_8	19,501,346	98.65 %	1162281	27,353,276	94.82 %
isolate_2_9	19,630,654	98.15 %			

a) Percentage of reads mapping to the non-redundant *K. pneumoniae* transcriptome

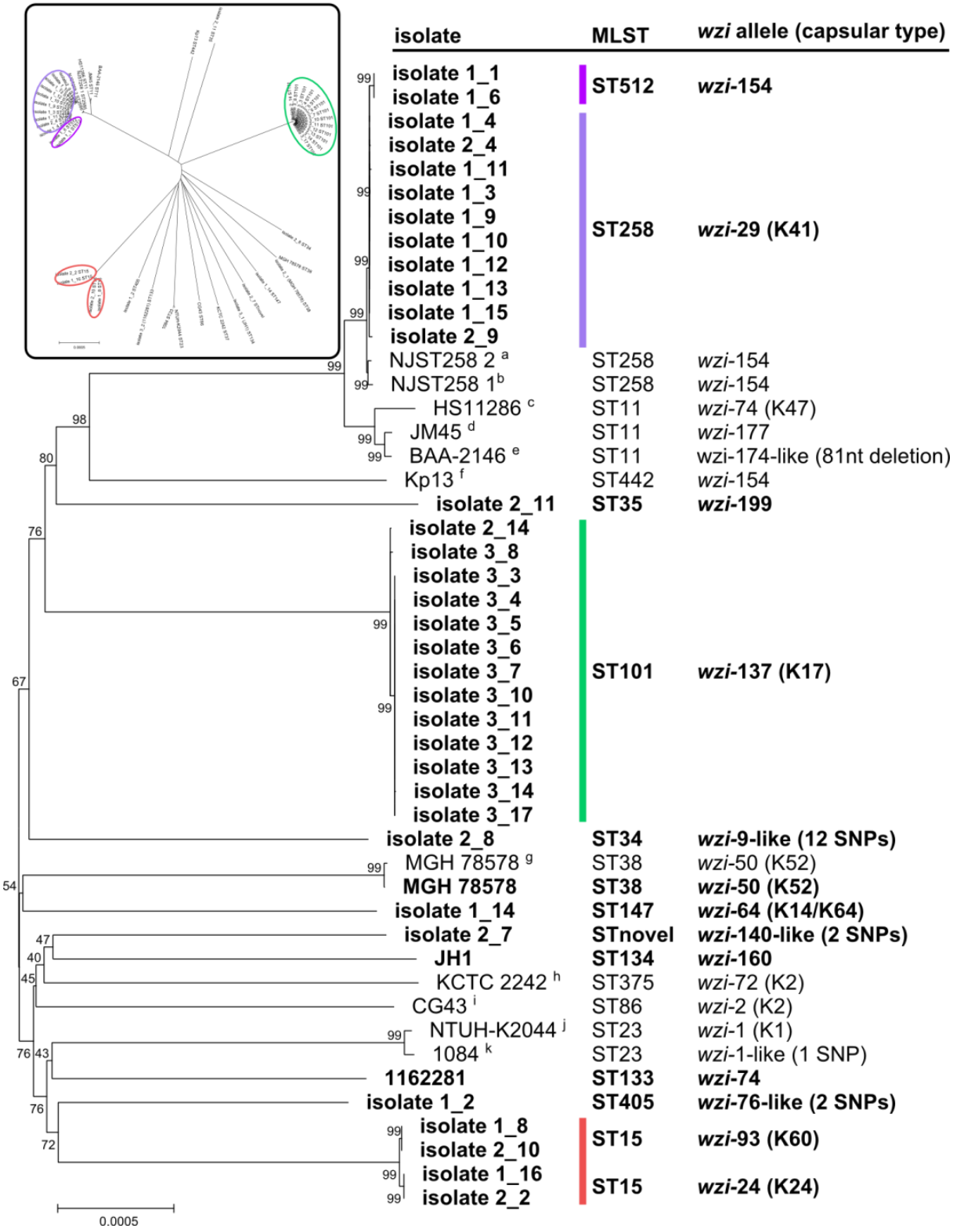

Figure 3.11: Phylogenetic relationship, multilocus sequence types and wzi types of all 37 clinical isolates and 11 reference strains.

The unrooted Neighbor Joining tree was constructed using the aligned sequences of 404 genes which were covered by at least 5 nucleotides at each position in all isolates. Bootstrapping values of 1000 replications are indicated at each branch. MLST and *wzi* type results are also listed for each isolate. *wzi* alleles without perfect matches are indicated by "*wzi*-like" and the nucleotide differences to the closest matching allele are shown in brackets. Isolates included in this study are written in

bold letters and reference genomes are indicated by a – k (see Table 2.7). Isolates belonging to the same MLST sequence type are highlighted in the same color. The scale indicates the number of base substitutions per site. The insert in the upper left corner shows the same tree in a radiation style to demonstrate phylogenetic distances

Our analysis revealed a broad phylogenetic distribution of the *K. pneumoniae* isolates included in this study. We detected 12 different multilocus sequence types (ST), one of which (isolate 2_7, MLST pattern: 2-2-2-1-1-1-91) has not been described before and also 12 different *wzi* types, three of which have not been described yet.

13 of the 37 isolates were of ST101 origin. ST101 isolates are distributed world-wide and are known to carry beta-lactamase OXA-48 and the extended spectrum beta-lactamase CTX-M-15 [231]. Furthermore, they have been reported to be involved in clinical outbreaks in Europe [232,233]. 11 of these 13 ST101 isolates have been isolated from the same hospital within a period of five months. They showed no sequence variation in the phylogenetic analysis indicating that these isolates are likely to have their origin in a single reservoir.

Additionally, we identified ten and two isolates, belonging to the broadly distributed multidrug-resistant high-risk clones ST258 and ST512 [234], respectively. Both sequence types are members of the clonal group CG258, sharing seven out of eight MLST alleles [235]. Isolates of the sequence type 258 are reported to be involved in several European and North American hospital outbreaks [236,237] and are the primary reason for the spread of KPC [234]. Here, the *K. pneumoniae* carbapenemase KPC-2 was identified in all ten ST258 isolates, whereas both ST512 isolates carried KPC-3. Of note, all other 25 sequenced clinical isolates were found to be KPC negative. Recent studies described the heterogeneous nature of ST258 isolates with two large clades ST258 I and ST258 II [172,230,238]. All ST258 isolates of this study were members of clade ST258 I (described as ST258a in [229]) due to the *wzi* allele *wzi*-29 (K41). The two ST512 isolates shared the same *wzi*-154 allele [239] with strains NJST258_1 and NJST258_2 of clade ST258 II and KP13 (ST442), indicating that the ST512 isolates evolved from an ST258 clade II ancestor as suggested previously [230].

Another successful and multidrug-resistant clone is ST15 [240-242]. Our collection contained four isolates of sequence type ST15 which split into two distinct phylogenetic groups based on 9 variable sites within the sequence of the 404 conserved genes. This separation was also supported by *wzi* sequencing, since two isolates (isolate 1_16 and isolate 2_2) shared allele *wzi*-24 (K24) (clade ST15 I) and two isolates (isolate 1_8 and isolate 2_10) shared *wzi*-93 (K60) (clade ST15 II). *wzi*-24 (clade I) has been identified previously in ST15 as well as ST59 isolates [149] and *wzi*-93 (clade II) has been identified in a New Delhi metallo-beta-lactamase positive isolate from Nepal [243]. The fact that within the group of ST15 isolates two different clades exist further illustrates the prominence of the *K. pneumoniae* capsular polysaccharide gene clusters as an evolutionary hotspot. The remaining seven isolates were of diverse phylogenetic origin.

3.3.2 The *K. pneumoniae* pan-genome

K. pneumoniae, like almost all other Gram-negative bacteria, shows a high variation in genome content. The size of the completely sequenced and annotated 11 genomes, which were used as a reference in this study, varies from 5.2 to 6.1 Mbp encoding for 4887 to 5577 genes per genome (see Table 2.7). Thus, in order to map a maximum of RNA sequencing reads from our collection of clinical isolates, we generated a *K. pneumoniae* pan-genome. This pan-genome is based on the 11 *K. pneumoniae* genomes which contain overall 57,312 chromosomal genes, with an average of 5,210 genes per strain. The non-redundant *K. pneumoniae* pan-genome contained 7859 genes (see supplementary table S3). 3336 of those genes were shared by all 11 reference strains ("core-genome") and 4523 genes were absent in at least one of the strains. Among the latter, 1598 genes were identified in only one of the reference genomes ("singletons"). Figure 3.12 depicts the development of the size of the pan-genome, core-genome and singletons by sequentially adding the genomic information of one genome to that of the others.

Based on the averages, it shows an exponential expansion for all 3 groups with the following formulae: pan-genome: $f(x) = 4958.2\ x^{0,1807}$, $R^2=1.0$; core-genome: $f(x) = 4891.5\ x^{-0,16}$, $R^2=0.998$ and singletons: $f(x) = 1135.7\ x^{0,1481}$, $R^2=0.996$). With x representing the number of completely sequenced genomes. Based on this extrapolated data, it is expected that the size of these groups would change by less than 2 % if genomic information of another genome would be added, less than 1 % by adding information of 20 genomes, and less than 0.5 % by adding 40 genomes in total.

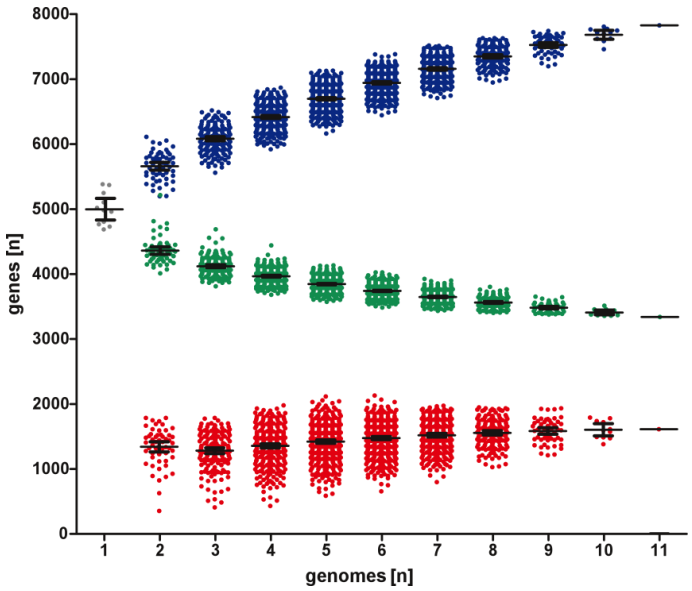

Figure 3.12: Analysis of the *Klebsiella pneumoniae* genomic content.

The amount of genes belonging to the pan-genome (blue dots) core genome (green dots) and unique genes (red dots) is plotted as a function of genomes sequentially added in all possible combinations. The number of genes in the single genomes is shown as gray dots. Black bars show mean with 95 % confidence intervals.

To further explore the genomic content of the pan-genome, we extracted for each gene the gene ontology (GO) information and simultaneously deduced the gene function using the COG database [244], where possible. As expected, the GO term analysis revealed an enrichment of house-keeping genes in the core-genome, which are essential to maintain cellular function and integrity (see Figure 3.13).

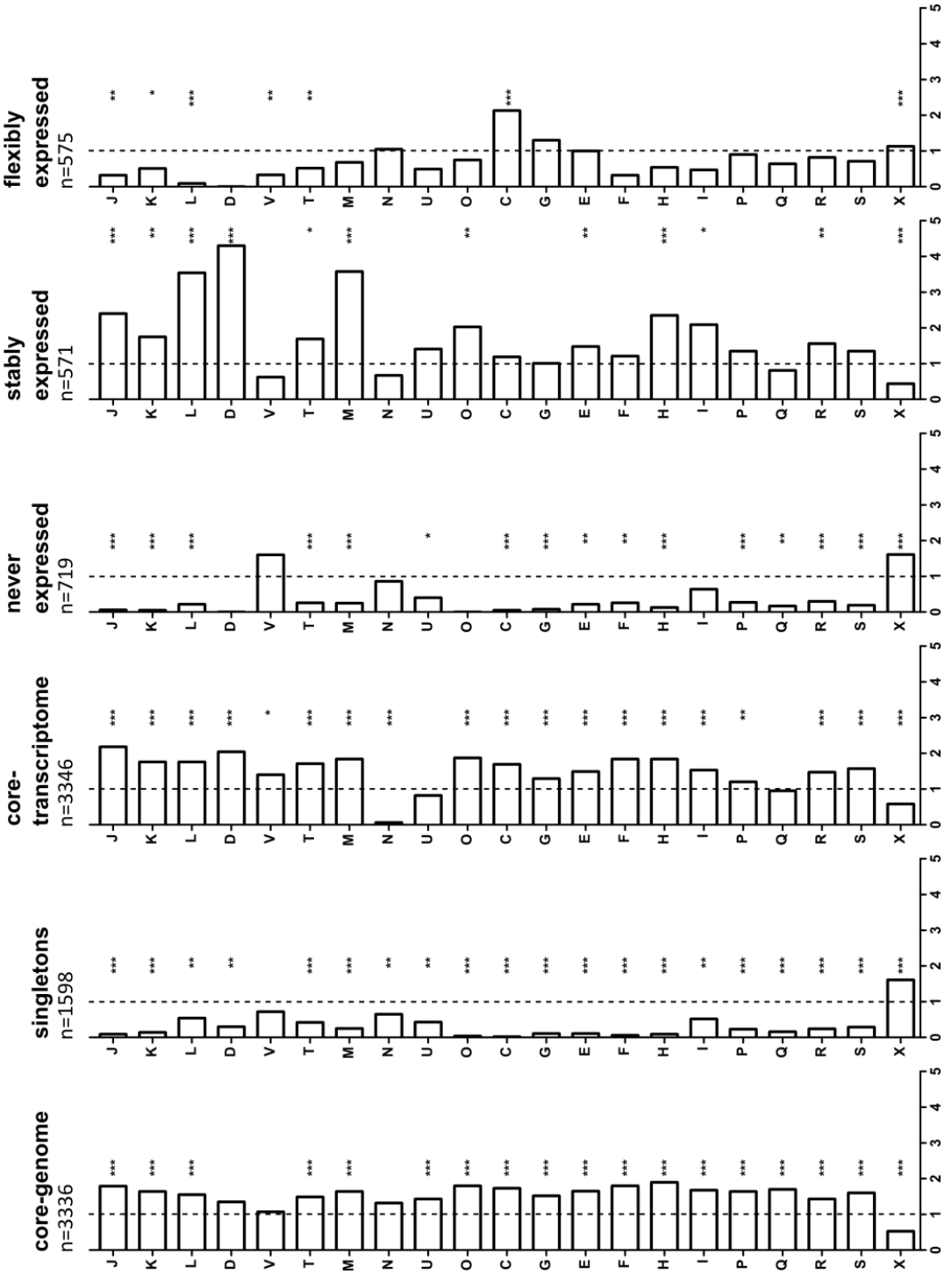

Figure 3.13: Functional annotation and analysis of different sets of genes.

This bar chart shows the relative enrichment of each functional category of genes within the core-genome, singletons, core-transcriptome, as well as never, stably and flexibly expressed genes in comparison to the pan-genome (dashed line).

Functional annotation was extracted from the COG database. The level of significance is indicated by asterisks with * < 0.05; ** < 0.01; *** < 0.001; hypergeometric test and Benjamini-Hochberg correction.

Functional categories are:

J	Translation, ribosomal structure and biogenesis	C	Energy production and conversion
K	Transcription	G	Carbohydrate transport and metabolism
L	Replication, recombination and repair	E	Amino acid transport and metabolism
D	Cell cycle control, cell division, chromosome partitioning	F	Nucleotide transport and metabolism
V	Defense mechanisms	H	Coenzyme transport and metabolism
T	Signal transduction mechanisms	I	Lipid transport and metabolism
M	Cell wall/membrane/envelope biogenesis	P	Inorganic ion transport and metabolism
N	Cell motility	Q	Secondary metabolites biosynthesis, transport and catabolism
U	Intracellular trafficking, secretion, and vesicular transport	R	General function prediction only
O	Posttranslational modification, protein turnover, chaperones	S	Function unknown
		X	not annotated

3.3.3 The *K. pneumoniae* transcriptional landscape

The distribution of normalized reads per kilo base (nRPK) [164], after mapping all RNA sequencing reads against the non-redundant *K. pneumoniae* pan-genome, was found to be continuous and unimodal (see Figure 3.14), with a median nRPK of 4.22 and a maximum of 24.01. Depending on the isolate, between 4744 and 5378 genes exhibited an expression value above the sensitivity limit of 2.20 nRPK (see chapter 2.10.1 for definition), thus demonstrating a very high number of transcribed genes per isolate under the chosen conditions. Of all 7859 genes in the pan-genome, we identified a large set of 3346 genes to be commonly expressed in all isolates above the threshold level. This core-transcriptome (highlighted in green in Figure 3.14B) accounted for 62 % to 71 % of all transcribed genes within one isolate and largely overlapped with the core-genome (2515 genes or 75 % of the core-genome was commonly transcribed). Due to this large overlap between core-genome and core-transcriptome, it was not surprising that the core-transcriptome likewise consisted mostly of genes with house-keeping functions, as revealed by a GO term enrichment analysis (Figure 3.13).

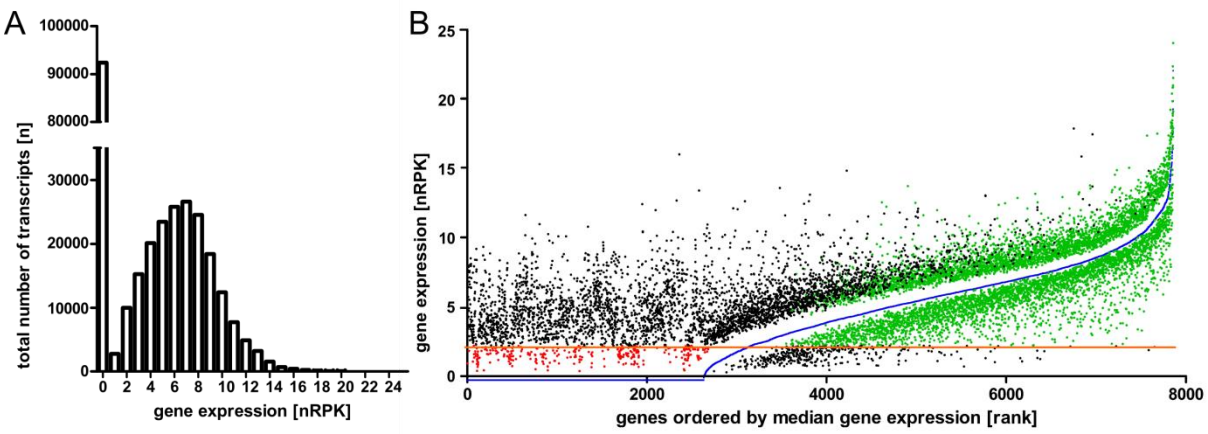

Figure 3.14: The *Klebsiella pneumoniae* transcriptional landscape.

A: Histogram showing the expression in nRPK of all 7859 genes in the pan-genome over all 37 isolates.

B: Expression levels of all genes in the *K. pneumoniae* pan-genome. The median, maximal and minimal expression value (in nRPK) of each gene is plotted. Genes are ranked according to their median gene expression on the x-axis (blue line). The yellow line denotes the expression sensitivity limit ($nRPK_0$=2.20). All genes with a maximal expression value below the sensitivity limit are regarded as never expressed under the given growth conditions and highlighted in red (n=719). All genes with a minimal gene expression value above the sensitivity limit are regarded as expressed in every isolate (core-transcriptome, n = 3346) and are highlighted in green.

On the other end of the scale we found 719 genes within the pan-genome that exhibited maximal expression values below the sensitivity limit (highlighted in red in Figure 3.14B). Those genes were not expressed in any clinical isolate under standard laboratory conditions. Interestingly, only eight of them belonged to the core-genome, whereas 473 (almost 66 %) of these never expressed genes were singletons and occurred only in single reference genomes.

With the aim to map RNA sequencing reads also to potentially non-chromosomally encoded genes, we performed a *de novo* assembly of all reads from the 37 isolates that did not map to the reference pan-genome. We found a total of 1482 genes with an average of 251 genes per isolate and a range from 57 to 419 that did not map to our reference pan-genome. 1258 (85 %) of these genes had homologs with at least 80 % sequence identity to genes that have been previously identified in *Klebsiella spp.*. 150 of the remaining 187 genes had homologs in other members of the Enterobacteriaceae family. While the majority of 60 % (900 out of 1486 genes) was encoding for hypothetical (including putative and predicted) proteins, many genes were found to be related to antibiotic and metal resistance, integrase/transposase, phage-related and involved in plasmid integrity. The complete list of genes potentially encoded on plasmids, integrons or other mobile elements is shown in supplementary table S4.

3.3.4 The *K. pneumoniae* gene expression variance

To gain further insights into the expression variance, we calculated the differential expression of each gene in any possible pairwise comparison of two of the 37 isolates (overall 666 comparisons). Pairwise gene comparison data were considered only if a gene in both isolates reached expression values above the sensitivity limit of 2.20 nRPK. The expression variance of one gene was defined as the fraction (between 0 and 1) of pairwise comparisons showing at least a two-fold differential expression as determined by DESeq [175]. Thus, for example, an expression variance of 0.1 means that 10% of the pairwise comparisons showed at least a two-fold difference in expression values. We obtained information about the expression variance of overall 5696 genes. Ribosomal RNA coding genes were excluded from this analysis due to the influence of rRNA removal during Illumina library preparation.

571 genes were found to be very stably expressed with an expression variance of 0.1 or less (see supplementary table S3). These included 28 genes which were never differentially expressed according to the DESeq analysis. On the other hand, 575 genes exhibited large gene expression variance, between 0.58 and 0.83. A GO term analysis (Figure 3.13) revealed enrichment of genes involved in translation, replication, cell cycle control, cell wall synthesis and coenzyme transport in the most stably expressed genes; whereas only genes involved in the class of energy production and conservation were highly enriched in the set of variably expressed genes. The stably expressed genes were slightly, but significantly higher expressed (average nRPK value of 6.82) compared to the variably expressed genes (average nRPK value of 6.05; two-tailed Student's t-test, P-value < 0.001). The core-transcriptome exhibited significantly lower expression variance (0.31) as compared to the set of genes that did not belong to the core-transcriptome (0.41); two-tailed Student's t-test, P-value < 0.001. Figure 3.15 shows a scatter plot of the expression variance of the core-transcriptome as compared to the individual minimal (gray dots) and maximal (black dots) gene expression values. We observed a rather homogenous expression pattern across the core-transcriptome with a smoothly increasing difference between the average minimal (bottom line) and maximal (top line) gene expression. The maximal gene expression correlated positively with the increasing expression variance. This was even more pronounced in the set of genes not belonging to the core-transcriptome (not shown).

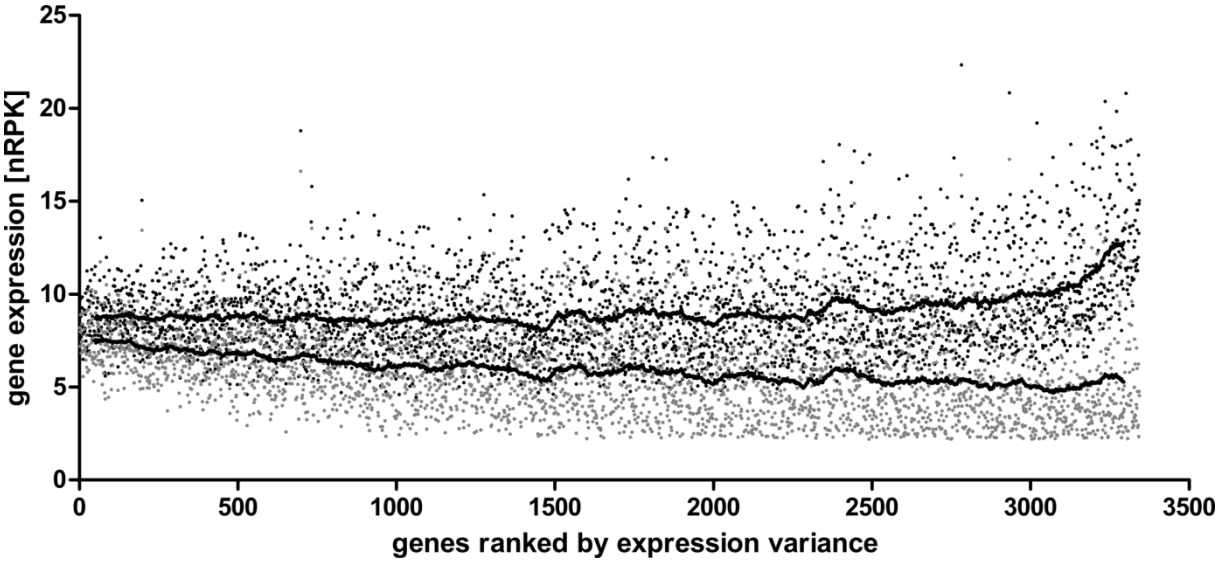

Figure 3.15: Expression variance of the core-transcriptome.

Black and gray dots show the maximal and minimal expression of all genes of the core-transcriptome (n=3346), respectively. Black lines show the moving average of minimal and maximal gene expression of 100 genes, respectively. The genes are ranked from left to right according to increasing values of their overall expression variance

3.3.5 Correlation between phylogenetic background and the core transcriptional profile

We next assessed whether and how the genetic background of the various clinical isolates impacts on global gene expression profiles. We performed a hierarchical clustering of all 37 *K. pneumoniae* isolates according to the overall similarity of the expression profile of all 7859 genes in the pan-genome (Figure 3.16A). Hierarchical clustering revealed three major sub-groups: the first included the two ST512 isolates together with all ten ST258 isolates, the second group included all except one ST101 isolates and the third group included the four ST15 isolates together with various other sequence types. A principal component analysis (PCA) (Figure 3.16C) also demonstrates a clear separation of the transcriptional profiles of all major phylogenetic linages within our set of isolates. This clustering might have been expected since the genomic composition i.e. the presence of distinct sets of accessory genes of the various MLST sequence types strongly influences the clustering.

To exclude the impact of the transcription of accessory genes, we next analyzed the clustering of the 37 clinical isolates based on variations within genes of the core-transcriptome. Remarkably, clustering of the expression profiles based solely on the core-transcriptome (Figure 3.16B) still revealed concordance with the phylogenetic clustering. Although the separation into distinct phylogenetic groups - becoming especially apparent in the PCA (Figure 3.16D) - was not as strong as observed for the hierarchical clustering based on the pan-genome, the phylogenetic groups could be clearly separated.

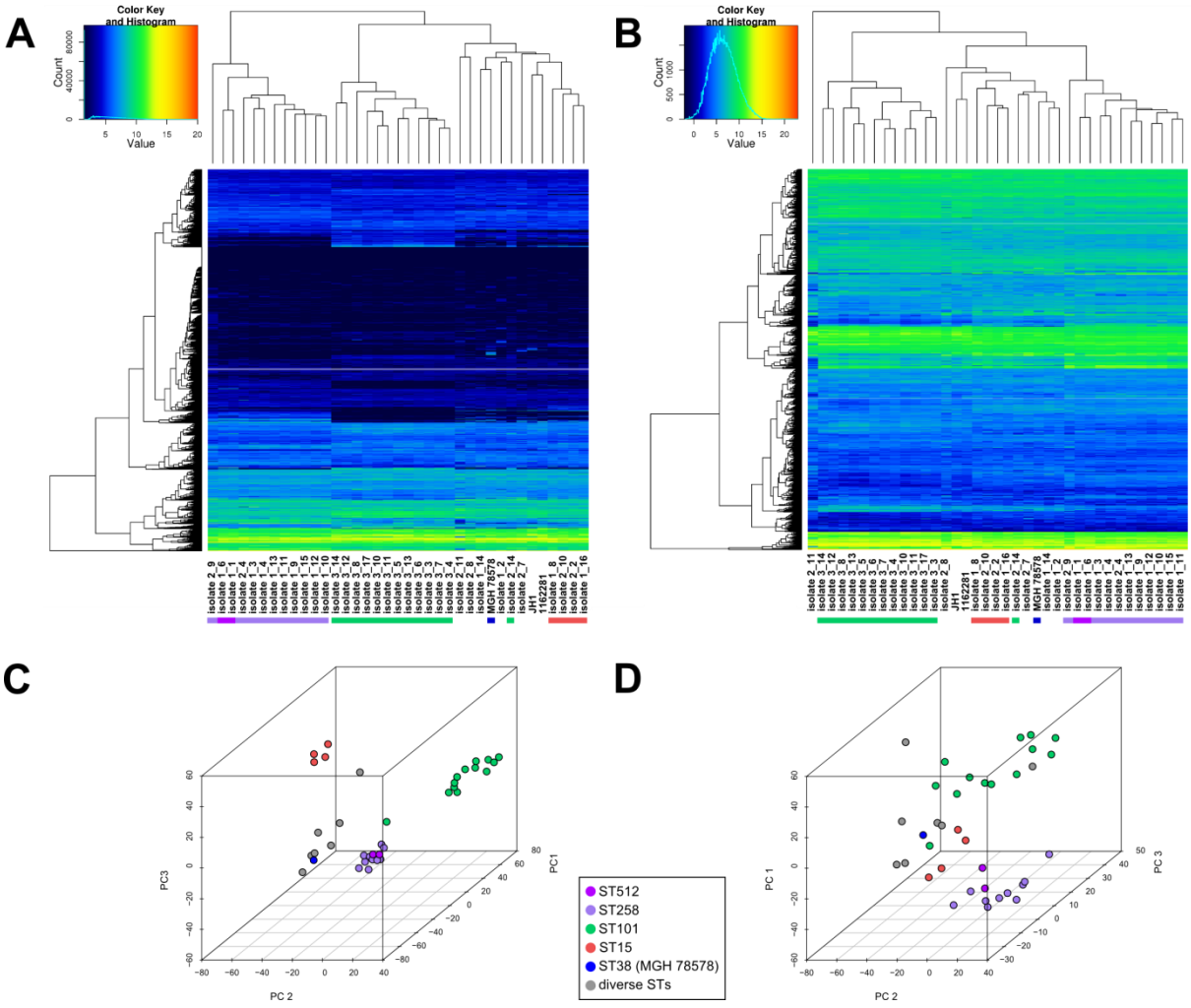

Figure 3.16: Phylogenetic relationship is reflected in the core-transcriptome.

The heat maps show the expression of the pan-genome (A) and core-transcriptome (B), respectively. Genes (vertical) are hierarchically clustered using Pearson correlation distances, and the isolates (horizontal) are clustered according to their Spearman rank correlation. The same datasets are shown in C and D as 3D principal component analyses. Sequence types are highlighted by colors: ST512 (magenta), ST258 (purple), ST101 (green), ST15 (orange) and ST38 (MGH 78578) (blue).

3.3.6 Virulence of *K. pneumoniae* in *Galleria* wax moth larvae is independent of the phylogenetic background

Since the overall expression profiles of the core-transcriptome seemed to be associated with a distinct *K. pneumoniae* sequence type, we wondered whether this global expression profile determines bacterial behavior which might contribute to the success of global clonal lineages. The larvae of the greater wax moth *Galleria mellonella* are widely used as a model to study the virulence of pathogens [153,245,246], including *K. pneumoniae* [150,239,247,248]. Here, we used the

G. mellonella infection model to test the virulence of the various isolates. Healthy *G. mellonella* larvae were injected with an average dose of 7.5 x 105 CFU *K. pneumoniae* and the larval survival was monitored for 72 hours at 37 °C (see Figure 3.17 and Table 3.8). Virulence differed greatly not only among the various MLST groups but also within them. Furthermore, isolates with the same capsular type, which was previously shown to play an important role in *K. pneumoniae* virulence [249], did not exhibit similar virulence profiles. Our data indicate that virulence-associated traits are independent from the phylogenetic background, and therefore are rather isolate specific.

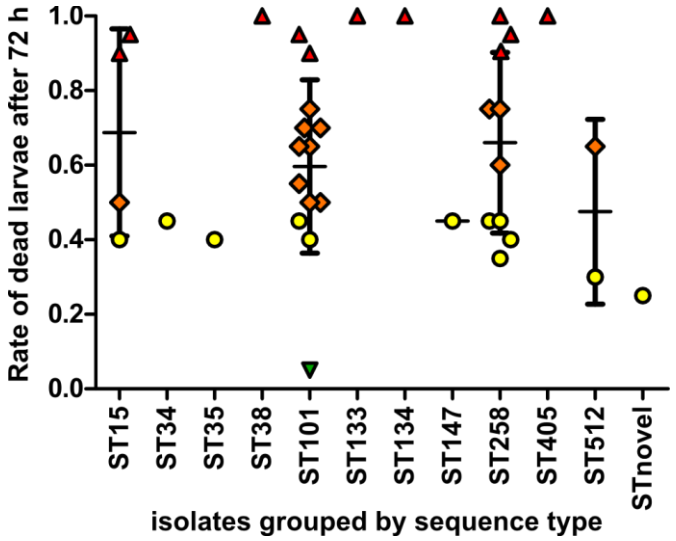

Figure 3.17: Galleria survival assay.

The graph shows the rate of dead larvae 72 hours post infection. Diamonds represent the mean of duplicate experiments with 10 larvae each. They are colored according to increasing rates of dead larvae (green ≤ 0.1; yellow <0.5; orange < 0.9 and red ≥ 0.9). Horizontal and vertical bars indicate mean and standard deviation of each phylogenetic group, respectively.

We found one isolate (isolate 3_8 of ST101) that exhibited a very low virulence. When we analyzed the growth behavior of all isolates in rich medium and in minimal medium supplemented with two different carbon sources (glucose and mannose, respectively; Table 3.8), this isolate exhibited a severe growth defect, which might explain its low virulence potential [239]. For all other isolates there was no correlation between growth and pathogenicity.

Table 3.8: Growth parameters in different media.

Isolate	Sequence type	surviving larvae after 72h	LB			BM2+glucose			BM2+mannitol		
			doubling time[a]	+/-	OD_{600} max	doubling time	+/-	OD_{600} max	doubling time	+/-	OD_{600} max
1_1	512	70 %	24.30	0.29	2.33	35.50	0.31	1.70	43.90	0.28	1.45
1_2	405	0 %	22.10	0.36	2.78	35.50	0.65	2.33	41.80	0.36	1.93
1_3	258	5 %	25.90	0.22	2.42	39.20	0.28	2.32	43.30	0.34	1.44
1_4	258	10 %	27.10	0.32	2.52	39.80	0.33	2.43	44.50	0.50	1.73
1_6	512	35 %	24.90	0.46	2.36	32.20	0.40	2.21	38.30	0.34	1.76
1_8	15	10 %	20.80	0.24	2.41	35.30	0.44	2.25	40.90	0.34	1.48
1_9	258	65 %	22.60	0.21	2.57	35.20	0.29	2.32	45.20	0.64	1.27
1_10	258	40 %	22.90	0.12	2.59	35.40	0.21	2.44	42.70	0.32	1.95
1_11	258	55 %	22.60	0.12	2.54	37.50	0.24	2.39	44.30	0.42	1.73
1_12	258	60 %	22.10	0.12	2.53	35.00	0.25	2.28	43.00	0.61	1.73
1_13	258	55 %	21.30	0.13	2.63	36.00	0.42	2.32	42.50	0.40	2.00
1_14	147	55 %	22.50	0.30	2.74	41.00	0.36	2.39	44.80	0.61	2.09
1_15	258	25 %	22.00	0.20	2.59	38.80	0.40	2.29	45.40	0.47	1.37
1_16	15	5 %	21.80	0.05	2.66	33.40	0.48	2.42	40.10	0.45	2.13
2_2	15	50 %	23.50	0.39	2.95	30.80	0.48	2.49	45.60	0.80	1.98
2_4	258	25 %	21.90	0.09	2.63	36.90	0.35	2.47	45.70	0.61	2.06
2_7	novel	75 %	22.40	0.21	2.77	38.10	0.14	2.24	42.30	0.20	1.81
2_8	34	55 %	22.30	0.25	2.69	38.50	0.36	2.35	44.00	0.69	1.35
2_9	258	0 %	21.30	0.19	2.69	36.30	0.30	2.24	41.70	0.57	1.40
2_10	15	60 %	19.60	0.56	3.19	44.10	0.49	2.22	41.60	0.49	1.89
2_11	35	60 %	21.00	0.41	2.74	36.30	0.80	2.31	42.40	0.78	1.87
2_14	101	45 %	22.80	0.46	2.67	37.40	0.56	2.26	42.90	0.41	1.75
3_3	101	50 %	22.50	0.42	2.70	39.20	0.48	2.18	42.90	0.68	1.84
3_4	101	30 %	22.70	0.47	2.78	36.80	0.45	2.20	42.80	0.63	1.89
3_5	101	10 %	22.60	0.44	2.75	34.40	0.38	2.16	39.90	0.53	1.80
3_6	101	30 %	23.00	0.52	2.76	35.60	0.42	2.23	41.80	0.69	1.89
3_7	101	35 %	23.00	0.38	2.75	35.60	0.39	2.18	44.70	0.58	1.90
3_8	101	95 %	24.10	0.17	2.42	38.30	0.31	1.11	44.60	0.50	1.03
3_10	101	50 %	22.20	0.46	2.73	34.80	0.40	2.15	39.00	0.57	1.78
3_11	101	60 %	22.30	0.46	2.73	35.10	0.36	2.15	40.30	0.49	1.80
3_12	101	25%	21.80	0.33	2.72	36.10	0.37	2.17	42.50	0.68	1.90
3_13	101	35 %	23.20	0.33	2.67	34.70	0.43	2.18	42.60	0.62	1.86
3_14	101	55 %	22.60	0.30	2.70	36.40	0.43	2.13	41.60	0.60	1.79
3_17	101	5 %	25.50	0.38	2.71	36.80	0.46	2.08	39.90	0.52	1.67
MGH 78578	38	0 %	23.30	0.52	2.76	44.70	0.44	2.19	57.40	0.33	1.92
JH1	134	0 %	22.20	0.39	2.67	35.80	0.38	1.94	50.70	0.37	1.48
1162281	133	0 %	22.10	0.27	2.30	34.40	0.28	2.06	40.10	0.65	1.77

a) Doubling time in min

To identify possible virulence-associated genetic determinants, the transcriptomes of 11 highly virulent isolates (≥ 90 % dead larvae after 72 hours, red diamonds in Figure 3.17) were compared with 12 lowly virulent isolates (between 10 % and 50 % dead larvae, yellow diamonds in Figure 3.17) and searched for differentially transcribed genes within these two subsets. However, we could not identify any statistically significant differences in gene expression profiles (data not shown).

Since virulence among the isolates could also be variable due to the presence of accessory genes on plasmids or integrons acquired by horizontal gene transfer [250], all reads that did not map to the *K. pneumoniae* pan-genome were extracted. A comparison of these accessory transcriptomes to the virulence factor data base (VFDB) [176] revealed the presence of several virulence-associated genes in the two sets of isolates (see supplementary table S5) but none of these were significantly enriched in the group of highly virulent isolates versus the lowly virulent ones.

3.3.7 ST258 isolates produce significantly less biofilm as compared to other MLST sequence types

In addition to virulence, the capability to form biofilms is a clinically relevant bacterial phenotype. We next analyzed the capability of each clinical isolate to produce biofilms by the use of a crystal violet assay (Figure 3.18A). Interestingly, as opposed to the virulence phenotype, the capability to produce biofilms seemed to be associated with the affiliation to a specific sequence type (Figure 3.18B). As shown previously [156], biofilm formation was significantly lower in ST258 isolates as compared to other isolates, with a median OD_{590} of 0.06 versus 0.28 for all other isolates, respectively (two-tailed Student's t-test, P-value < 0.01). The isolate with the highest absorbance in the crystal violet assay was the one isolate of ST101 (isolate 3_8) that already exhibited a non-virulent phenotype in the *Galleria* assay and showed a severe growth defect in minimal media. Among all other isolates, growth was not associated with high or low biofilm formation.

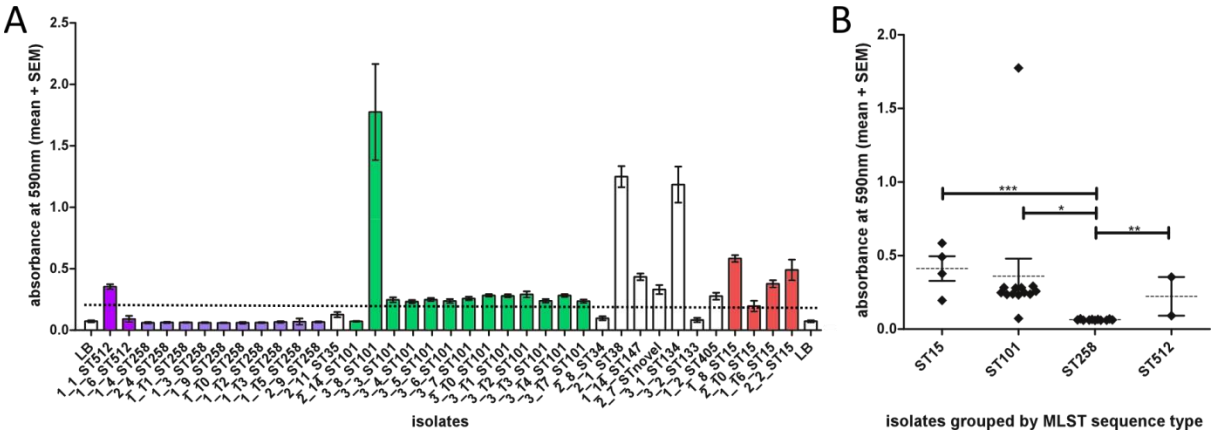

Figure 3.18: Quantitative analysis of biofilm formation by *K. pneumoniae* clinical isolates.

A: The raw absorbance at 590 nm of 8 replicate measurements with standard error of the mean (SEM). Isolate are arranged according to their MLST sequence type. The dashed line shows the separation into high and low biofilm producing isolates (which corresponds to three times the medium control (absorbance at 590nm = 0.187)).
B: Differences in biofilm formation as determined by crystal violet staining between groups of isolates belonging to the same MLST type were analyzed using two-tailed Student's t-test.

We classified the clinical isolates according to their ability to form biofilm into high producers (OD_{590} > 0.187, 11 isolates (all but one ST101 isolate were not included due to their probable clonal nature)) and low producers (OD_{590} < 0.187, 15 isolates) and analyzed whether we can detect group specific gene expression profiles using Wilcoxon's rank-sum test. Retrieved P-values were furthermore adjusted by the Benjamini-Hochberg correction to control the false-discovery rate.

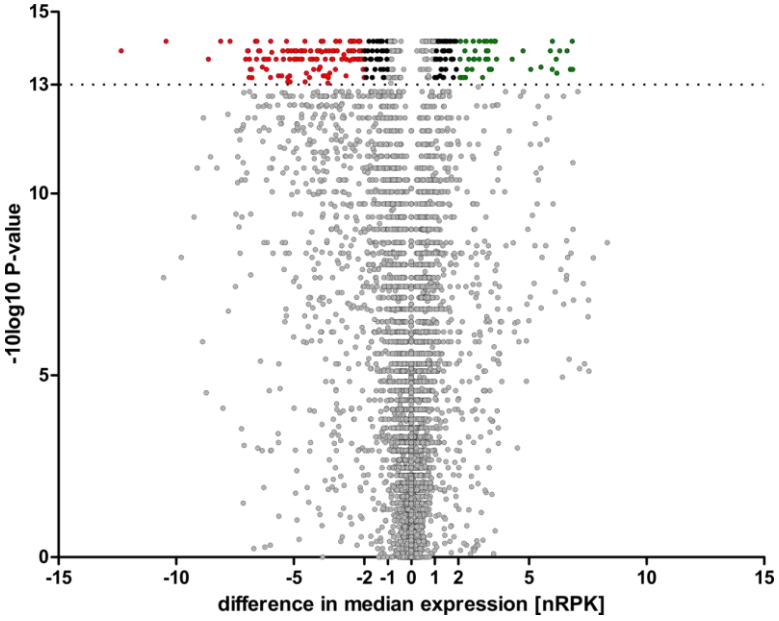

Figure 3.19: Transcriptome-wide association of genes involved in biofilm formation.
Volcano plot showing differentially expressed genes in biofilm forming isolates compared to non-biofilm forming isolates. Colored dots indicate genes that display large differences in their median gene expression (x-axis) as well as high statistical significance (-log10 of P-value, y-axis) with red and green indicating a fold change of ≥ 4 (nRPK of 2), respectively and black having a fold-change of ≥ 2 (nRPK of 1). Genes which are statistically not significantly expressed or having a fold-change less than 2 are shown in gray. The dotted line indicates P = 0.05, with genes above having P-values < 0.05.

In this transcriptome-wide association study, we could identify a total of 165 genes whose expression was significantly different in the high biofilm forming group as compared to the low biofilm forming group (Figure 3.19). Out of these 159 genes, 46 genes were more than 4-fold upregulated in biofilm forming isolates (indicated as green dots in Figure 3.19) and 38 genes were upregulated on intermediate levels between 2- and 4-fold (black dots). The list of 46 genes which were at least 4-fold higher expressed (Figure 3.19 and Table 3.9) included *mrkA,* encoding the major pilin subunit of type

3 fimbriae [251], which has been shown previously to be crucial for binding to abiotic surfaces [252]. The remaining genes of the *mrk* operon, *mrkB* to *mrkF,* were also found to be higher expressed, although with a corrected P-value higher than 0.05. MrkB, MrkC and MrkF are chaperones, outer membrane usher and minor pilin subunit, respectively [253]. MrkD is the adhesive subunit of type 3 fimbriae and has been shown to facilitate binding to extracellular matrix proteins [254]. Another fimbrial cluster of three genes (D364_17530, D364_17540 and D364_17550) from a fimbria coding operon of *K. pneumoniae* CG43 was also significantly higher expressed in the biofilm forming isolates. Besides fimbrial genes, the genes *acsA*, *bcsB* and *bcsC* were identified to be higher expressed. They all are involved in cellulose synthesis, an extracellular polysaccharide found in bacterial biofilms [255]. It has been shown that the cellulose synthase BcsB is activated via cyclic di-GMP [256], a bacterial second messenger well known for its control of biofilm formation [257]. Another operon which was higher expressed was the fumarat reductase operon. Although, only *frdD* is listed in Table 3.9, *frdA, frdB* and *frdC* were also expressed on higher levels, but just below our strict threshold of a median difference by at least 2 nRPK (indicating a 4-fold stronger expression). It has been shown that inhibition of the fumarate reductase in *Porphyromonas gingivalis* significantly inhibited biofilm formation [258]. Furthermore, the outer membrane protein *ompW* was expressed at higher levels in the biofilm forming isolates. It has been shown previously that the *ompW* homolog in *P. aeruginosa oprG* is highly expressed in biofilms [259] and an *oprG* deletion mutant produced lower biofilm volumes as compared to the wild-type [260]. Figure 3.20 depicts the gene expression profile of the clinical isolates for the 46 genes found to be higher expressed in the biofilm-proficient isolates. Clearly, a reduced expression of the majority of these genes became apparent within the low biofilm producing ST258 isolates.

Table 3.9: List of genes being highly expressed in biofilm forming isolates

gene_name / locus	dnRPK	gene_name / locus	dnRPK
bcsB	2.66	A79E_2827	3.62
bcsC	2.67	A79E_2841	3.03
A79E_0470	5.91	*ompW* (*yciD*)	3.26
A79E_0471	6.76	A79E_3106	3.57
A79E_0472	2.58	*dmsA*	2.07
ttdA	3.40	A79E_4441	6.15
ttdB	2.27	*ulaC* (*ptxA*)	2.30
A79E_0491	2.09	*ulaB* (*sgaB*)	2.36
mrkA	6.00	*frdD*	2.21
dalT	2.31	D364_02760	6.30
A79E_2240	3.19	D364_02765	6.86
A79E_2397	4.75	D364_17515	5.08
A79E_2413	6.18	D364_17530	2.71
A79E_2451	5.51	D364_17540	3.26
A79E_2489	2.12	D364_17550	6.62
A79E_2492	2.07	*acsA*	2.89
A79E_2600	3.31	KP13_01340	4.29
A79E_2740	2.63	KP13_04177	6.84
A79E_2741	3.16	KP13_32375	2.45
astB	3.38	KPN2242_20090	5.99
astD	3.10	KPN_01389	2.37
A79E_2744	3.20	KPN_01390	3.36
astC	2.88	KPN_01391	3.52

d-nRPK: Difference in nRPK between the groups of high and low biofilm forming isolates

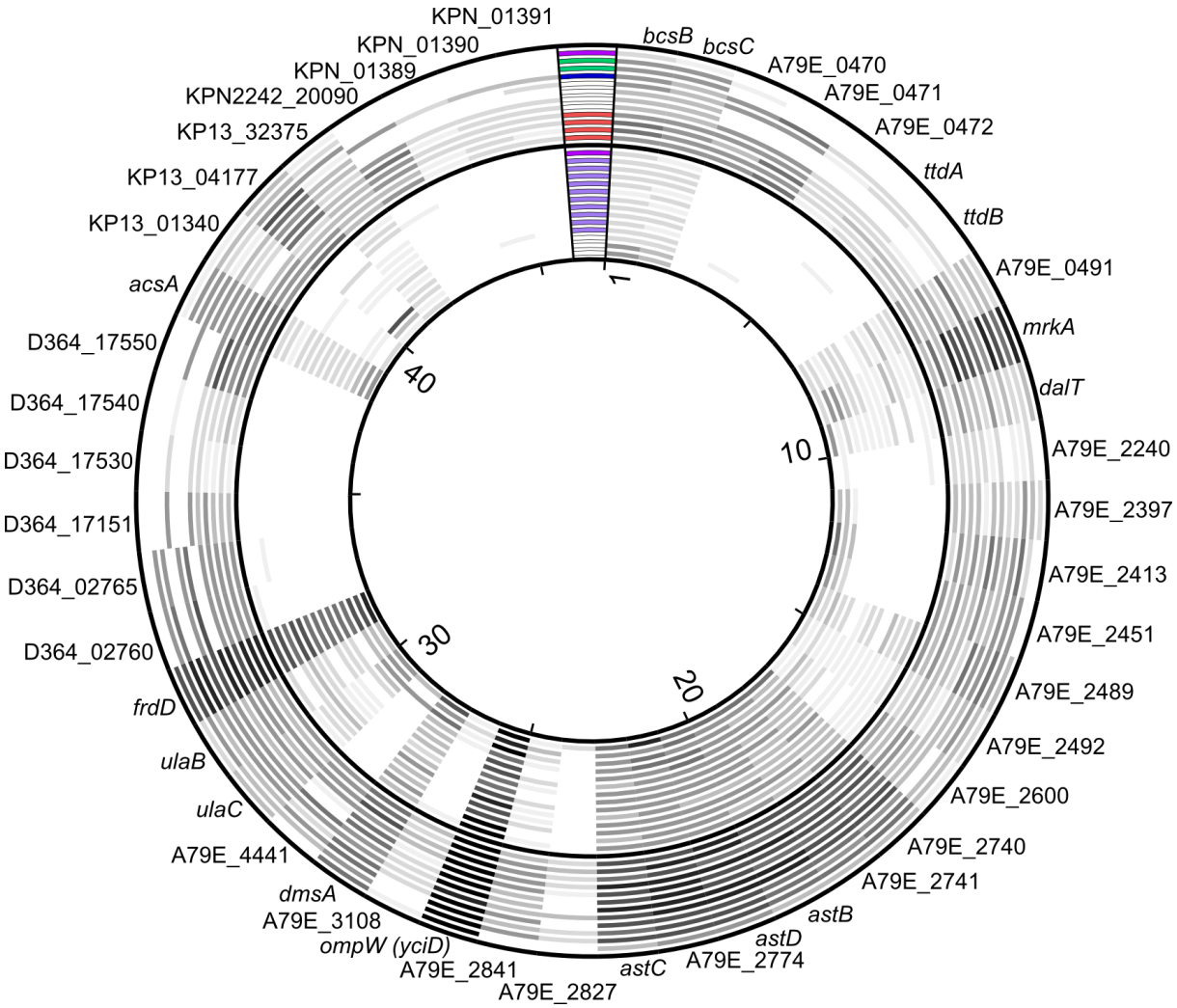

Figure 3.20: Differences in gene expression between high and low biofilm forming isolates

The circular plot shows the normalized read counts (in nRPK) of all genes which were identified to be highly expressed in biofilm forming *K. pneumoniae* isolates. Expression varies from 13 nRPK (dark gray) to 0 nRPK (white). All 46 genes are labeled on the outside. Isolates are represented as rings and are arranged according to their biofilm phenotype. The 12 high biofilm forming isolates are shown in the outer rings, followed by the 14 low biofilm forming isolates in the inner rings. The MLST type is indicated as colored segments: ST512 (magenta), ST258 (purple), ST101 (green), ST15 (orange) and ST38 (MGH 78578) (blue).

3.4 Overview of antibiotic resistance determinants in *K. pneumoniae* clinical isolates

The antibiotic susceptibility profile of each isolate (see Table 2.3 and Table 2.4) was determined using the automated Vitek2 system (bioMérieux) and according to CLSI antibiotic resistance breakpoints [142], most of the isolates were categorized as multidrug-resistant (resistant to three or more antimicrobial classes) [213] with the highest rate of resistance to penicillin and fluoroquinolone antibiotics (see Figure 3.21). The collection included also two isolates which were susceptible to all antibiotics with the only exception of ampicillin.

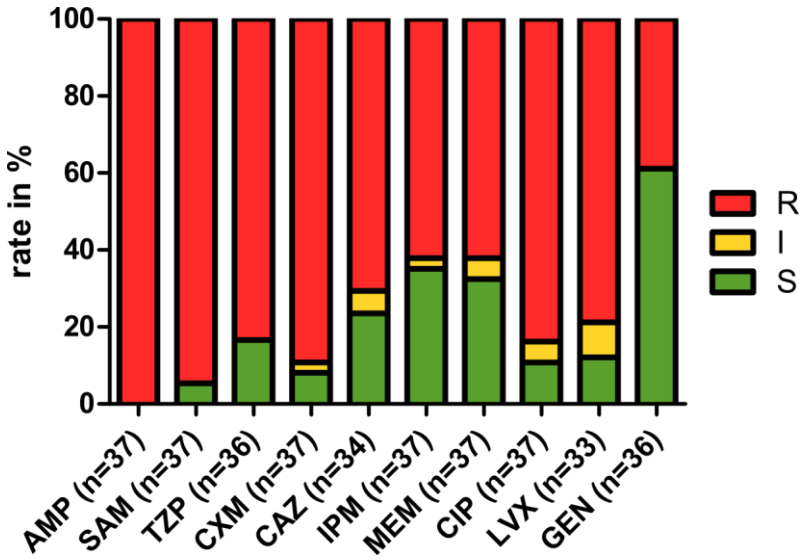

Figure 3.21: Antibiotic resistance in the clinical *K. pneumoniae* isolates

The figure shows the percentage of resistant (R; red columns), intermediate (I, yellow columns) and sensitive (S, green columns) isolates to ten antibiotics of different classes. Antibiotic resistance breakpoints are evaluated according to CLSI guidelines [142].

AMP, ampicillin; SAM, ampicillin-sulbactam; TZP, piperacillin-tazobactam; CXM, cefuroxime-axetil; CAZ, ceftazidime; IPM, imipenem; MEM, meropenem; CIP, ciprofloxacin; LVX, levofloxacin; GEN, gentamicin.

In order to provide an overview of the mechanisms leading to antibiotic resistance, different strategies were used to analyze the RNA-seq data: i) horizontally acquired resistance enzymes were identified via a *de-novo* assembly of all reads which did not map to the pan-genome; ii) chromosomal mutations in the QRDRs of *gyrA*, *gyrB*, *parC* and *parE* were extracted using SAMtools and iii) differences in expression profiles of genes known to be involved in antibiotic resistance were analyzed.

3.4.1 Beta-lactam resistance

The main driver of beta-lactam resistance in Gram-negative bacteria is the presence of beta-lactamases, enzymes that are able to cleave the lactam ring and hydrolyze these antibiotics [261]. Although further mechanisms like an enhanced expression of efflux pumps [86], reduced membrane permeability [113] or target modification through mutations in penicillin-binding proteins [262] are known to contribute to a reduced susceptibility, beta-lactamases are the primary and most common cause of resistance to these drugs [261,263,264].

3.4.1.1 Carbapenemases

Table 3.10 shows all horizontally acquired beta-lactamases that were identified in the accessory transcriptome of all isolates. The analyses revealed the presence of carbapenemase KPC-2 in all ST258 isolates and KPC-3 in both ST512 isolates. These findings were additionally confirmed by Sanger sequencing of bla_{KPC} PCR products. The association of ST258 and ST512 isolates with KPC enzymes is well known and the global dissemination of ST258 clones including its close relatives is the main driver of the global KPC spread [237,265,266]. All KPC expressing isolates were non-susceptible to the carbapenem meropenem. In all other KPC negative isolates which were resistant to meropenem (of note, only ST101 isolates) the carbapenemase OXA-48 could be identified, an oxacillinase with strong carbapenem-hydrolyzing activity [267]. The other two identified OXA beta-lactamases OXA-1 and OXA-9 are narrow-spectrum beta-lactamases without carbapenem or cephalosporin hydrolyzing activity [268,269]. The carbenicillinase CARB-2 (first reported in *P. aeruginosa* and designated PSE-1 [270]), a beta-lactamase capable to hydrolyze carbapenems, was identified in one isolate (1162281). But since this isolate was fully susceptible to meropenem, the influence of CARB-2 on the MIC cannot be estimated here.

In conclusion, meropenem non-susceptibility can be explained almost entirely by the presence of either KPC or OXA-48 carbapenemases. Only one single isolate (1_16) showed reduced susceptibility on an intermediate level without expressing a carbapenemase. The elevated resistance level might be explained by porin alterations [271]. Due to incomplete sequence coverage for most porins, involvement of porin alteration in meropenem non-susceptibility in this isolate cannot be determined.

3.4.1.2 Extended spectrum beta-lactamases

Almost all isolates contained further beta-lactamases or extended-spectrum beta-lactamases (ESBLs) of different classes of TEM, SHV and CTX-M types. The sequences of these types of ESBLs are highly variable and the spectrum of hydrolyzed beta-lactam antibiotics varies largely between the different variants of these enzymes [272,273]. For example, the TEM variants TEM-1 and TEM-2 are no ESBLs,

whereas the variant TEM-3 (differs from TEM-2 by two amino acid substitutions [274]) is able to hydrolyze the third-generation cephalosporins cefotaxime and ceftazidime. Likewise, the SHV variants SHV-1 or SHV-11 are no ESBLs but the variant SHV-2 has cefotaxime (and to a lesser degree ceftazidime) hydrolyzing activity [275] which is facilitated by a single amino acid substitution of glycine to serine at position 238 [272].

The CTX-M beta-lactamases are the most widespread enzymes and most of them provide a high level of resistance to cefotaxime but only few are able to hydrolyze ceftazidime [276]. One of these examples is the variant CTX-M-15 that differs from its parental enzyme CTX-M-9 (which does not hydrolyze ceftazidime) by a single mutation of aspartic acid to glycine at position 240 [277].

Besides ESBLs, third-generation cephalosporins are also hydrolyzed by KPC enzymes [278], whereas all OXA carbapenemases (including OXA-48) do not or only very poorly hydrolyze cefotaxime and ceftazidime [264].

Six out of the 37 isolates had the CTX-M-15 variant (including all ST15 isolates) and the association of CTX-M-15 with sequence types 15 and 147 has been previously described [240,279]. The transcript of another 11 isolates showed close relation to CTX-M-9 (exclusively in ST101 isolates) and one isolate had the CTX-M-1 variant. SHV beta-lactamases, one of the most common ESBLs [280] with more than 180 known variants (http://www.lahey.org/studies/), were expressed in all ST258 isolates and in MGH 78578; all of them could be identified as SHV-11. CTX-M- and SHV-enzymes are usually plasmid encoded but have been integrated into the chromosome of two reference strains (Kpn2146 and 1084, respectively) and are therefore included in the pan-genome used in this study as a reference to map RNA-seq reads (see Figure 3.22). TEM beta-lactamases were identified in 29 isolates, but in 13 of them the transcript could not be typed due to low sequence coverage. The remaining 16 isolates showed the variant TEM-1.

Due to this partially low sequencing coverage and the resulting uncertainties in the determination of the exact type of TEM, SHV and CTX-M beta-lactamases, it was not possible to elucidate the influence of ESBLs on the ceftazidime resistance phenotype. Therefore, ESBL typing needs to be improved e.g. by directed Sanger resequencing of single genes or by whole genome sequencing.

Table 3.10: Expressed beta-lactamases in all *K. pneumoniae* clinical isolates

Origin	Isolate	MLST	MEM	CAZ	KPC	OXA	CARB	TEM	SHV	CTX-M
Medizinisches Labor Ostsachsen, Goerlitz, Germany	isolate 1_1	512	R ≥ 16	R ≥ 64	KPC-3			TEM-1		
	isolate 1_2	405	S ≤ 0.25	I 8		OXA-1		TEM-1		CTX-M-15
	isolate 1_3	258	R ≥ 16	R ≥ 64	KPC-2				SHV-11	
	isolate 1_4	258	R ≥ 16	R ≥ 64	KPC-2				SHV-11	
	isolate 1_6	512	R >32	R ≥ 64	KPC-3			TEM-1		
	isolate 1_8	15	S ≤ 0.25	n.d.		OXA-1		TEM-1		CTX-M-15
	isolate 1_9	258	R ≥ 16	R ≥ 64	KPC-2			TEM-1	SHV-11	
	isolate 1_10	258	R ≥ 16	n.d.	KPC-2	OXA-9		TEM-1	SHV-11	
	isolate 1_11	258	R 4	R ≥ 64	KPC-2			TEM-1	SHV-11	
	isolate 1_12	258	R 8	R ≥ 64	KPC-2			TEM-1	SHV-11	
	isolate 1_13	258	R ≥ 16	R ≥ 64	KPC-2				SHV-11	
	isolate 1_15	258	I 2	R ≥ 64	KPC-2			TEM-1	SHV-11	
	isolate 1_16	15	I 2	R ≥ 64		OXA1		TEM-1		CTX-M-15
	isolate 2_2	15	S ≤ 0.25	R ≥ 64		OXA1		TEM-1		CTX-M-15
	isolate 2_4	258	R 16	n.d.	KPC-2				SHV-11	
	isolate 2_8	34	S ≤ 0.25	S 4						CTX-M-1
	isolate 2_9	258	R 8	R ≥ 64	KPC-2				SHV-11	
	isolate 2_10	15	S ≤ 0.25	I 8		OXA-1		TEM-1		CTX-M-15
	isolate 2_14	101	S 1	R ≥ 64		OXA1		TEM-1		
Charite-Universitätsmedizin, Berlin, Germany	isolate 3_3	101	R ≥ 16	R 16		OXA-9 + OXA-48		TEM-like		CTX-M-9-like
	isolate 3_4	101	R ≥ 16	R 16		OXA-9 + OXA-48		TEM-like		CTX-M-9-like
	isolate 3_5	101	R ≥ 16	S 4		OXA-9 + OXA-48		TEM-like		CTX-M-9-like
	isolate 3_6	101	R ≥ 16	R 16		OXA-9 + OXA-48		TEM-like		CTX-M-9-like
	isolate 3_7	101	R ≥ 16	S 4		OXA-9 + OXA-48		TEM-like		CTX-M-9-like
	isolate 3_8	101	R 8	R 64		OXA-1 + OXA48		TEM-like		CTX-M-like
	isolate 3_10	101	R ≥ 16	R 16		OXA-9 + OXA-48		TEM-like		CTX-M-9-like
	isolate 3_11	101	R ≥ 16	R 16		OXA-9 + OXA-48		TEM-like		CTX-M-9-like
	isolate 3_12	101	R 8	S 4		OXA-9 + OXA-48		TEM-like		CTX-M-9-like
	isolate 3_13	101	R 8	R 16		OXA-48		TEM-like		CTX-M-9-like
	isolate 3_14	101	R 16	R 16		OXA-48		TEM-like		CTX-M-9-like
	isolate 3_17	101	R 8	S 4		OXA-9 + OXA-48		TEM-like		CTX-M-9-like
Private practice, Salzgitter, Germany	isolate 1_14	147	S ≤ 0.25	R ≥ 64				TEM-1		CTX-M-15
	isolate 2_7	novel	S ≤ 0.25	S ≤ 1						
	isolate 2_11	35	S ≤ 0.25	S ≤ 1				TEM-1		
previously published	MGH 78578	38	S ≤ 0.25	R ≥ 64		OXA-9*		TEM-1	SHV-11	
	JH1	134	S ≤ 0.25	S ≤ 1						
	1162281	133	S ≤ 0.25	R ≥ 64			CARB-2	TEM-like		

* Sequence contains a premature stop codon at nucleotide position 336, -like: identified sequences contained SNPs or was incomplete, therefore the closest hit is given; MEM, meropenem; CAZ, ceftazidime; MICs in µg/ml, breakpoints according to CLSI [142].

3.4.2 Aminoglycoside resistance

Resistance to aminoglycosides arises from several mechanisms like alteration of the ribosomal binding sites (only for streptomycin), a decreased intracellular concentration of the drug and the expression of aminoglycoside-modifying enzymes (AMEs) which inactivate the antibiotic [128]. Whereas a reduction in drug uptake through membrane impermeabilization occurs mostly in *P. aeruginosa* and the clinical significance of an active efflux remains uncertain, the main mechanism of aminoglycoside resistance in *K. pneumoniae* is the acquisition of these AMEs. [128].

In this set of clinical isolates, enzymes from the three main classes of AMEs, namely N-acetyltransferases (AAC), O-phosphotransferases (APH), and O-nucleotidyltransferases (ANT), were present in all but five isolates (see Table 3.11). Whereas only few isolates expressed ANT and APH enzymes, most of the isolates contained AAC(6')-Ib C or its variant AAC(6')-Ib cr. Due to insufficient read coverage, the exact type could not be determined. Enzymes of the AAC(6')-I subgroup confer resistance to tobramycin, kanamycin, netilmicin and either amikacin or gentamicin. Whereas AAC(6')-Ib C (encoded by *aacA4*) does not show activity against gentamicin [281,282], the variants AAC(6')-Ib cr (encoded by *aac(6')-Ib'-cr*) and AAC(6')-Ib' (encoded by *aac(6')-Ib'*) do have gentamicin modifying activity [110,283]. Therefore, the exact type of N-acetyltransferase is of importance and needs to be clarified in further studies.

Besides the known involvement of AMEs in aminoglycoside resistance, there are reports of an involvement of bacterial efflux contributing to aminoglycoside resistance. The *K. pneumoniae* homologs of the *E. coli* RND multidrug efflux transport acrD [284] as well as the MFS transporter *mdfA* (also named *kdeA* [285]) and *bcr* [286] are known to extrude aminoglycosides [287]. These three genes were homogenously expressed at medium levels in all isolates (nRPK values between 3.5 and 6.8, see also Figure 3.22) and although the influence on aminoglycoside resistance could be clearly shown *in-vitro*, their involvement in a clinical setting still remains unclear.

Table 3.11: Horizontally acquired aminoglycoside modifying enzymes

Origin	Isolate	MLST	GEN	AAC	ANT	APH
Medizinisches Labor Ostsachsen, Goerlitz, Germany	isolate 1_1	512	S ≤ 1			
	isolate 1_2	405	R ≥ 16	AAC(6')-Ib cr-like		APH(3")-Ib + APH(6)-Id
	isolate 1_3	258	S 4	AAC(6')-Ib C-like		
	isolate 1_4	258	S 4	AAC(6')-Ib C-like		
	isolate 1_6	512	S 4	AAC(6')-Ib C-like		
	isolate 1_8	15	S ≤ 1	AAC(6')-Ib-cr-like + AAC(3)-Ia C		
	isolate 1_9	258	S 4	AAC(6')-Ib C-like		
	isolate 1_10	258	S ≤ 1	AAC(6')-Ib C-like		
	isolate 1_11	258	S 4	AAC(6')-Ib C-like		
	isolate 1_12	258	S 4	AAC(6')-Ib C-like		
	isolate 1_13	258	S 4	AAC(6')-Ib C-like		
	isolate 1_15	258	S 4	AAC(6')-Ib C-like		
	isolate 1_16	15	R ≥ 16	AAC(6')-Ib cr-like	ANT(3")-Ia	
	isolate 2_2	15	R ≥ 16	AAC(6')-Ib cr-like		
	isolate 2_4	258	S 4	AAC(6')-Ib C-like		
	isolate 2_8	34	S ≤ 1			
	isolate 2_9	258	S 4	AAC(6')-Ib C-like		
	isolate 2_10	15	S ≤ 1	AAC(6')-Ib-cr-like + AAC(3)-Ia C		
	isolate 2_14	101	R ≥ 16	AAC(6')-Ib cr-like		
Charite-Universitätsmedizin, Berlin, Germany	isolate 3_3	101	R ≥ 16	AAC(6')-Ib C-like	ANT(3")-Ia*	APH(6)-Id
	isolate 3_4	101	S ≤ 1	AAC(6')-Ib C-like		APH(6)-Id
	isolate 3_5	101	S ≤ 1			APH(6)-Id
	isolate 3_6	101	R ≥ 16	AAC(6')-Ib C-like	ANT(3")-Ia*	APH(6)-Id
	isolate 3_7	101	R ≥ 16	AAC(6')-Ib C-like		APH(6)-Id
	isolate 3_8	101	R ≥ 16	AAC(6')-Ib cr-like		
	isolate 3_10	101	R ≥ 16	AAC(6')-Ib C-like	ANT(3")-Ia*	APH(6)-Id
	isolate 3_11	101	R ≥ 16	AAC(6')-Ib C-like	ANT(3")-Ia*	APH(6)-Id
	isolate 3_12	101	R ≥ 16	AAC(6')-Ib C-like		APH(6)-Id
	isolate 3_13	101	S ≤ 1			APH(6)-Id
	isolate 3_14	101	S ≤ 1			APH(6)-Id
	isolate 3_17	101	R ≥ 16	AAC(6')-Ib C-like		
Private practice, Salzgitter, Germany	isolate 1_14	147	S ≤ 1	AAC(6')-Ib C-like		
	isolate 2_7	novel	S ≤ 1			
	isolate 2_11	35	n.d.			
previously published	MGH 78578	38	R ≥ 16	AAC(6')-Ib C-like	ANT(2")-Ia	
	JH1	134	S ≤ 1			
	1162281	133	R 8		ANT(2")-Ia	

* only fragments were identified; aminoglycoside modifying enzymes are named according to [132]; -like: identified sequences contained SNPs or was incomplete, therefore the closest hit is given; GEN, gentamicin MIC in µg/ml, breakpoints according to CLSI [142].

3.4.3 Fluoroquinolone resistance

Fluoroquinolone resistance is primarily conferred via mutations in the gyrase subunits GyrA and GyrB as well as mutations in the topoisomerase IV subunits ParC and ParE. In particular, high levels of ciprofloxacin resistance are mostly determined by mutations in *gyrA* at amino acid position 83 in combination with mutations in *parC* at position 87. Besides these chromosomal target mutations an enhanced efflux [86] and the presence of transferable quinolone resistance genes [111] like Qnr [288] or AAC(6')-Ib-cr [110] are known to be involved in the development of fluoroquinolone resistance.

To provide insights into the nature and dimension of ciprofloxacin resistance in our panel of clinical *K. pneumoniae* isolates, chromosomal mutations within the four fluoroquinolone target genes and the presence of plasmid-mediated quinolone resistance (PMQR) determinants were evaluated. Using transcriptomic data, several mutations in the QRDR of *gyrA*, *gyrB* and *parC* were determined, while no mutations in *parE* could be detected (see Table 3.12). Furthermore several types of Qnr proteins and the aminoglycoside acetyltransferase AAC(6')-Ib-cr were identified in the majority of isolates.

Our analysis revealed the presence of *gyrA* mutations at amino acid position 83 (S83I, S83F and S83Y, respectively) in all ciprofloxacin non-susceptible isolates and moreover, all but two non-susceptible isolates harbored additionally a non-synonymous mutation in *parC* at position 87 (always S80I). Further mutations in *gyrA* at amino acid position 87 and in *gyrB* at position 466 were also identified, although always in combination with mutations in *gyrA* and *parC*. Therefore the influence of these mutations on the ciprofloxacin MIC cannot be clarified based on this dataset.

Both non-susceptible isolates without a mutation of *gyrA* in combination with *parC* expressed PMQR determinants, which are most likely responsible for the reduced susceptibility [289]. One of these two isolates (1162281) expressed *qnrA1* [290] along with a S83F mutation in *gyrA*, whereas the other isolate (1_2) expressed the aminoglycoside acetyltransferase encoding gene *aac(6')-Ib-cr* in combination with *qnrB1* [291]. Since all other isolates expressing plasmid encoded enzymes do also have *gyrA* and *parC* double mutations, the specific influence on the MIC of these enzymes remains unclear.

Table 3.12: QRDR mutations and horizontally acquired fluoroquinolone resistance enzymes

Origin	Isolate	MLST	CIP	*gyrA* S83	*gyrA* D87	*gyrB* E466	*parC* S80	AAC(6')-Ib-cr	Qnr
Medizinisches Labor Ostsachsen, Goerlitz, Germany	isolate 1_1	512	R ≥ 4	S83I	-	E466D	S80I		
	isolate 1_2	405	I 2		-	-	-	AAC(6')-Ib-cr-like	QnrB1
	isolate 1_3	258	R ≥ 4	S83I	-	E466D	S80I		
	isolate 1_4	258	R ≥ 4	S83I	-	E466D	S80I		
	isolate 1_6	512	R ≥ 4	S83I	-	E466D	S80I		
	isolate 1_8	15	R ≥ 4	S83F	D87A	-	S80I	AAC(6')-Ib-cr-like	
	isolate 1_9	258	R ≥ 4	S83I	-	E466D	S80I		
	isolate 1_10	258	R ≥ 4	S83I	-	E466D	S80I		
	isolate 1_11	258	R ≥ 4	S83I	-	E466D	S80I		
	isolate 1_12	258	R ≥ 4	S83I	-	E466D	S80I		
	isolate 1_13	258	R ≥ 4	S83I	-	E466D	S80I		
	isolate 1_15	258	R ≥ 4	S83I	-	E466D	S80I		
	isolate 1_16	15	R ≥ 4	S83F	D87A	-	S80I	AAC(6')-Ib-cr-like	
	isolate 2_2	15	R ≥ 4	S83F	D87A	-	S80I	AAC(6')-Ib-cr-like	
	isolate 2_4	258	R ≥ 4	S83I	-	E466D	S80I		
	isolate 2_8	34	S ≤ 0.25	-	-	-	-		
	isolate 2_9	258	R ≥ 4	S83I	-	-	S80I		
	isolate 2_10	15	R ≥ 4	S83F	D87A	-	S80I	AAC(6')-Ib-cr-like	
	isolate 2_14	101	R ≥ 4	S83Y	D87N	-	S80I	AAC(6')-Ib-cr-like	
Charite-Universitätsmedizin, Berlin, Germany	isolate 3_3	101	R ≥ 4	S83Y	D87N	-	S80I		QnrS1
	isolate 3_4	101	R ≥ 4	S83Y	D87N	-	S80I		QnrS1
	isolate 3_5	101	R ≥ 4	S83Y	D87N	-	S80I		QnrS1
	isolate 3_6	101	R ≥ 4	S83Y	D87N	-	S80I		QnrS1
	isolate 3_7	101	R ≥ 4	S83Y	D87N	-	S80I		
	isolate 3_8	101	R ≥ 4	S83Y	D87N	-	S80I	AAC(6')-Ib-cr-like	
	isolate 3_10	101	R ≥ 4	S83Y	D87N	-	S80I		QnrS1
	isolate 3_11	101	R ≥ 4	S83Y	D87N	-	S80I		QnrS1
	isolate 3_12	101	R ≥ 4	S83Y	D87N	-	S80I		QnrS1
	isolate 3_13	101	R ≥ 4	S83Y	D87N	-	S80I		
	isolate 3_14	101	R ≥ 4	S83Y	D87N	-	S80I		
	isolate 3_17	101	R ≥ 4	S83Y	D87N	-	S80I		QnrS1
Private practice, Salzgitter, Germany	isolate 1_14	147	R ≥ 4	S83I	-	-	S80I		
	isolate 2_7	novel	S ≤ 0.25	-	-	-	-		
	isolate 2_11	35	I 2	S83I	-	-	S80I		
previously published	MGH 78578	38	S 1	S83Y	-	-	-		
	JH1	134	S ≤ 0.25	-	-	-	-		
	1162281	133	R ≥ 4	S83F	-	-	-		QnrA1

–: the wild type allele was present; -like: identified sequences contained SNPs or was incomplete, therefore the closest hit is given; CIP, ciprofloxacin MIC in µg/ml, breakpoints according to CLSI [142].

3.4.4 Influence of other, non-specific resistance mechanisms

Besides the presence of horizontally acquired resistance enzymes and specific target mutations, the enhanced expression of efflux pumps, porins and beta-lactamases are well known examples of mechanisms that confer antibiotic resistance [292]. Figure 3.22 gives a broad overview about the expression of 65 genes involved in antibiotic resistance over all 37 clinical isolates. The figure illustrates the expression of six described and putative beta-lactamases, six porins and 53 genes

involved in the extrusion of antibacterial compounds. All efflux genes are arranged into the following clusters: i) Resistance-Nodulation-Cell Division (RND) Superfamily, ii) Major Facilitator Superfamily (MFS), iii) Small Multidrug Resistance (SMR) proteins, iv) ATP-binding Cassette (ABC) transporter, and v) Multi-antimicrobial extrusion (MATE) transporter. The operon structure of efflux pumps is indicated on the outside of the graph.

Figure 3.22 reveals a low and uniform expression of most efflux systems, only *acrAB* and *oqxAB* were expressed on high levels in this set of clinical isolates. The pump with the highest average expression was the RND efflux pump AcrAB with nRPK values of *acrA* and *acrB* of 9.98 and 10.69, respectively. AcrAB is known to be involved in beta-lactam and fluoroquinolone resistance in *K. pneumoniae* as well as *E. coli* [293-295]. Whereas *acrAB* was highly expressed in all isolates, only *oqxA* and *oqxB* were highly variably expressed. The RND efflux system OqxAB is composed of the membrane fusion protein OqxA and the multidrug efflux transporter OqxB [296] and is involved in resistance to fluoroquinolone, cephalosporin, and glycylcycline antibiotics in *K. pneumoniae* [295,297]. The expression of *oqxAB* is tightly regulated by the negative GntR-type transcriptional regulator OqxR and overexpression of this pump usually requires either mutations in OqxR, rendering the negative regulator ineffective or an upregulation of the transcriptional AraC-type activator RarA [298,299].

Sequence analyses revealed that all isolates overexpressing this efflux pump harbored mutations within *oqxR*, whereas all other 22 isolates do not have altered amino acid sequences of this transcriptional repressor. All ST258 and ST512 isolates contained a SNP in *oqxR* (T389C) which caused the amino acid substitution V130A. Two other isolates, 1162281 and 1_16, contained also amino acid alterations in OqxR (V137A and A117E, respectively) and isolate 1_8 had an insertion of 24 nucleotides after nucleotide position 206 which most likely led to a nonfunctional OqxR protein. Interestingly, the gene encoding the positive regulator RarA is always overexpressed when mutations in *oqxR* occur (data not shown) and therefore the strong expression of *rarA* might enhance the effect of the *oqxR* mutation on the expression of *oqxAB* [298].

Besides beta-lactamases and efflux genes, Figure 3.22 shows additionally the expression of six outer membrane proteins (porins) which are known to be involved in antibiotic resistance. Porins are water-filled channels in the bacterial cell membrane and facilitate the uptake of hydrophilic compounds [83]. Whereas *K. pneumoniae* possesses several, diverse porins, only the two major non-specific porins OmpK35 (homolog of the *E. coli* porin *ompF*) and OmpK36 (homolog of the *E. coli* porin *ompC*) play an eminent role in the clinical setting [300]. Loss of OmpK35 is known to be involved in resistance to fluoroquinolones [301], cephalosporins, carbapenems, and chloramphenicol [302] and loss of OmpK36 plays a critical role in the development of carbapenem resistance [303].

Only four out of the six porins were expressed at high levels in the panel of 37 clinical isolates analyzed here in this thesis; *ompN* and *ompS* showed only a negligible expression. Remarkably, all

ST258 isolates expressed porins generally lower as compared to all other isolates (including the two ST512 isolates). The expression of *ompK35*, *ompK36* and *ompC* was 4-fold lower and the expression of *ompW* even 16-fold lower. Besides this effect, no correlation between phylogeny and porin expression could be detected. Despite high expression values, a detailed and comparative sequence analysis was not possible for most of the porins due to an uneven distributed read coverage leaving large parts of these genes without reliable sequence information. Nevertheless, several mutations could be clearly identified in *ompK35* as compared to the sequence of the reference strain 1084: All ST258 and both ST512 isolates showed a deletion of a G in codon 40 and all ST101 harbored an insertion of a single G in codon 61. These two mutations are causing a frameshift in the open reading frame and therefore most-likely render the protein nonfunctional. Additionally to these two indels, at least two isolates showed missense mutations causing an amino acid exchange in the sequence of *ompK35*: D159N in isolate 1_3 and I183V in isolate 2-9 which are located in the external loop L4 and in the beta-strands between loops L4 and L5, respectively [302]. The influence of deleterious mutations in *ompK35* and *ompK36* was shown in clinical samples and could be demonstrated *in vitro* in an isogenic background [302,304]. Therefore it is very likely that porin disruptions also contribute to antibiotic resistance in this set of clinical isolates, but further studies are needed to determine the exact influence of these mutations on the MIC.

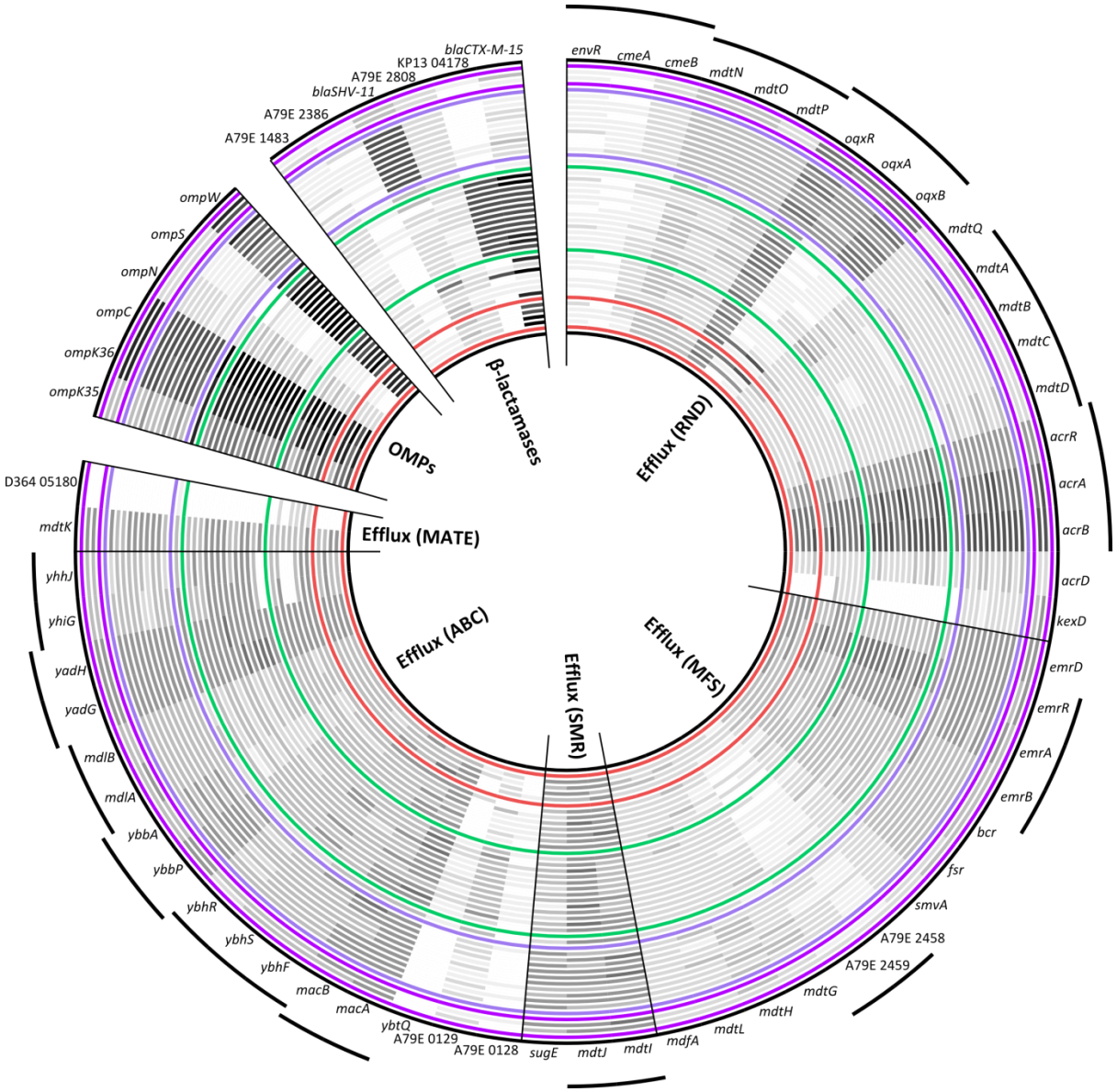

Figure 3.22: Expression of antibiotic resistance associated genes.

The circular plot shows the normalized read counts (in nRPK) of 65 genes which are described to be associated with antibiotic resistance. Expression varies from 16 nRPK (dark gray) to 0 nRPK (white). Genes are arranged in segments according to the functional class of their product with indicated operon structures on the outside. Isolates are represented as rings and are arranged according to their phylogenic relationship (see Figure 3.11). Isolates with the same MLST profile are framed by colored rings: ST512 (magenta), ST258 (purple), ST101 (green) and ST15 (red).

4 Discussion

4.1 Antimicrobial resistance is a major global threat

Hospital and community acquired infections with Gram-negative pathogens have an dramatic and increasing impact on human health, due to the emerging threat of multidrug resistant and highly virulent clinical isolates. Two of the most worrisome examples of Gram-negative pathogens are the Gammaproteobacteria *Pseudomonas aeruginosa* and *Klebsiella pneumoniae*, since infections with these pathogens are reaching alarming rates in the clinical setting. The U.S. CDC classified carbapenem-resistant Enterobacteriaceae (including *K. pneumoniae*) as an urgent public health threat (representing the highest out of five categories) requiring "urgent and aggressive action" [48]. Furthermore, extended spectrum beta-lactamase (ESBL) producing Enterobacteriaceae as well as multidrug-resistant *P. aeruginosa* were classified as microorganisms with a threat level of serious (the second highest level) demanding "prompt and sustained action" to guarantee that these problems do not grow in the future [48]. In 1999 the U.S. CDC, FDA and the National Institutes of Health (NIH) created the "Interagency Task Force on Antimicrobial" to combat antimicrobial resistance in a concerted manner. They released their "Action Plan to Combat Antimicrobial Resistance" in 2001 with the latest update from 2012 as a "blueprint for specific, coordinated actions to address the growing threat of antimicrobial resistance" (available at http://www.cdc.gov/drugresistance/pdf/action-plan-2012.pdf). In this plan, the consortium highlighted the following focus areas of four overarching categories of i) surveillance, ii) prevention and control, iii) research, and iv) product development, with the aim to develop novel treatment strategies to contain the spread of multidrug resistant Gram-negative pathogens.

4.2 Nature and dimension of QRDR mutations

In this thesis, a combination of Sanger sequencing, pyrosequencing, quantitative real-time PCRs and RNA-seq was used to determine the nature and frequency of hot spot mutations in the QRDRs of the genes *gyrA* and *gyrB* encoding the DNA-gyrase as well as *parC* and *parE* encoding the topoisomerase IV and the involvement of bacterial efflux in fluoroquinolone resistance in a panel of 172 clinical *P. aeruginosa* isolates. Most of those isolates were resistant to multiple antimicrobial agents (data not shown) and the majority (including all ciprofloxacin resistant strains) expressed at least one SNP within one of the QRDRs. In accordance with several previous studies [192-198], the by far most frequently observed mutation was within the QRDR of *gyrA*, with the amino acid substitution T83I being the prevailing mutation, whereas mutations in *gyrB* were less frequent [197,199,200]. In *gyrB*,

the majority of mutations were found at amino acid positions 466 to 468; however we also found one isolate with an insertion of CCG (Proline) at position 458 and two I529V mutations which have not been described previously. Five different *parE* mutations and three *parC* mutations were found, interestingly all *parC* mutations exclusively in strains that harbored the predominant *gyrA* T83I mutation. Single *parC* mutations were not found in the panel of MDR *P. aeruginosa* – as also observed in previous studies [195,200]. Additionally, it could be shown in the isogenic background of the *P. aeruginosa* reference strain PA14 that the *parC* mutations S87W and S87L only contribute to an increased fluoroquinolone resistance in the presence of a *gyrA* mutation. This has been indicated previously by several studies on fluoroquinolone resistance in clinical isolates of different species like *E. coli* [201,305-307], *P. aeruginosa* [203] or *Streptococcus pneumoniae* [308,309], but has never been shown in an isogenic background of *P. aeruginosa* so far. The data shown here strongly indicates that *parC* mutations only occur as secondary mutations increasing the resistance towards fluoroquinolones synergistically with previously acquired *gyrA* mutations.

With this combined approach of different sequencing strategies, 53 and 23 strains with a single mutation in either *gyrA* or *gyrB,* respectively, were identified. However, those strains exhibited MIC values that spanned a broad range between 1 µg/ml and > 8 µg/ml. In contrast, and as already described in several previous studies [195,197,205], double mutations in *gyrA* and *parC* always revealed high level ciprofloxacin resistance with MICs of 8 µg/ml or more in clinical MDR strains. Accordingly, the introduction of the most frequent SNPs within the QRDRs of *gyrA* and *gyrB* into the susceptible reference stain PA14 only conferred MIC values of 1 - 2 µg/ml, whereas the introduction of a secondary mutation in the *parC* QRDR always resulted in high level ciprofloxacin resistance. This broad MIC range in clinical *P. aeruginosa gyrA* mutants has been observed in studies before [202,203] and although it is tempting to speculate that this can be explained by a differential efflux pumps expression [199,204], no clear association of increased MICs in *gyrA* mutants and an increased expression of efflux pumps could be demonstrated previously [203,205,206]. Similarly, in this study, the large variation of MIC values in isolates with only single mutations within the QRDRs could not be linked to an additional differential expression of one or more of the four major efflux pumps involved in ciprofloxacin resistance as determined by either qRT-PCR in 29 selected clinical isolates (see **Table** 3.2 and Figure 3.3) or by RNA-seq (see Figure 3.7) Additionally, we found that complementation with the wild-type *gyrA* gene led to a 2- to 8-fold reduction in fluoroquinolone resistance irrespective of the original resistance level. These results indicate that mutations within the *gyrA* QRDR add to a preexisting isolate-specific resistance level of unknown origin.

4.3 Unbiased phenotype-genotype correlation reveals that ciprofloxacin resistance is predominantly determined by specific QRDR mutations

Three comprehensive screenings of *P. aeruginosa* mutant libraries have shown that approximately 100 to 200 genes are involved in the intrinsic ciprofloxacin resistome [133,135,136]. These publications could show that antibiotic resistance might be the result of complex and multifactorial networks of interactions among bacterial proteins of diverse functional categories. To determine which of the gene inactivations identified in these large mutant screening, if any, play a role in fluoroquinolone resistance in the clinical setting and to identify possible additional mechanisms of fluoroquinolone resistance that go beyond the known resistance determinants of target mutations and increased efflux, the complete transcriptome of a large and phylogenetic diverse collection of clinical isolates was studied in its full complexity.

High throughput sequencing of messenger RNAs (RNA-seq) offers the ability to study gene expression at single nucleotide resolution. Therefore, it allows not only the measurement of transcript abundancies but also the detection of point mutations, deletions and insertions of transcribed genes. Hence, RNA-seq provides an advantage over whole genome sequencing to obtain information of both transcript abundancies and sequence variations in a single approach. Thus, it gives the possibility to draw global phenotype-genotype correlations to study the interplay of genome and transcriptome [310-312]. Recently, RNA-seq has been applied successfully in the elucidation of ceftolozane resistance by the group of Antonio Oliver in collaboration with our group. Ceftolozane is a novel beta-lactam antibiotic of the cephalosporin class which is used in combination with the beta-lactamase inhibitor tazobactam for the treatment of complicated urinary tract infections, complicated intra-abdominal infections, and ventilator-associated bacterial pneumonia [313]. Resistance of *P. aeruginosa* to ceftolozane requires changes in gene expression as well as amino acid alterations. By using RNA-seq, it was possible to identify multiple mutations leading to an overexpression of *ampC* as well as to describe the structural modification of this chromosomal beta-lactamase in a single approach [314].

Here, RNA-seq was used to study the mechanisms leading to fluoroquinolone resistance in a phylogenetically broad and diverse panel of 159 clinical *P. aeruginosa* isolates in an unbiased manner. By performing whole transcriptome comparisons, it was possible to identify 15 single nucleotide polymorphisms which were highly enriched in non-susceptible isolates. Among these 15 identified SNPs, four SNPs lead to an amino-acid substitution in the corresponding gene product. The by far best hits, which showed the highest significance, were the fluoroquinolone resistance determining mutations of T83I in *gyrA* and S87L/W in *parC*. The finding that SNPs in *gyrA* and *parC*, and especially combinations thereof, are an absolute requirement in of high level ciprofloxacin

resistance is further supported by the comparison of only highly-resistant isolates with a MIC of ≥ 8 µg/ml with the susceptible ones. In this comparison, only the SNPs in *gyrA* (T83I) and *parC* (S87L/W) were highly significantly enriched in the group of resistant isolates.

Besides the two mutations within the QRDRs of *gyrA* and *parC*, two additional non-synonymous SNPs, located in the genes *kynU* (PA14_37610) and *glmU* (PA14_73220), were significantly enriched in the comparison of non-susceptible versus susceptible isolates. *kynU* encodes the enzyme kynureninase which is involved in the aerobic degradation of tryptophan via the anthranilate pathway [315]. Anthranilate in turn serves as a precursor of the quorum-sensing signal molecules 4-hydroxy-2-alkylquinolines which regulate numerous virulence genes and are associated with iron chelation [316,317]. Therefore it has been suggested previously, that the cellular supply of anthranilate could provide a viable drug target whose disruption could lessen the virulence of *P. aeruginosa* [318]. GlmU is a bifunctional acetyltransferase/uridyltransferase enzyme facilitating the biosynthesis of UDP-N-acetylglucosamine which is involved in the biosynthesis of lipopolysaccharide, peptidoglycan and teichoic acid components of bacterial cell walls [319]. Since GlmU is an essential enzyme in both Gram-negative and Gram-positive bacteria and furthermore lacks a homolog in eukaryotes, it is regarded as a potential antibacterial target [320].

Both genes were previously not associated with resistance to antimicrobial drugs in the aforementioned four global transposon mutagenesis screenings. Although they seem to be correlated with fluoroquinolone resistance here, correlation does not necessarily imply causation. Therefore further studies, e.g. the incorporation of these SNPs in an isogenic background, are required to elucidate the involvement of these SNPs in the development of antimicrobial resistance and furthermore the proficiency of these enzymes to act as a potential novel drug target.

4.4 Occurrence of certain QRDR mutations in distinct niches

It has been observed before that highly resistant *P. aeruginosa* strains harboring a double *gyrA* and *parC* mutation are almost exclusively isolated from non-CF patients, whereas in CF single mutations within the QRDRs dominate [202,209,321]. Interestingly, in accordance with these previous reports, 26 of the 30 *gyrA/parC* mutants with available patient information were isolated from non-CF patients. It has been suggested that higher drug levels of ciprofloxacin in non-CF patients might account for this phenomenon, since drug levels in CF-sputum were found to be significantly lower than in blood [322]. Although the lower drug concentration levels might select for intermediate resistant strains in distinct niches, it might also indicate that there is a co-selection of single mutations in QRDRs with other phenotypic traits that provide the strains with a selective advantage.

Thereby, the unique environment of the CF lung might play a significant role and potentially influences the process of mutation and selection [321].

The broad use of the fluoroquinolones is known to be a risk factor for the development of resistant strains, however, the lower the MIC of a first-step mutation the higher is the likelihood that those mutations will be cleared from an infectious site under antimicrobial therapy. 74 of the 172 *P. aeruginosa* isolates studied here harbored a single mutation within only one of the QRDR and 48 of those showed MIC values of 2 µg/ml or less. Although these *P. aeruginosa* isolates are categorized as susceptible or intermediate, it remains to be shown that it is safe to treat them with fluoroquinolones [111]. This is a key factor to consider in the treatment of Pseudomonas infections in CF patients, since drug concentrations in the CF lung do not reach sufficient levels [323] and sub-inhibitory concentrations might promote population diversification [324].

The stepwise enrichment of fluoroquinolone resistance mutations has been described previously in several *in vitro* studies [325-327]. Mutants at each step are enriched when drug concentrations fall within a specific range called the mutant selection window [98,328]. Furthermore, even antibiotic concentrations below the MIC might select for resistance-conferring mutations. In a recent study, it could be demonstrated that ciprofloxacin concentrations at 1/10 the MIC were sufficient to select fluoroquinolone-resistant mutants *de novo* in *E. coli* [329]. Although low level resistance conferred by first-step mutations in the QRDRs does not prevent bacterial killing in the presence of sufficient levels of a quinolone, they may substantially enhance the number of (secondary) resistant mutants that can be selected from this population. In line with this, it has been demonstrated that deletion of efflux pumps significantly reduces the frequency of emerging fluoroquinolone-resistant isolates [211,327]. A key to preventing fluoroquinolone resistance in *P. aeruginosa* may therefore be to strictly avoid the use of low doses of fluoroquinolones and thus to preclude the emergence of first-step mutations that confer resistance to fluoroquinolones.

4.5 The global *K. pneumoniae* transcriptional landscape

The alarming increase of infections caused by multidrug-resistant pathogens poses a serious threat to human health, the global economy and to society in general [65,68,72]. To successfully combat infections it is crucial to understand the molecular processes of bacterial adaptation to infection-relevant habitats; especially, since the effectiveness of proven antibiotics to control bacterial infections is diminishing and novel treatment-strategies and -targets are urgently needed. Over the past decade, there were multiple reports on the epidemic dissemination of multidrug-resistant Enterobacteriaceae, among which the carbapenemase-producing organisms have been some of the most concerning [33]. The spread of certain epidemic clones that are involved in numerous hospital outbreaks worldwide is an emerging and a major concern [234] and infections with carbapenem-resistant Enterobacteriaceae are common in German intensive care units [330]. The global success of these clonal lineages of multidrug-resistant pathogens is expected to be determined by a complex interplay between pathogenicity, epidemicity, and antibiotic resistance. While the impact on virulence and fitness of several individual antibiotic resistance mechanisms on the global success of the bacterial pathogens seems to be established, other specific adaptive traits that may explain the success of epidemic high-risk clones remain largely unexplored [223]. Understanding the reasons for the success of these clones could be crucial for designing specific and targeted treatment and infection control strategies.

In the cross-sectional study described in chapters 3.3 and 3.4, the advantages of deep transcriptome sequencing (RNA-seq) were exploited to gain an unbiased view on the global transcriptional landscape of clinical *K. pneumoniae* isolates. Besides valuable transcriptomic information, RNA-seq allows for the extraction of the genomic sequences on the single nucleotide level of sufficiently transcribed genes, which, together with multilocus sequence typing [186] and capsular typing based on the *wzi* gene sequence [149,230], provided detailed insights into the phylogenetic relationship of the 37 clinical *K. pneumoniae* isolates studied in this work. The phylogenetic data revealed that most of the clinical isolates belong to the two sequence types ST101 and ST258 - including the closely related isolates of ST512. Both groups comprise world-wide distributed, often multidrug-resistant epidemic clones with a high risk potential. Of note, while 12 out of 13 ST101 isolates in this study seemed to originate from a common reservoir and therefore could likely be involved in a hospital outbreak, the ST258 isolates were less closely related and were obtained from various hospitals.

In this study, unprecedented high-resolution transcriptome data of clinical *K. pneumoniae* isolates was recorded in its full complexity. We combined the transcriptome data with an analysis of infection relevant phenotypes such as of biofilm formation and virulence in a *Galleria* infection model and explored potential biological parameters that may explain the success of these high-risk clones. By

using a pan-genome as a reference assembled from 11 previously published and publicly available genome sequences, we observed that a large set of 3346 genes was expressed in all isolates. These genes showed great overlap (75 %) with the core-genome consisting of 3336 genes and, like the core-genome, consists mostly of genes with central house-keeping functions. Most strikingly, we found clustering of isolates based on differential expression profiles of those commonly expressed genes. These results are in stark contrast to those obtained from *Pseudomonas aeruginosa* [331] and *Escherichia coli* [332]. The size of the core-genome with 3336 genes is very similar to the one of *E. coli* with approximately 3000 genes [333], considering the average *K. pneumoniae* genome is around 10 % larger with a size of 5.5 Mb as compared to *E. coli* with 5.1 Mb; nevertheless, the phylogenetic background in *E. coli* was only reflected in the overall gene expression profiles, which included accessory gene sets, lacking subgroup-specific differences in core-genome expression profiles [332]. In *P. aeruginosa* even the acquisition of accessory genes seemed to be isolate specific and was independent of the phylogenetic background [331].

Since *K. pneumoniae* ST258 isolates showed striking sequence type specific differences in their global expression profiles, we sought to correlate the expression profiles with the infection relevant phenotypes of virulence and biofilm formation. In a *Galleria* infection model, virulence has been shown to correlate to resistance to human serum [239] and was linked to the occurrence of the K1 and K2 capsular type [248]. However, none of our isolates were of K1 or K2 type. Nevertheless, we observed differences in the virulence of the isolates between the various sequence types, but also within isolates of the same sequence type. These results clearly indicate that virulence - as measured under the chosen experimental conditions in the *Galleria* infection model - is not associated with a particular sequence type. The same variation in virulence was previously described for ST258 isolates containing the *wzi*-154 allele (which is also shared by ST512 isolates) in a *Galleria* infection model, macrophage killing assay and human serum resistance assay [239]. Thus, it seems that *K. pneumoniae* virulence is not exclusively determined by the capsular type or a sequence type, but rather that certain yet to be identified virulence traits contribute to the bacterial pathogenicity. The analysis of *ex vivo* transcriptomes recorded during the course of infection [332,334-336] might provide valuable information on how this pathogen adapts to the host.

Biofilm formation experiments showed that all ST258 isolates formed only poor biofilms, while in most of the other clinical strains biofilm formation was more common [156]. Classifying the strains into biofilm-proficient and -deficient isolates revealed differential expression of 90 genes, some of which have previously been linked to biofilm formation. 41 of those belonged to the core-transcriptome. These results indicate that the high-risk clone ST258 has adopted poor biofilm formation as a common trait, and this trait is determined by distinct changes in the transcriptome. This finding might be unexpected since the capability to form biofilms has been associated with more

successful survival in the clinical environment [337]. Nevertheless, the finding that the ST258 isolates share a non-biofilm-specific gene expression profile within their core-transcriptome strongly implicates that this trait confers to an advantageous phenotype that might be linked to the establishment and maintenance of an infection within the human host but it might also be linked to a more successful spreading or survival of this clonal linage in the hospital setting. Further studies are inevitable to explore a possible correlation of the incidence of the ST258 *K. pneumoniae* sequence type with distinct patient or hospital environmental settings that might privilege biofilm-deficient isolates and whether there are specific hospital settings that favor the dissemination of ST258 isolates over those of other epidemic clones.

4.6 Genetic determinants of antibiotic resistance in clinical *K. pneumoniae* isolates

In order to gain detailed insights into the molecular mechanism leading to antimicrobial resistance in the clinical *K. pneumoniae* isolates, this comprehensive RNA-seq data set was analyzed for the occurrence of horizontally acquired enzymes, chromosomal mutations and differences in gene expression. Although antimicrobial resistance in Gram-negative bacteria can be caused by a plethora of diverse and variable resistance conferring mechanisms, it was very surprising to see, that resistance to the most important classes of fluoroquinolones, carbapenems and aminoglycosides can be explained by the presence of just a few resistance determinants (see Figure 4.1)

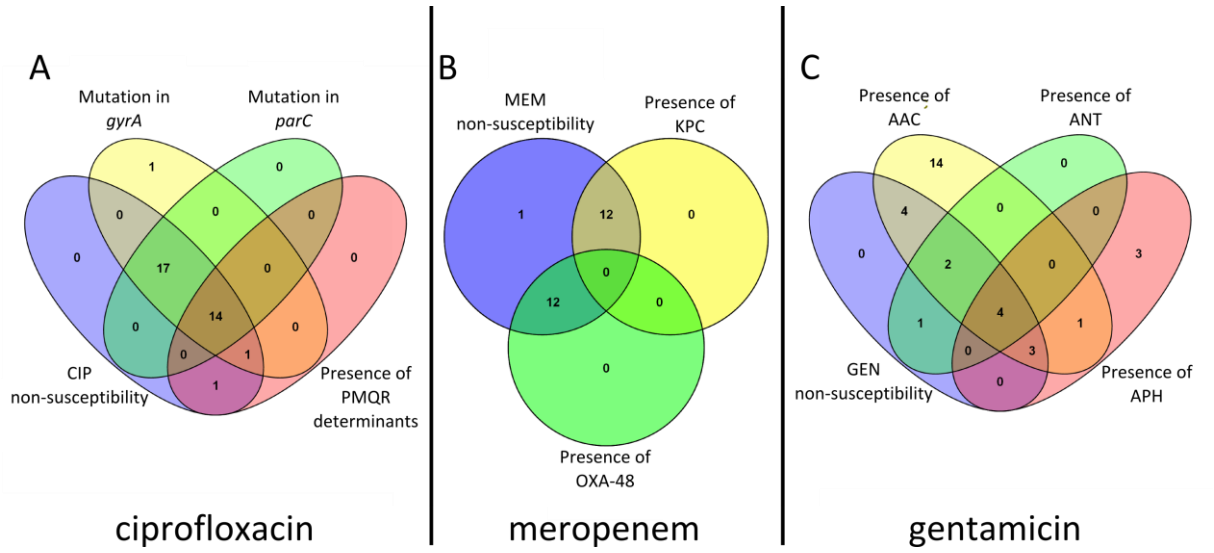

Figure 4.1: Overlap of antibiotic non-susceptibility with occurrence of certain antibiotic resistance determinants.

The Venn diagrams show the overlap of antibiotic non-susceptibility and the occurrence of certain resistance determining mechanisms for ciprofloxacin (A), meropenem (B) and gentamicin (C). All isolates which were non-susceptible (classified as

either resistant or intermediate according to CLSI guidelines [142]) were taken into account for the graphs. All resistance determinants are listed in more detail in Tables 3.11-13. Venn diagrams were created using VENNY [338].
CIP, ciprofloxacin, MEM, meropenem, GEN, gentamicin, PMQR, plasmid-mediated quinolone resistance

Similarly to *P. aeruginosa*, fluoroquinolone resistance in this panel of *K. pneumoniae* isolates is largely dependent on target mutations within *gyrA* and *parC*, whereas further mechanisms like enhanced efflux and the occurrence of plasmid mediated quinolone seem to play a minor role. Almost all non-susceptible isolates exhibited a mutation within the QRDRs of *gyrA* and *parC*, rendering these SNPs appropriate resistance markers. Only a single non-susceptible isolates could be detected which did not show any amino acid alterations in these genes. Nevertheless, non-susceptibility in this isolate can be explained by the presence of the plasmid-mediated quinolone resistance determinants AAC(6')-Ib-cr and QnrB1.

Carbapenem resistance is known to be facilitated by an interplay of diminished drug uptake through porin deficiencies and the production of carbapenem hydrolyzing enzymes. Here, in all but one isolates non-susceptibility to meropenem can be attributed to the expression of either KPC or OXA-48 carbapenemases and furthermore, none of these determinants were identified in susceptible isolates. Only a single isolate, which showed intermediate resistance to meropenem, does not exhibit detectable resistance mechanisms.

The most prevalent mechanism causing aminoglycoside resistance in Enterobacteriaceae is the presence of certain, mainly horizontally acquired, AMEs and consequently, all non-susceptible isolates contained at least one of these enzymes. On the contrary, the majority of susceptible isolates also contained at least one AME, mostly of AAC(6')-type. Since AMEs are highly specific in their substrate spectrum and activity varies greatly between their different types [132], it is crucial to identify AMEs precisely to study the mechanism causing aminoglycoside resistance. For example, the N-acetyltransferase AAC(6')-Ib-C does not confer resistance to gentamicin [281,282], whereas the variants AAC(6')-Ib' [283] and AAC(6')-Ib-cr [110] are known for their gentamicin inhibiting nature. Here, due to low or incomplete sequencing coverage of AMEs in many isolates, it was not possible to extract the complete sequence and therefore their exact type could not be determined. Further additional studies, e.g. Sanger sequencing of resistance cassettes, are needed to be able to draw conclusions on the aminoglycoside resistance conferring mechanisms.

Although our results suggest that deep transcriptome sequencing is highly valuable in identifying molecular mechanisms associated with antimicrobial resistance, in several *K. pneumoniae* isolates the resistance phenotypes could not be explained to its full extend by the presence or absence of known resistance markers. This highlights one of the pitfalls of RNA-seq where the detection of mutations or presence of genes is highly dependent on the expression thereof. The combination of RNA-seq with complimentary analysis such as whole genome sequencing will therefore allow

researchers to study the molecular mechanisms leading to antimicrobial resistance in their full complexity. So far, several studies have used whole genome sequencing to identify antimicrobial resistance -related factors and correlated this information with susceptibility data, but all of them lacked information about transcript abundancies [339-343]. To our knowledge, only one study used the combination of whole genome and transcriptome sequencing to study antimicrobial resistance. In this publication, Wright and colleagues could successfully elucidate colistin resistance in clinical *K. pneumoniae* isolates [227].

4.7 Prediction of antibiotic resistance based on genotypic data

The recent major advances in (next generation) sequencing technologies have positioned this valuable method to become an essential tool to control antibiotic resistance. Highly increasing accuracy, rapidly falling costs and ever decreasing turnaround times will facilitate the implementation of whole-genome sequencing into diagnostic and public health microbiology in the near future [344]. In clinical microbiology next generation sequencing has the power to tackle three essential tasks at the same time: species identification, determination of its properties e.g. antibiotic resistance and virulence and infection control through surveillance [345]. Recent studies demonstrated the power of whole genome sequencing as an analytical tool to investigate clinical outbreaks. Köser *et al.* studied an outbreak of methicillin-resistant *S. aureus* to identify transmission events and delivered valuable information within a clinically relevant time frame of 1.5 days from DNA extraction to sequence analysis [346]. Snitkin and colleagues combined whole-genome sequencing with epidemiological data to reveal the transmission route of an outbreak of carbapenem-resistant *K. pneumoniae* and therefore provided valuable information for clinicians [47]. Reuter *et al.* accurately discriminated between outbreak and non-outbreak isolates of several Gram-negative pathogens and demonstrated that whole genome sequencing was superior to conventional typing methods [347]. Recent advances in sample preparation have even enabled whole genome sequencing directly from single bacterial colonies [348], thereby dramatically decreasing the time between isolation of a pathogen and identification of its species and properties.

Currently, microbiological diagnosis involves the pathogen identification followed by antimicrobial susceptibility testing via various, highly standardized methods like broth microdilution, antimicrobial gradients, disc diffusion or automated systems (e.g. Vitek2). However, antimicrobial susceptibility depends substantially on the growth of bacteria and requires usually 16 hours, but can be significantly longer in the case of slow growing organisms like Mycobacteria [349]. An early and rapid reporting of antibiotic susceptibility is crucial to facilitate a quick, efficient and successful treatment with appropriate antibiotics and has both clinical and financial benefits [350]. Hence, novel molecular

approaches facilitating fast and reliable pathogen identification and susceptibility testing are needed. A promising strategy to detect molecular markers of antibiotic resistance is the application of reliable and cost-effective targeted resequencing methods.

Microarray analysis has been widely used to detect antibiotic resistance genes in clinical isolates of various origins and current arrays have the capability to analyze the presence of numerous sequences of a broad range of organisms. The recently published NanoCHIP® enables the detection of 400 resistance markers of carbapenemase producing *K. pneumoniae*, methicillin-resistant S*. aureus* and vancomycin-resistant *Enterococcus* directly from swab cultures in a single approach [351]. However, the application of microarrays in clinical antibiotic susceptibility testing bears some major disadvantages, since the design of microarrays is labor-intensive and errors introduced during probe synthesis are problematic. Furthermore the production of custom microarrays is expensive and its inflexibility makes the use of an microarray inefficient for clinical diagnostics [352].

Another promising technology for microorganism typing and detection of genomic antibiotic resistance markers is the application of mass spectrometry to analyze nucleic acid sequences [353]. One example is the MassARRAY® iPLEX® genotyping platform (former Sequenom, now Agena Bioscience) which detects distinct mass differences of the four nucleotides by coupling single base primer extension PCRs with matrix-assisted laser desorption/ionization time-of-flight mass spectrometry (MALDI-TOF). MassARRAY allows the detection of SNPs, indels and copy number variants and, when using cDNA, can also be applied to quantify differential gene expression [354,355]. MassARRAY genotyping is a time- and cost-effective high-throughput method which simultaneously exhibits excellent sensitivity and specificity. It has already been applied to detect resistance determinants in human cancer cells [356], mosquitoes [357], viruses [358,359] and bacteria [360]. Furthermore, it has successfully been used in the typing of clonal lineages of *Mycobacterium tuberculosis* [361], *Neisseria gonorrhoeae* [362] and *Yersinia pestis* [363].

In conclusion, the application of novel genotyping methods, for example whole genome sequencing, microarrays or genotyping via mass spectrometry, is becoming the method of choice for monitoring pathogens and identification of outbreaks in research facilities [345]. However, the implementation in the clinic requires exhaustive knowledge about the nature and impact of molecular resistance determinants. Therefore, further studies on the cellular processes leading to antimicrobial resistance, like the ones presented in this thesis, are needed to accurately predict antibiotic resistance based on genotypic data.

5 Appendix

The following supplementary files are stored on a compact disc and have been attached at the end of this thesis:

supplementary file S1:	resistance_genes.fasta
supplementary table S2:	QRDR mutations and expression of the four major efflux pumps in clinical *P. aeruginosa* isolates
supplementary table S3:	Complete list of the K. pneumoniae pan-genome with information about transcription conservation and variation
supplementary table S4:	Complete list of the accessory transcriptomes of clinical *K. pneumoniae* isolates
supplementary table S5:	Identified virulence associate genes in the accessory transcriptome of clinical *K. pneumoniae* isolates

6 References

1. Cooper TF, Rozen DE, Lenski RE (2003) Parallel changes in gene expression after 20,000 generations of evolution in Escherichiacoli. Proc Natl Acad Sci U S A 100: 1072-1077.
2. Tavares LS, Silva CS, de Souza VC, da Silva VL, Diniz CG, et al. (2013) Strategies and molecular tools to fight antimicrobial resistance: resistome, transcriptome, and antimicrobial peptides. Front Microbiol 4: 412.
3. Boucher HW, Talbot GH, Bradley JS, Edwards JE, Gilbert D, et al. (2009) Bad bugs, no drugs: no ESKAPE! An update from the Infectious Diseases Society of America. Clin Infect Dis 48: 1-12.
4. (2005) Bergey's Manual of Systematic Bacteriology, Volume 2: The Proteobacteria; Garrity GB, J. D, Krieg NR, Staley JR, editors: Springer-Verlag.
5. Parsek TLYaMR (2006) Pseudomonas aeruginosa. In: Dworkin M, Falkow, S., Rosenberg, E., Schleifer, K. & Stackebrandt, E.,, editor. The Prokaryotes Springer Verlag.
6. Stover CK, Pham XQ, Erwin AL, Mizoguchi SD, Warrener P, et al. (2000) Complete genome sequence of Pseudomonas aeruginosa PAO1, an opportunistic pathogen. Nature 406: 959-964.
7. Green SK, Schroth MN, Cho JJ, Kominos SK, Vitanza-jack VB (1974) Agricultural plants and soil as a reservoir for Pseudomonas aeruginosa. Appl Microbiol 28: 987-991.
8. Palleroni NJ (1984) Genus I. Pseudomonas Migula 1984. In: Holt NRKaJG, editor. Bergey's Manual of Systematic Bacteriology. Baltimore: Williams and Wilkins.
9. Silby MW, Winstanley C, Godfrey SA, Levy SB, Jackson RW (2011) Pseudomonas genomes: diverse and adaptable. FEMS Microbiol Rev 35: 652-680.
10. Williams HD, Zlosnik JE, Ryall B (2007) Oxygen, cyanide and energy generation in the cystic fibrosis pathogen Pseudomonas aeruginosa. Adv Microb Physiol 52: 1-71.
11. Eschbach M, Schreiber K, Trunk K, Buer J, Jahn D, et al. (2004) Long-term anaerobic survival of the opportunistic pathogen Pseudomonas aeruginosa via pyruvate fermentation. J Bacteriol 186: 4596-4604.
12. Costerton JW, Stewart PS, Greenberg EP (1999) Bacterial biofilms: a common cause of persistent infections. Science 284: 1318-1322.
13. (1998) National Nosocomial Infections Surveillance (NNIS) System report, data summary from October 1986-April 1998, issued June 1998. Am J Infect Control 26: 522-533.
14. Sievert DM, Ricks P, Edwards JR, Schneider A, Patel J, et al. (2013) Antimicrobial-resistant pathogens associated with healthcare-associated infections: summary of data reported to the National Healthcare Safety Network at the Centers for Disease Control and Prevention, 2009-2010. Infect Control Hosp Epidemiol 34: 1-14.
15. Gaynes R, Edwards JR, National Nosocomial Infections Surveillance S (2005) Overview of nosocomial infections caused by gram-negative bacilli. Clin Infect Dis 41: 848-854.
16. Blanc DS, Petignat C, Janin B, Bille J, Francioli P (1998) Frequency and molecular diversity of Pseudomonas aeruginosa upon admission and during hospitalization: a prospective epidemiologic study. Clin Microbiol Infect 4: 242-247.
17. Sader HS, Farrell DJ, Flamm RK, Jones RN (2014) Antimicrobial susceptibility of Gram-negative organisms isolated from patients hospitalized in intensive care units in United States and European hospitals (2009-2011). Diagn Microbiol Infect Dis 78: 443-448.
18. Franzetti F, Cernuschi M, Esposito R, Moroni M (1992) Pseudomonas infections in patients with AIDS and AIDS-related complex. J Intern Med 231: 437-443.
19. Bendig JW, Kyle PW, Giangrande PL, Samson DM, Azadian BS (1987) Two neutropenic patients with multiple resistant Pseudomonas aeruginosa septicaemia treated with ciprofloxacin. J R Soc Med 80: 316-317.

20. Richards MJ, Edwards JR, Culver DH, Gaynes RP (2000) Nosocomial infections in combined medical-surgical intensive care units in the United States. Infect Control Hosp Epidemiol 21: 510-515.
21. Lyczak JB, Cannon CL, Pier GB (2000) Establishment of Pseudomonas aeruginosa infection: lessons from a versatile opportunist. Microbes Infect 2: 1051-1060.
22. Gellatly SL, Hancock RE (2013) Pseudomonas aeruginosa: new insights into pathogenesis and host defenses. Pathog Dis 67: 159-173.
23. Rowe SM, Miller S, Sorscher EJ (2005) Cystic fibrosis. N Engl J Med 352: 1992-2001.
24. Boucher RC, Cotton CU, Gatzy JT, Knowles MR, Yankaskas JR (1988) Evidence for reduced Cl- and increased Na+ permeability in cystic fibrosis human primary cell cultures. J Physiol 405: 77-103.
25. Rice LB (2008) Federal funding for the study of antimicrobial resistance in nosocomial pathogens: no ESKAPE. J Infect Dis 197: 1079-1081.
26. Walsh C (2003) Antibiotics: Actions, Origins, Resistance: ASM Press.
27. Walsh C (2000) Molecular mechanisms that confer antibacterial drug resistance. Nature 406: 775-781.
28. Alekshun MN, Levy SB (2007) Molecular mechanisms of antibacterial multidrug resistance. Cell 128: 1037-1050.
29. Yigit H, Queenan AM, Anderson GJ, Domenech-Sanchez A, Biddle JW, et al. (2001) Novel carbapenem-hydrolyzing beta-lactamase, KPC-1, from a carbapenem-resistant strain of Klebsiella pneumoniae. Antimicrob Agents Chemother 45: 1151-1161.
30. Kumarasamy KK, Toleman MA, Walsh TR, Bagaria J, Butt F, et al. (2010) Emergence of a new antibiotic resistance mechanism in India, Pakistan, and the UK: a molecular, biological, and epidemiological study. Lancet Infect Dis 10: 597-602.
31. Daikos GL, Markogiannakis A (2011) Carbapenemase-producing Klebsiella pneumoniae: (when) might we still consider treating with carbapenems? Clin Microbiol Infect 17: 1135-1141.
32. Rapp RP, Urban C (2012) Klebsiella pneumoniae carbapenemases in Enterobacteriaceae: history, evolution, and microbiology concerns. Pharmacotherapy 32: 399-407.
33. Nordmann P, Cuzon G, Naas T (2009) The real threat of Klebsiella pneumoniae carbapenemase-producing bacteria. Lancet Infect Dis 9: 228-236.
34. Podschun R, Ullmann U (1998) Klebsiella spp. as nosocomial pathogens: epidemiology, taxonomy, typing methods, and pathogenicity factors. Clin Microbiol Rev 11: 589-603.
35. Livermore DM, Hope R, Brick G, Lillie M, Reynolds R, et al. (2008) Non-susceptibility trends among Enterobacteriaceae from bacteraemias in the UK and Ireland, 2001-06. J Antimicrob Chemother 62 Suppl 2: ii41-54.
36. Correa L, Martino MD, Siqueira I, Pasternak J, Gales AC, et al. (2013) A hospital-based matched case-control study to identify clinical outcome and risk factors associated with carbapenem-resistant Klebsiella pneumoniae infection. BMC Infect Dis 13: 80.
37. Liu YC, Cheng DL, Lin CL (1986) Klebsiella pneumoniae liver abscess associated with septic endophthalmitis. Arch Intern Med 146: 1913-1916.
38. Wang JH, Liu YC, Lee SS, Yen MY, Chen YS, et al. (1998) Primary liver abscess due to Klebsiella pneumoniae in Taiwan. Clin Infect Dis 26: 1434-1438.
39. Struve C, Bojer M, Krogfelt KA (2008) Characterization of Klebsiella pneumoniae type 1 fimbriae by detection of phase variation during colonization and infection and impact on virulence. Infect Immun 76: 4055-4065.
40. Brisse S, Fevre C, Passet V, Issenhuth-Jeanjean S, Tournebize R, et al. (2009) Virulent clones of Klebsiella pneumoniae: identification and evolutionary scenario based on genomic and phenotypic characterization. PLoS One 4: e4982.
41. Domenico P, Salo RJ, Cross AS, Cunha BA (1994) Polysaccharide capsule-mediated resistance to opsonophagocytosis in Klebsiella pneumoniae. Infect Immun 62: 4495-4499.
42. Campos MA, Vargas MA, Regueiro V, Llompart CM, Alberti S, et al. (2004) Capsule polysaccharide mediates bacterial resistance to antimicrobial peptides. Infect Immun 72: 7107-7114.

43. Fung CP, Siu LK (2007) Virulence of Klebsiella pneumoniae serotype K2 should not be underestimated in K. pneumoniae liver abscess. Clin Infect Dis 45: 1530-1531; author reply 1532-1533.
44. Hart CA (1993) Klebsiellae and neonates. J Hosp Infect 23: 83-86.
45. Orskov I (1952) Nosocomial infections with Klebsiella in lesions of the urinary tract. Acta Pathol Microbiol Scand Suppl 93: 259-271.
46. Lockhart SR, Abramson MA, Beekmann SE, Gallagher G, Riedel S, et al. (2007) Antimicrobial resistance among Gram-negative bacilli causing infections in intensive care unit patients in the United States between 1993 and 2004. J Clin Microbiol 45: 3352-3359.
47. Snitkin ES, Zelazny AM, Thomas PJ, Stock F, Group NCSP, et al. (2012) Tracking a hospital outbreak of carbapenem-resistant Klebsiella pneumoniae with whole-genome sequencing. Sci Transl Med 4: 148ra116.
48. U.S. Department of Health and human Services - Centers for Disease Control and Prevention (2013) Antibiotic Resistance Threats in the United States.
49. Waksman SA (1947) What is an antibiotic or an antibiotic substance? Mycologia 39: 565-569.
50. Aminov RI (2010) A brief history of the antibiotic era: lessons learned and challenges for the future. Front Microbiol 1: 134.
51. Sepkowitz KA (2011) One hundred years of Salvarsan. N Engl J Med 365: 291-293.
52. Schatz A, Waksman SA (1944) Effect of Streptomycin and Other Antibiotic Substances upon Mycobacterium tuberculosis and Related Organisms. Experimental Biology and Medicine 57: 244-248
53. Demain AL, Sanchez S (2009) Microbial drug discovery: 80 years of progress. J Antibiot (Tokyo) 62: 5-16.
54. Coates AR, Halls G, Hu Y (2011) Novel classes of antibiotics or more of the same? Br J Pharmacol 163: 184-194.
55. Hall BG, Barlow M (2004) Evolution of the serine beta-lactamases: past, present and future. Drug Resist Updat 7: 111-123.
56. Baltz R (2005) Antibiotic discovery from actinomycetes: will a renaissance follow the decline and fall. SIM News 55: 186-196.
57. D'Costa VM, King CE, Kalan L, Morar M, Sung WW, et al. (2011) Antibiotic resistance is ancient. Nature 477: 457-461.
58. Davies J, Davies D (2010) Origins and evolution of antibiotic resistance. Microbiol Mol Biol Rev 74: 417-433.
59. Abraham EP, Chain E (1988) An enzyme from bacteria able to destroy penicillin. 1940. Rev Infect Dis 10: 677-678.
60. Fleming A (1946) Chemotherapy, Yesterday, Today and Tomorrow. Linacre lecture, Cambridge University press.
61. Meziane-Cherif D, Courvalin P (2014) Antibiotic resistance: to the rescue of old drugs. Nature 510: 477-478.
62. Silver LL (2011) Challenges of antibacterial discovery. Clin Microbiol Rev 24: 71-109.
63. Palmer AC, Kishony R (2013) Understanding, predicting and manipulating the genotypic evolution of antibiotic resistance. Nat Rev Genet 14: 243-248.
64. Spellberg B, Guidos R, Gilbert D, Bradley J, Boucher HW, et al. (2008) The epidemic of antibiotic-resistant infections: a call to action for the medical community from the Infectious Diseases Society of America. Clin Infect Dis 46: 155-164.
65. World Health Organization (2012) The evolving threat of antimicrobial resistance: options for action.
66. Obritsch MD, Fish DN, MacLaren R, Jung R (2005) Nosocomial infections due to multidrug-resistant Pseudomonas aeruginosa: epidemiology and treatment options. Pharmacotherapy 25: 1353-1364.

67. Aloush V, Navon-Venezia S, Seigman-Igra Y, Cabili S, Carmeli Y (2006) Multidrug-resistant Pseudomonas aeruginosa: risk factors and clinical impact. Antimicrob Agents Chemother 50: 43-48.
68. Giske CG, Monnet DL, Cars O, Carmeli Y, ReAct-Action on Antibiotic R (2008) Clinical and economic impact of common multidrug-resistant gram-negative bacilli. Antimicrob Agents Chemother 52: 813-821.
69. Lister PD, Wolter DJ, Hanson ND (2009) Antibacterial-resistant Pseudomonas aeruginosa: clinical impact and complex regulation of chromosomally encoded resistance mechanisms. Clin Microbiol Rev 22: 582-610.
70. Hegreness M, Shoresh N, Damian D, Hartl D, Kishony R (2008) Accelerated evolution of resistance in multidrug environments. Proc Natl Acad Sci U S A 105: 13977-13981.
71. Papp-Wallace KM, Endimiani A, Taracila MA, Bonomo RA (2011) Carbapenems: past, present, and future. Antimicrob Agents Chemother 55: 4943-4960.
72. Cinel I, Dellinger RP (2007) Advances in pathogenesis and management of sepsis. Curr Opin Infect Dis 20: 345-352.
73. Levy SB, Marshall B (2004) Antibacterial resistance worldwide: causes, challenges and responses. Nat Med 10: S122-129.
74. Infectious Diseases Society of A, Spellberg B, Blaser M, Guidos RJ, Boucher HW, et al. (2011) Combating antimicrobial resistance: policy recommendations to save lives. Clin Infect Dis 52 Suppl 5: S397-428.
75. van Duin D, Kaye KS, Neuner EA, Bonomo RA (2013) Carbapenem-resistant Enterobacteriaceae: a review of treatment and outcomes. Diagn Microbiol Infect Dis 75: 115-120.
76. ECDC/EMEA Joint Technical Report (2009) The bacterial challenge: time to react.
77. So AD, Gupta N, Cars O (2010) Tackling antibiotic resistance. BMJ 340: c2071.
78. Review on Antimicrobial Resistance (2014) Antimicrobial Resistance: Tackling a Crisis for the Health and Wealth of Nations. .
79. Hamilton-Miller JM (1997) Living in the 'post-antibiotic era': could the use of probiotics be an effective strategy? Clin Microbiol Infect 3: 2-3.
80. Hede K (2014) Antibiotic resistance: An infectious arms race. Nature 509: S2-3.
81. Breidenstein EB, de la Fuente-Nunez C, Hancock RE (2011) Pseudomonas aeruginosa: all roads lead to resistance. Trends Microbiol 19: 419-426.
82. Fernandez L, Breidenstein EB, Hancock RE (2011) Creeping baselines and adaptive resistance to antibiotics. Drug Resist Updat 14: 1-21.
83. Fernandez L, Hancock RE (2012) Adaptive and mutational resistance: role of porins and efflux pumps in drug resistance. Clin Microbiol Rev 25: 661-681.
84. Nikaido H (1994) Prevention of drug access to bacterial targets: permeability barriers and active efflux. Science 264: 382-388.
85. Strateva T, Yordanov D (2009) Pseudomonas aeruginosa - a phenomenon of bacterial resistance. J Med Microbiol 58: 1133-1148.
86. Poole K (2005) Efflux-mediated antimicrobial resistance. J Antimicrob Chemother 56: 20-51.
87. Putman M, van Veen HW, Konings WN (2000) Molecular properties of bacterial multidrug transporters. Microbiol Mol Biol Rev 64: 672-693.
88. Zgurskaya HI, Nikaido H (2000) Multidrug resistance mechanisms: drug efflux across two membranes. Mol Microbiol 37: 219-225.
89. Ziha-Zarifi I, Llanes C, Kohler T, Pechere JC, Plesiat P (1999) In vivo emergence of multidrug-resistant mutants of Pseudomonas aeruginosa overexpressing the active efflux system MexA-MexB-OprM. Antimicrob Agents Chemother 43: 287-291.
90. Llanes C, Hocquet D, Vogne C, Benali-Baitich D, Neuwirth C, et al. (2004) Clinical strains of Pseudomonas aeruginosa overproducing MexAB-OprM and MexXY efflux pumps simultaneously. Antimicrob Agents Chemother 48: 1797-1802.

91. Yamamoto M, Ueda A, Kudo M, Matsuo Y, Fukushima J, et al. (2009) Role of MexZ and PA5471 in transcriptional regulation of mexXY in Pseudomonas aeruginosa. Microbiology 155: 3312-3321.
92. Jeannot K, Sobel ML, El Garch F, Poole K, Plesiat P (2005) Induction of the MexXY efflux pump in Pseudomonas aeruginosa is dependent on drug-ribosome interaction. J Bacteriol 187: 5341-5346.
93. Morita Y, Sobel ML, Poole K (2006) Antibiotic inducibility of the MexXY multidrug efflux system of Pseudomonas aeruginosa: involvement of the antibiotic-inducible PA5471 gene product. J Bacteriol 188: 1847-1855.
94. Chen H, Hu J, Chen PR, Lan L, Li Z, et al. (2008) The Pseudomonas aeruginosa multidrug efflux regulator MexR uses an oxidation-sensing mechanism. Proc Natl Acad Sci U S A 105: 13586-13591.
95. Schweizer HP (2003) Efflux as a mechanism of resistance to antimicrobials in Pseudomonas aeruginosa and related bacteria: unanswered questions. Genet Mol Res 2: 48-62.
96. Mima T, Joshi S, Gomez-Escalada M, Schweizer HP (2007) Identification and characterization of TriABC-OpmH, a triclosan efflux pump of Pseudomonas aeruginosa requiring two membrane fusion proteins. J Bacteriol 189: 7600-7609.
97. Yang L, Chen L, Shen L, Surette M, Duan K (2011) Inactivation of MuxABC-OpmB transporter system in Pseudomonas aeruginosa leads to increased ampicillin and carbenicillin resistance and decreased virulence. J Microbiol 49: 107-114.
98. Drlica K, Zhao X (1997) DNA gyrase, topoisomerase IV, and the 4-quinolones. Microbiol Mol Biol Rev 61: 377-392.
99. Hooper DC, Wolfson JS (1991) Fluoroquinolone antimicrobial agents. N Engl J Med 324: 384-394.
100. Shorr AF (2009) Review of studies of the impact on Gram-negative bacterial resistance on outcomes in the intensive care unit. Crit Care Med 37: 1463-1469.
101. Gasink LB, Fishman NO, Weiner MG, Nachamkin I, Bilker WB, et al. (2006) Fluoroquinolone-resistant Pseudomonas aeruginosa: assessment of risk factors and clinical impact. Am J Med 119: 526 e519-525.
102. Drlica K, Hiasa H, Kerns R, Malik M, Mustaev A, et al. (2009) Quinolones: action and resistance updated. Curr Top Med Chem 9: 981-998.
103. Froelich-Ammon SJ, Osheroff N (1995) Topoisomerase poisons: harnessing the dark side of enzyme mechanism. J Biol Chem 270: 21429-21432.
104. Ruiz J (2003) Mechanisms of resistance to quinolones: target alterations, decreased accumulation and DNA gyrase protection. J Antimicrob Chemother 51: 1109-1117.
105. Hooper DC, Wolfson JS (1989) Bacterial resistance to the quinolone antimicrobial agents. Am J Med 87: 17S-23S.
106. Yoshida H, Bogaki M, Nakamura M, Nakamura S (1990) Quinolone resistance-determining region in the DNA gyrase gyrA gene of Escherichia coli. Antimicrob Agents Chemother 34: 1271-1272.
107. Barnard FM, Maxwell A (2001) Interaction between DNA gyrase and quinolones: effects of alanine mutations at GyrA subunit residues Ser(83) and Asp(87). Antimicrob Agents Chemother 45: 1994-2000.
108. Tran JH, Jacoby GA (2002) Mechanism of plasmid-mediated quinolone resistance. Proc Natl Acad Sci U S A 99: 5638-5642.
109. Perichon B, Courvalin P, Galimand M (2007) Transferable resistance to aminoglycosides by methylation of G1405 in 16S rRNA and to hydrophilic fluoroquinolones by QepA-mediated efflux in Escherichia coli. Antimicrob Agents Chemother 51: 2464-2469.
110. Robicsek A, Strahilevitz J, Jacoby GA, Macielag M, Abbanat D, et al. (2006) Fluoroquinolone-modifying enzyme: a new adaptation of a common aminoglycoside acetyltransferase. Nat Med 12: 83-88.
111. Robicsek A, Jacoby GA, Hooper DC (2006) The worldwide emergence of plasmid-mediated quinolone resistance. Lancet Infect Dis 6: 629-640.

112. Strahilevitz J, Jacoby GA, Hooper DC, Robicsek A (2009) Plasmid-mediated quinolone resistance: a multifaceted threat. Clin Microbiol Rev 22: 664-689.
113. Poole K (2004) Resistance to beta-lactam antibiotics. Cell Mol Life Sci 61: 2200-2223.
114. Fisher JF, Meroueh SO, Mobashery S (2005) Bacterial resistance to beta-lactam antibiotics: compelling opportunism, compelling opportunity. Chem Rev 105: 395-424.
115. Worthington RJ, Melander C (2013) Overcoming resistance to beta-lactam antibiotics. J Org Chem 78: 4207-4213.
116. Wise EM, Jr., Park JT (1965) Penicillin: its basic site of action as an inhibitor of a peptide cross-linking reaction in cell wall mucopeptide synthesis. Proc Natl Acad Sci U S A 54: 75-81.
117. Tipper DJ, Strominger JL (1965) Mechanism of action of penicillins: a proposal based on their structural similarity to acyl-D-alanyl-D-alanine. Proc Natl Acad Sci U S A 54: 1133-1141.
118. Essack SY (2001) The development of beta-lactam antibiotics in response to the evolution of beta-lactamases. Pharm Res 18: 1391-1399.
119. Zapun A, Contreras-Martel C, Vernet T (2008) Penicillin-binding proteins and beta-lactam resistance. FEMS Microbiol Rev 32: 361-385.
120. Kong KF, Schneper L, Mathee K (2010) Beta-lactam antibiotics: from antibiosis to resistance and bacteriology. APMIS 118: 1-36.
121. Moore NM, Flaws ML (2011) Treatment strategies and recommendations for Pseudomonas aeruginosa infections. Clin Lab Sci 24: 52-56.
122. Pitout JD, Laupland KB (2008) Extended-spectrum beta-lactamase-producing Enterobacteriaceae: an emerging public-health concern. Lancet Infect Dis 8: 159-166.
123. Nordmann P, Poirel L (2002) Emerging carbapenemases in Gram-negative aerobes. Clin Microbiol Infect 8: 321-331.
124. Livermore DM, Woodford N (2000) Carbapenemases: a problem in waiting? Curr Opin Microbiol 3: 489-495.
125. Pfeifer Y, Cullik A, Witte W (2010) Resistance to cephalosporins and carbapenems in Gram-negative bacterial pathogens. Int J Med Microbiol 300: 371-379.
126. Nordmann P, Poirel L, Walsh TR, Livermore DM (2011) The emerging NDM carbapenemases. Trends Microbiol 19: 588-595.
127. McKenna M (2013) Antibiotic resistance: the last resort. Nature 499: 394-396.
128. Mingeot-Leclercq MP, Glupczynski Y, Tulkens PM (1999) Aminoglycosides: activity and resistance. Antimicrob Agents Chemother 43: 727-737.
129. Davis BD, Chen LL, Tai PC (1986) Misread protein creates membrane channels: an essential step in the bactericidal action of aminoglycosides. Proc Natl Acad Sci U S A 83: 6164-6168.
130. Davis BD (1987) Mechanism of bactericidal action of aminoglycosides. Microbiol Rev 51: 341-350.
131. Becker B, Cooper MA (2013) Aminoglycoside antibiotics in the 21st century. ACS Chem Biol 8: 105-115.
132. Ramirez MS, Tolmasky ME (2010) Aminoglycoside modifying enzymes. Drug Resist Updat 13: 151-171.
133. Breidenstein EB, Khaira BK, Wiegand I, Overhage J, Hancock RE (2008) Complex ciprofloxacin resistome revealed by screening a Pseudomonas aeruginosa mutant library for altered susceptibility. Antimicrob Agents Chemother 52: 4486-4491.
134. Schurek KN, Marr AK, Taylor PK, Wiegand I, Semenec L, et al. (2008) Novel genetic determinants of low-level aminoglycoside resistance in Pseudomonas aeruginosa. Antimicrob Agents Chemother 52: 4213-4219.
135. Fajardo A, Martinez-Martin N, Mercadillo M, Galan JC, Ghysels B, et al. (2008) The neglected intrinsic resistome of bacterial pathogens. PLoS One 3: e1619.
136. Dötsch A, Becker T, Pommerenke C, Magnowska Z, Jansch L, et al. (2009) Genomewide identification of genetic determinants of antimicrobial drug resistance in Pseudomonas aeruginosa. Antimicrob Agents Chemother 53: 2522-2531.

137. Martinez JL, Baquero F (2002) Interactions among strategies associated with bacterial infection: pathogenicity, epidemicity, and antibiotic resistance. Clin Microbiol Rev 15: 647-679.
138. Wright GD (2007) The antibiotic resistome: the nexus of chemical and genetic diversity. Nat Rev Microbiol 5: 175-186.
139. He J, Baldini RL, Deziel E, Saucier M, Zhang Q, et al. (2004) The broad host range pathogen Pseudomonas aeruginosa strain PA14 carries two pathogenicity islands harboring plant and animal virulence genes. Proc Natl Acad Sci U S A 101: 2530-2535.
140. Woodcock DM, Crowther PJ, Doherty J, Jefferson S, DeCruz E, et al. (1989) Quantitative evaluation of Escherichia coli host strains for tolerance to cytosine methylation in plasmid and phage recombinants. Nucleic Acids Res 17: 3469-3478.
141. Simon R PU, Pühler A (1983) A broad host range mobilization system for in vivo genetic engineering: Transposon mutagenesis in gram negative bacteria. Biotechnology.
142. CLSI (2013) Performance Standards for Antimicrobial Susceptibility Testing; Twenty-Third Informational Supplement. Wayne, PA: Clinical and Laboratory Standards Institute.
143. Kumar V, Sun P, Vamathevan J, Li Y, Ingraham K, et al. (2011) Comparative genomics of Klebsiella pneumoniae strains with different antibiotic resistance profiles. Antimicrob Agents Chemother 55: 4267-4276.
144. Rozen S, Skaletsky H (2000) Primer3 on the WWW for general users and for biologist programmers. Methods Mol Biol 132: 365-386.
145. Heeb S, Blumer C, Haas D (2002) Regulatory RNA as mediator in GacA/RsmA-dependent global control of exoproduct formation in Pseudomonas fluorescens CHA0. J Bacteriol 184: 1046-1056.
146. Hoang TT, Karkhoff-Schweizer RR, Kutchma AJ, Schweizer HP (1998) A broad-host-range Flp-FRT recombination system for site-specific excision of chromosomally-located DNA sequences: application for isolation of unmarked Pseudomonas aeruginosa mutants. Gene 212: 77-86.
147. Bruchmann S, Dötsch A, Nouri B, Chaberny IF, Häussler S (2013) Quantitative contributions of target alteration and decreased drug accumulation to Pseudomonas aeruginosa fluoroquinolone resistance. Antimicrob Agents Chemother 57: 1361-1368.
148. Tomas M, Doumith M, Warner M, Turton JF, Beceiro A, et al. (2010) Efflux pumps, OprD porin, AmpC beta-lactamase, and multiresistance in Pseudomonas aeruginosa isolates from cystic fibrosis patients. Antimicrob Agents Chemother 54: 2219-2224.
149. Brisse S, Passet V, Haugaard AB, Babosan A, Kassis-Chikhani N, et al. (2013) wzi Gene sequencing, a rapid method for determination of capsular type for Klebsiella strains. J Clin Microbiol 51: 4073-4078.
150. McLaughlin MM, Advincula MR, Malczynski M, Barajas G, Qi C, et al. (2014) Quantifying the clinical virulence of Klebsiella pneumoniae producing carbapenemase Klebsiella pneumoniae with a Galleria mellonella model and a pilot study to translate to patient outcomes. BMC Infect Dis 14: 31.
151. Ho SN, Hunt HD, Horton RM, Pullen JK, Pease LR (1989) Site-directed mutagenesis by overlap extension using the polymerase chain reaction. Gene 77: 51-59.
152. Wiegand I, Hilpert K, Hancock RE (2008) Agar and broth dilution methods to determine the minimal inhibitory concentration (MIC) of antimicrobial substances. Nat Protoc 3: 163-175.
153. Pustelny C, Brouwer S, Musken M, Bielecka A, Dotsch A, et al. (2013) The peptide chain release factor methyltransferase PrmC is essential for pathogenicity and environmental adaptation of Pseudomonas aeruginosa PA14. Environ Microbiol 15: 597-609.
154. Overhage J, Bains M, Brazas MD, Hancock RE (2008) Swarming of Pseudomonas aeruginosa is a complex adaptation leading to increased production of virulence factors and antibiotic resistance. J Bacteriol 190: 2671-2679.
155. Hall BG, Acar H, Nandipati A, Barlow M (2014) Growth rates made easy. Mol Biol Evol 31: 232-238.

156. Naparstek L, Carmeli Y, Navon-Venezia S, Banin E (2014) Biofilm formation and susceptibility to gentamicin and colistin of extremely drug-resistant KPC-producing Klebsiella pneumoniae. J Antimicrob Chemother 69: 1027-1034.
157. Maldonado N.C. SdRC, Cecilia M. and Nader-Macias M.E. (2007) A simple technique to detect Klebsiella biofilm-forming-strains. Inhibitory potential of Lactobacillus fermentum CRL 1058 whole cells and products. In: Mendez-Vilas A, editor. Communicating Current Research and Educational Topics and Trends in Applied Microbiology: FORMATEX. pp. 52-59.
158. Mordhorst IL, Claus H, Ewers C, Lappann M, Schoen C, et al. (2009) O-acetyltransferase gene neuO is segregated according to phylogenetic background and contributes to environmental desiccation resistance in Escherichia coli K1. Environ Microbiol 11: 3154-3165.
159. Doostzadeh J, Shokralla S, Absalan F, Jalili R, Mohandessi S, et al. (2008) High throughput automated allele frequency estimation by pyrosequencing. PLoS One 3: e2693.
160. Royo JL, Hidalgo M, Ruiz A (2007) Pyrosequencing protocol using a universal biotinylated primer for mutation detection and SNP genotyping. Nat Protoc 2: 1734-1739.
161. Tamura K, Stecher G, Peterson D, Filipski A, Kumar S (2013) MEGA6: Molecular Evolutionary Genetics Analysis version 6.0. Mol Biol Evol 30: 2725-2729.
162. Livak KJ, Schmittgen TD (2001) Analysis of relative gene expression data using real-time quantitative PCR and the 2(-Delta Delta C(T)) Method. Methods 25: 402-408.
163. Cabot G, Ocampo-Sosa AA, Tubau F, Macia MD, Rodriguez C, et al. (2011) Overexpression of AmpC and efflux pumps in Pseudomonas aeruginosa isolates from bloodstream infections: prevalence and impact on resistance in a Spanish multicenter study. Antimicrob Agents Chemother 55: 1906-1911.
164. Dotsch A, Eckweiler D, Schniederjans M, Zimmermann A, Jensen V, et al. (2012) The Pseudomonas aeruginosa transcriptome in planktonic cultures and static biofilms using RNA sequencing. PLoS One 7: e31092.
165. Martinez J, Martinez L, Rosenblueth M, Silva J, Martinez-Romero E (2004) How are gene sequence analyses modifying bacterial taxonomy? The case of Klebsiella. Int Microbiol 7: 261-268.
166. Sridhar J, Sambaturu N, Sabarinathan R, Ou HY, Deng Z, et al. (2010) sRNAscanner: a computational tool for intergenic small RNA detection in bacterial genomes. PLoS One 5: e11970.
167. Wu KM, Li LH, Yan JJ, Tsao N, Liao TL, et al. (2009) Genome sequencing and comparative analysis of Klebsiella pneumoniae NTUH-K2044, a strain causing liver abscess and meningitis. J Bacteriol 191: 4492-4501.
168. Shin SH, Kim S, Kim JY, Lee S, Um Y, et al. (2012) Complete genome sequence of the 2,3-butanediol-producing Klebsiella pneumoniae strain KCTC 2242. J Bacteriol 194: 2736-2737.
169. Liu P, Li P, Jiang X, Bi D, Xie Y, et al. (2012) Complete genome sequence of Klebsiella pneumoniae subsp. pneumoniae HS11286, a multidrug-resistant strain isolated from human sputum. J Bacteriol 194: 1841-1842.
170. Lin AC, Liao TL, Lin YC, Lai YC, Lu MC, et al. (2012) Complete genome sequence of Klebsiella pneumoniae 1084, a hypermucoviscosity-negative K1 clinical strain. J Bacteriol 194: 6316.
171. Ramos PI, Picao RC, Almeida LG, Lima NC, Girardello R, et al. (2014) Comparative analysis of the complete genome of KPC-2-producing Klebsiella pneumoniae Kp13 reveals remarkable genome plasticity and a wide repertoire of virulence and resistance mechanisms. BMC Genomics 15: 54.
172. Deleo FR, Chen L, Porcella SF, Martens CA, Kobayashi SD, et al. (2014) Molecular dissection of the evolution of carbapenem-resistant multilocus sequence type 258 Klebsiella pneumoniae. Proc Natl Acad Sci U S A 111: 4988-4993.
173. Hudson CM, Bent ZW, Meagher RJ, Williams KP (2014) Resistance determinants and mobile genetic elements of an NDM-1-encoding Klebsiella pneumoniae strain. PLoS One 9: e99209.
174. Lunter G, Goodson M (2011) Stampy: a statistical algorithm for sensitive and fast mapping of Illumina sequence reads. Genome Res 21: 936-939.

175. Anders S, Huber W (2010) Differential expression analysis for sequence count data. Genome Biol 11: R106.
176. Chen L, Xiong Z, Sun L, Yang J, Jin Q (2012) VFDB 2012 update: toward the genetic diversity and molecular evolution of bacterial virulence factors. Nucleic Acids Res 40: D641-645.
177. Liu B, Pop M (2009) ARDB--Antibiotic Resistance Genes Database. Nucleic Acids Res 37: D443-447.
178. Schulz MH, Zerbino DR, Vingron M, Birney E (2012) Oases: robust de novo RNA-seq assembly across the dynamic range of expression levels. Bioinformatics 28: 1086-1092.
179. Uchiyama I (2003) MBGD: microbial genome database for comparative analysis. Nucleic Acids Res 31: 58-62.
180. Uchiyama I, Mihara M, Nishide H, Chiba H (2013) MBGD update 2013: the microbial genome database for exploring the diversity of microbial world. Nucleic Acids Res 41: D631-635.
181. Li H, Handsaker B, Wysoker A, Fennell T, Ruan J, et al. (2009) The Sequence Alignment/Map format and SAMtools. Bioinformatics 25: 2078-2079.
182. Sievers F, Higgins DG (2014) Clustal Omega, accurate alignment of very large numbers of sequences. Methods Mol Biol 1079: 105-116.
183. Sievers F, Wilm A, Dineen D, Gibson TJ, Karplus K, et al. (2011) Fast, scalable generation of high-quality protein multiple sequence alignments using Clustal Omega. Mol Syst Biol 7: 539.
184. Winsor GL, Lam DK, Fleming L, Lo R, Whiteside MD, et al. (2011) Pseudomonas Genome Database: improved comparative analysis and population genomics capability for Pseudomonas genomes. Nucleic Acids Res 39: D596-600.
185. Letunic I, Bork P (2011) Interactive Tree Of Life v2: online annotation and display of phylogenetic trees made easy. Nucleic Acids Res 39: W475-478.
186. Diancourt L, Passet V, Verhoef J, Grimont PA, Brisse S (2005) Multilocus sequence typing of Klebsiella pneumoniae nosocomial isolates. J Clin Microbiol 43: 4178-4182.
187. Dimmer EC, Huntley RP, Alam-Faruque Y, Sawford T, O'Donovan C, et al. (2012) The UniProt-GO Annotation database in 2011. Nucleic Acids Res 40: D565-570.
188. Thorvaldsdottir H, Robinson JT, Mesirov JP (2013) Integrative Genomics Viewer (IGV): high-performance genomics data visualization and exploration. Brief Bioinform 14: 178-192.
189. Ewing B, Hillier L, Wendl MC, Green P (1998) Base-calling of automated sequencer traces using phred. I. Accuracy assessment. Genome Res 8: 175-185.
190. Ewing B, Green P (1998) Base-calling of automated sequencer traces using phred. II. Error probabilities. Genome Res 8: 186-194.
191. Gorgani N, Ahlbrand S, Patterson A, Pourmand N (2009) Detection of point mutations associated with antibiotic resistance in Pseudomonas aeruginosa. Int J Antimicrob Agents 34: 414-418.
192. Yoshida H, Nakamura M, Bogaki M, Nakamura S (1990) Proportion of DNA gyrase mutants among quinolone-resistant strains of Pseudomonas aeruginosa. Antimicrob Agents Chemother 34: 1273-1275.
193. Nakano M, Deguchi T, Kawamura T, Yasuda M, Kimura M, et al. (1997) Mutations in the gyrA and parC genes in fluoroquinolone-resistant clinical isolates of Pseudomonas aeruginosa. Antimicrob Agents Chemother 41: 2289-2291.
194. Jalal S, Wretlind B (1998) Mechanisms of quinolone resistance in clinical strains of Pseudomonas aeruginosa. Microb Drug Resist 4: 257-261.
195. Mouneimne H, Robert J, Jarlier V, Cambau E (1999) Type II topoisomerase mutations in ciprofloxacin-resistant strains of Pseudomonas aeruginosa. Antimicrob Agents Chemother 43: 62-66.
196. Takenouchi T, Sakagawa E, Sugawara M (1999) Detection of gyrA mutations among 335 Pseudomonas aeruginosa strains isolated in Japan and their susceptibilities to fluoroquinolones. Antimicrob Agents Chemother 43: 406-409.
197. Lee JK, Lee YS, Park YK, Kim BS (2005) Alterations in the GyrA and GyrB subunits of topoisomerase II and the ParC and ParE subunits of topoisomerase IV in ciprofloxacin-resistant clinical isolates of Pseudomonas aeruginosa. Int J Antimicrob Agents 25: 290-295.

198. Cambau E, Perani E, Dib C, Petinon C, Trias J, et al. (1995) Role of mutations in DNA gyrase genes in ciprofloxacin resistance of Pseudomonas aeruginosa susceptible or resistant to imipenem. Antimicrob Agents Chemother 39: 2248-2252.
199. Oh H, Stenhoff J, Jalal S, Wretlind B (2003) Role of efflux pumps and mutations in genes for topoisomerases II and IV in fluoroquinolone-resistant Pseudomonas aeruginosa strains. Microb Drug Resist 9: 323-328.
200. Akasaka T, Tanaka M, Yamaguchi A, Sato K (2001) Type II topoisomerase mutations in fluoroquinolone-resistant clinical strains of Pseudomonas aeruginosa isolated in 1998 and 1999: role of target enzyme in mechanism of fluoroquinolone resistance. Antimicrob Agents Chemother 45: 2263-2268.
201. Bagel S, Hullen V, Wiedemann B, Heisig P (1999) Impact of gyrA and parC mutations on quinolone resistance, doubling time, and supercoiling degree of Escherichia coli. Antimicrob Agents Chemother 43: 868-875.
202. Jalal S, Ciofu O, Hoiby N, Gotoh N, Wretlind B (2000) Molecular mechanisms of fluoroquinolone resistance in Pseudomonas aeruginosa isolates from cystic fibrosis patients. Antimicrob Agents Chemother 44: 710-712.
203. Higgins PG, Fluit AC, Milatovic D, Verhoef J, Schmitz FJ (2003) Mutations in GyrA, ParC, MexR and NfxB in clinical isolates of Pseudomonas aeruginosa. Int J Antimicrob Agents 21: 409-413.
204. Wang DD, Sun TY, Hu YJ (2007) Contributions of efflux pumps to high level resistance of Pseudomonas aeruginosa to ciprofloxacin. Chin Med J (Engl) 120: 68-70.
205. Rejiba S, Aubry A, Petitfrere S, Jarlier V, Cambau E (2008) Contribution of ParE mutation and efflux to ciprofloxacin resistance in Pseudomonas aeruginosa clinical isolates. J Chemother 20: 749-752.
206. Dunham SA, McPherson CJ, Miller AA (2010) The relative contribution of efflux and target gene mutations to fluoroquinolone resistance in recent clinical isolates of Pseudomonas aeruginosa. Eur J Clin Microbiol Infect Dis 29: 279-288.
207. El Amin N, Giske CG, Jalal S, Keijser B, Kronvall G, et al. (2005) Carbapenem resistance mechanisms in Pseudomonas aeruginosa: alterations of porin OprD and efflux proteins do not fully explain resistance patterns observed in clinical isolates. APMIS 113: 187-196.
208. Pai H, Kim J, Lee JH, Choe KW, Gotoh N (2001) Carbapenem resistance mechanisms in Pseudomonas aeruginosa clinical isolates. Antimicrob Agents Chemother 45: 480-484.
209. Henrichfreise B, Wiegand I, Pfister W, Wiedemann B (2007) Resistance mechanisms of multiresistant Pseudomonas aeruginosa strains from Germany and correlation with hypermutation. Antimicrob Agents Chemother 51: 4062-4070.
210. Mulet X, Moya B, Juan C, Macia MD, Perez JL, et al. (2011) Antagonistic interactions of Pseudomonas aeruginosa antibiotic resistance mechanisms in planktonic but not biofilm growth. Antimicrob Agents Chemother 55: 4560-4568.
211. Lomovskaya O, Lee A, Hoshino K, Ishida H, Mistry A, et al. (1999) Use of a genetic approach to evaluate the consequences of inhibition of efflux pumps in Pseudomonas aeruginosa. Antimicrob Agents Chemother 43: 1340-1346.
212. Roy PH, Tetu SG, Larouche A, Elbourne L, Tremblay S, et al. (2010) Complete genome sequence of the multiresistant taxonomic outlier Pseudomonas aeruginosa PA7. PLoS One 5: e8842.
213. Magiorakos AP, Srinivasan A, Carey RB, Carmeli Y, Falagas ME, et al. (2012) Multidrug-resistant, extensively drug-resistant and pandrug-resistant bacteria: an international expert proposal for interim standard definitions for acquired resistance. Clin Microbiol Infect 18: 268-281.
214. Tsugawa H, Suzuki H, Muraoka H, Ikeda F, Hirata K, et al. (2011) Enhanced bacterial efflux system is the first step to the development of metronidazole resistance in Helicobacter pylori. Biochem Biophys Res Commun 404: 656-660.
215. Schmalstieg AM, Srivastava S, Belkaya S, Deshpande D, Meek C, et al. (2012) The antibiotic resistance arrow of time: efflux pump induction is a general first step in the evolution of mycobacterial drug resistance. Antimicrob Agents Chemother 56: 4806-4815.

216. Morita Y, Tomida J, Kawamura Y (2012) Primary mechanisms mediating aminoglycoside resistance in the multidrug-resistant Pseudomonas aeruginosa clinical isolate PA7. Microbiology 158: 1071-1083.
217. Murata T, Gotoh N, Nishino T (2002) Characterization of outer membrane efflux proteins OpmE, OpmD and OpmB of Pseudomonas aeruginosa: molecular cloning and development of specific antisera. FEMS Microbiol Lett 217: 57-63.
218. Chuanchuen R, Murata T, Gotoh N, Schweizer HP (2005) Substrate-dependent utilization of OprM or OpmH by the Pseudomonas aeruginosa MexJK efflux pump. Antimicrob Agents Chemother 49: 2133-2136.
219. Krzywinski M, Schein J, Birol I, Connors J, Gascoyne R, et al. (2009) Circos: an information aesthetic for comparative genomics. Genome Res 19: 1639-1645.
220. Komp Lindgren P, Karlsson A, Hughes D (2003) Mutation rate and evolution of fluoroquinolone resistance in Escherichia coli isolates from patients with urinary tract infections. Antimicrob Agents Chemother 47: 3222-3232.
221. Pasca MR, Dalla Valle C, De Jesus Lopes Ribeiro AL, Buroni S, Papaleo MC, et al. (2012) Evaluation of fluoroquinolone resistance mechanisms in Pseudomonas aeruginosa multidrug resistance clinical isolates. Microb Drug Resist 18: 23-32.
222. Wang Z, Gerstein M, Snyder M (2009) RNA-Seq: a revolutionary tool for transcriptomics. Nat Rev Genet 10: 57-63.
223. Chen L, Mathema B, Chavda KD, DeLeo FR, Bonomo RA, et al. (2014) Carbapenemase-producing Klebsiella pneumoniae: molecular and genetic decoding. Trends Microbiol 22: 686-696.
224. Seo JH, Hong JS, Kim D, Cho BK, Huang TW, et al. (2012) Multiple-omic data analysis of Klebsiella pneumoniae MGH 78578 reveals its transcriptional architecture and regulatory features. BMC Genomics 13: 679.
225. Kim D, Hong JS, Qiu Y, Nagarajan H, Seo JH, et al. (2012) Comparative analysis of regulatory elements between Escherichia coli and Klebsiella pneumoniae by genome-wide transcription start site profiling. PLoS Genet 8: e1002867.
226. Li J, Liu F, Wang Q, Ge P, Woo PC, et al. (2014) Genomic and transcriptomic analysis of NDM-1 Klebsiella pneumoniae in spaceflight reveal mechanisms underlying environmental adaptability. Sci Rep 4: 6216.
227. Wright MS, Suzuki Y, Jones MB, Marshall SH, Rudin SD, et al. (2014) Genomic and transcriptomic analyses of colistin-resistant clinical isolates of Klebsiella pneumoniae reveal multiple pathways of resistance. Antimicrob Agents Chemother.
228. Ogawa W, Li DW, Yu P, Begum A, Mizushima T, et al. (2005) Multidrug resistance in Klebsiella pneumoniae MGH78578 and cloning of genes responsible for the resistance. Biol Pharm Bull 28: 1505-1508.
229. Wright MS, Perez F, Brinkac L, Jacobs MR, Kaye K, et al. (2014) Population structure of KPC-producing Klebsiella pneumoniae isolates from midwestern U.S. hospitals. Antimicrob Agents Chemother 58: 4961-4965.
230. D'Andrea MM, Amisano F, Giani T, Conte V, Ciacci N, et al. (2014) Diversity of capsular polysaccharide gene clusters in Kpc-producing Klebsiella pneumoniae clinical isolates of sequence type 258 involved in the Italian epidemic. PLoS One 9: e96827.
231. Potron A, Poirel L, Rondinaud E, Nordmann P (2013) Intercontinental spread of OXA-48 beta-lactamase-producing Enterobacteriaceae over a 11-year period, 2001 to 2011. Euro Surveill 18.
232. Pitart C, Sole M, Roca I, Fabrega A, Vila J, et al. (2011) First outbreak of a plasmid-mediated carbapenem-hydrolyzing OXA-48 beta-lactamase in Klebsiella pneumoniae in Spain. Antimicrob Agents Chemother 55: 4398-4401.
233. Poulou A, Voulgari E, Vrioni G, Koumaki V, Xidopoulos G, et al. (2013) Outbreak caused by an ertapenem-resistant, CTX-M-15-producing Klebsiella pneumoniae sequence type 101 clone carrying an OmpK36 porin variant. J Clin Microbiol 51: 3176-3182.

234. Woodford N, Turton JF, Livermore DM (2011) Multiresistant Gram-negative bacteria: the role of high-risk clones in the dissemination of antibiotic resistance. FEMS Microbiol Rev 35: 736-755.
235. Breurec S, Guessennd N, Timinouni M, Le TA, Cao V, et al. (2013) Klebsiella pneumoniae resistant to third-generation cephalosporins in five African and two Vietnamese major towns: multiclonal population structure with two major international clonal groups, CG15 and CG258. Clin Microbiol Infect 19: 349-355.
236. Grundmann H, Livermore DM, Giske CG, Canton R, Rossolini GM, et al. (2010) Carbapenem-non-susceptible Enterobacteriaceae in Europe: conclusions from a meeting of national experts. Euro Surveill 15.
237. Kitchel B, Rasheed JK, Patel JB, Srinivasan A, Navon-Venezia S, et al. (2009) Molecular epidemiology of KPC-producing Klebsiella pneumoniae isolates in the United States: clonal expansion of multilocus sequence type 258. Antimicrob Agents Chemother 53: 3365-3370.
238. Chen L, Mathema B, Pitout JD, DeLeo FR, Kreiswirth BN (2014) Epidemic Klebsiella pneumoniae ST258 is a hybrid strain. MBio 5: e01355-01314.
239. Diago-Navarro E, Chen L, Passet V, Burack S, Ulacia-Hernando A, et al. (2014) Carbapenem-resistant Klebsiella pneumoniae exhibit variability in capsular polysaccharide and capsule associated virulence traits. J Infect Dis 210: 803-813.
240. Damjanova I, Toth A, Paszti J, Hajbel-Vekony G, Jakab M, et al. (2008) Expansion and countrywide dissemination of ST11, ST15 and ST147 ciprofloxacin-resistant CTX-M-15-type beta-lactamase-producing Klebsiella pneumoniae epidemic clones in Hungary in 2005--the new 'MRSAs'? J Antimicrob Chemother 62: 978-985.
241. Liapis E, Pantel A, Robert J, Nicolas-Chanoine MH, Cavalie L, et al. (2014) Molecular epidemiology of OXA-48-producing Klebsiella pneumoniae in France. Clin Microbiol Infect.
242. Rodrigues C, Machado E, Ramos H, Peixe L, Novais A (2014) Expansion of ESBL-producing Klebsiella pneumoniae in hospitalized patients: A successful story of international clones (ST15, ST147, ST336) and epidemic plasmids (IncR, IncFII). Int J Med Microbiol.
243. Stoesser N, Giess A, Batty EM, Sheppard AE, Walker AS, et al. (2014) Genome sequencing of an extended series of NDM-producing Klebsiella pneumoniae isolates from neonatal infections in a Nepali hospital characterizes the extent of community- versus hospital-associated transmission in an endemic setting. Antimicrob Agents Chemother 58: 7347-7357.
244. Tatusov RL, Galperin MY, Natale DA, Koonin EV (2000) The COG database: a tool for genome-scale analysis of protein functions and evolution. Nucleic Acids Res 28: 33-36.
245. Giannouli M, Palatucci AT, Rubino V, Ruggiero G, Romano M, et al. (2014) Use of larvae of the wax moth Galleria mellonella as an in vivo model to study the virulence of Helicobacter pylori. BMC Microbiol 14: 228.
246. Alghoribi MF, Gibreel TM, Dodgson AR, Beatson SA, Upton M (2014) Galleria mellonella infection model demonstrates high lethality of ST69 and ST127 uropathogenic E. coli. PLoS One 9: e101547.
247. Wand ME, McCowen JW, Nugent PG, Sutton JM (2013) Complex interactions of Klebsiella pneumoniae with the host immune system in a Galleria mellonella infection model. J Med Microbiol 62: 1790-1798.
248. Insua JL, Llobet E, Moranta D, Perez-Gutierrez C, Tomas A, et al. (2013) Modeling Klebsiella pneumoniae pathogenesis by infection of the wax moth Galleria mellonella. Infect Immun 81: 3552-3565.
249. Yu VL, Hansen DS, Ko WC, Sagnimeni A, Klugman KP, et al. (2007) Virulence characteristics of Klebsiella and clinical manifestations of K. pneumoniae bloodstream infections. Emerg Infect Dis 13: 986-993.
250. Darmon E, Leach DR (2014) Bacterial genome instability. Microbiol Mol Biol Rev 78: 1-39.
251. Allen BL, Gerlach GF, Clegg S (1991) Nucleotide sequence and functions of mrk determinants necessary for expression of type 3 fimbriae in Klebsiella pneumoniae. J Bacteriol 173: 916-920.

252. Langstraat J, Bohse M, Clegg S (2001) Type 3 fimbrial shaft (MrkA) of Klebsiella pneumoniae, but not the fimbrial adhesin (MrkD), facilitates biofilm formation. Infect Immun 69: 5805-5812.
253. Huang YJ, Liao HW, Wu CC, Peng HL (2009) MrkF is a component of type 3 fimbriae in Klebsiella pneumoniae. Res Microbiol 160: 71-79.
254. Jagnow J, Clegg S (2003) Klebsiella pneumoniae MrkD-mediated biofilm formation on extracellular matrix- and collagen-coated surfaces. Microbiology 149: 2397-2405.
255. Zogaj X, Bokranz W, Nimtz M, Romling U (2003) Production of cellulose and curli fimbriae by members of the family Enterobacteriaceae isolated from the human gastrointestinal tract. Infect Immun 71: 4151-4158.
256. Morgan JL, McNamara JT, Zimmer J (2014) Mechanism of activation of bacterial cellulose synthase by cyclic di-GMP. Nat Struct Mol Biol 21: 489-496.
257. Romling U, Galperin MY, Gomelsky M (2013) Cyclic di-GMP: the first 25 years of a universal bacterial second messenger. Microbiol Mol Biol Rev 77: 1-52.
258. Dashper S, Ang CS, Liu SW, Paolini R, Veith P, et al. (2010) Inhibition of Porphyromonas gingivalis biofilm by oxantel. Antimicrob Agents Chemother 54: 1311-1314.
259. Mikkelsen H, Duck Z, Lilley KS, Welch M (2007) Interrelationships between colonies, biofilms, and planktonic cells of Pseudomonas aeruginosa. J Bacteriol 189: 2411-2416.
260. Ritter A, Com E, Bazire A, Goncalves Mdos S, Delage L, et al. (2012) Proteomic studies highlight outer-membrane proteins related to biofilm development in the marine bacterium Pseudoalteromonas sp. D41. Proteomics 12: 3180-3192.
261. Livermore DM (1995) beta-Lactamases in laboratory and clinical resistance. Clin Microbiol Rev 8: 557-584.
262. Moya B, Dötsch A, Juan C, Blazquez J, Zamorano L, et al. (2009) Beta-lactam resistance response triggered by inactivation of a nonessential penicillin-binding protein. PLoS Pathog 5: e1000353.
263. Davies J (1994) Inactivation of antibiotics and the dissemination of resistance genes. Science 264: 375-382.
264. Walther-Rasmussen J, Hoiby N (2006) OXA-type carbapenemases. J Antimicrob Chemother 57: 373-383.
265. Leavitt A, Carmeli Y, Chmelnitsky I, Goren MG, Ofek I, et al. (2010) Molecular epidemiology, sequence types, and plasmid analyses of KPC-producing Klebsiella pneumoniae strains in Israel. Antimicrob Agents Chemother 54: 3002-3006.
266. Lopez JA, Correa A, Navon-Venezia S, Correa AL, Torres JA, et al. (2011) Intercontinental spread from Israel to Colombia of a KPC-3-producing Klebsiella pneumoniae strain. Clin Microbiol Infect 17: 52-56.
267. Poirel L, Heritier C, Tolun V, Nordmann P (2004) Emergence of oxacillinase-mediated resistance to imipenem in Klebsiella pneumoniae. Antimicrob Agents Chemother 48: 15-22.
268. Zhou XY, Bordon F, Sirot D, Kitzis MD, Gutmann L (1994) Emergence of clinical isolates of Escherichia coli producing TEM-1 derivatives or an OXA-1 beta-lactamase conferring resistance to beta-lactamase inhibitors. Antimicrob Agents Chemother 38: 1085-1089.
269. Dortet L, Radu I, Gautier V, Blot F, Chachaty E, et al. (2008) Intercontinental travels of patients and dissemination of plasmid-mediated carbapenemase KPC-3 associated with OXA-9 and TEM-1. J Antimicrob Chemother 61: 455-457.
270. Huovinen P, Jacoby GA (1991) Sequence of the PSE-1 beta-lactamase gene. Antimicrob Agents Chemother 35: 2428-2430.
271. Wozniak A, Villagra NA, Undabarrena A, Gallardo N, Keller N, et al. (2012) Porin alterations present in non-carbapenemase-producing Enterobacteriaceae with high and intermediate levels of carbapenem resistance in Chile. J Med Microbiol 61: 1270-1279.
272. Bradford PA (2001) Extended-spectrum beta-lactamases in the 21st century: characterization, epidemiology, and detection of this important resistance threat. Clin Microbiol Rev 14: 933-951, table of contents.

273. Paterson DL, Bonomo RA (2005) Extended-spectrum beta-lactamases: a clinical update. Clin Microbiol Rev 18: 657-686.
274. Sougakoff W, Goussard S, Gerbaud G, Courvalin P (1988) Plasmid-mediated resistance to third-generation cephalosporins caused by point mutations in TEM-type penicillinase genes. Rev Infect Dis 10: 879-884.
275. Knothe H, Shah P, Krcmery V, Antal M, Mitsuhashi S (1983) Transferable resistance to cefotaxime, cefoxitin, cefamandole and cefuroxime in clinical isolates of Klebsiella pneumoniae and Serratia marcescens. Infection 11: 315-317.
276. Bonnet R (2004) Growing group of extended-spectrum beta-lactamases: the CTX-M enzymes. Antimicrob Agents Chemother 48: 1-14.
277. Poirel L, Gniadkowski M, Nordmann P (2002) Biochemical analysis of the ceftazidime-hydrolysing extended-spectrum beta-lactamase CTX-M-15 and of its structurally related beta-lactamase CTX-M-3. J Antimicrob Chemother 50: 1031-1034.
278. Livermore DM, Woodford N (2006) The beta-lactamase threat in Enterobacteriaceae, Pseudomonas and Acinetobacter. Trends Microbiol 14: 413-420.
279. Ewers C, Stamm I, Pfeifer Y, Wieler LH, Kopp PA, et al. (2014) Clonal spread of highly successful ST15-CTX-M-15 Klebsiella pneumoniae in companion animals and horses. J Antimicrob Chemother 69: 2676-2680.
280. Paterson DL, Hujer KM, Hujer AM, Yeiser B, Bonomo MD, et al. (2003) Extended-spectrum beta-lactamases in Klebsiella pneumoniae bloodstream isolates from seven countries: dominance and widespread prevalence of SHV- and CTX-M-type beta-lactamases. Antimicrob Agents Chemother 47: 3554-3560.
281. Nobuta K, Tolmasky ME, Crosa LM, Crosa JH (1988) Sequencing and expression of the 6'-N-acetyltransferase gene of transposon Tn1331 from Klebsiella pneumoniae. J Bacteriol 170: 3769-3773.
282. Shaw KJ, Rather PN, Hare RS, Miller GH (1993) Molecular genetics of aminoglycoside resistance genes and familial relationships of the aminoglycoside-modifying enzymes. Microbiol Rev 57: 138-163.
283. Lambert T, Ploy MC, Courvalin P (1994) A spontaneous point mutation in the aac(6')-Ib' gene results in altered substrate specificity of aminoglycoside 6'-N-acetyltransferase of a Pseudomonas fluorescens strain. FEMS Microbiol Lett 115: 297-304.
284. Rosenberg EY, Ma D, Nikaido H (2000) AcrD of Escherichia coli is an aminoglycoside efflux pump. J Bacteriol 182: 1754-1756.
285. Ping Y, Ogawa W, Kuroda T, Tsuchiya T (2007) Gene cloning and characterization of KdeA, a multidrug efflux pump from Klebsiella pneumoniae. Biol Pharm Bull 30: 1962-1964.
286. Nishino K, Yamaguchi A (2001) Analysis of a complete library of putative drug transporter genes in Escherichia coli. J Bacteriol 183: 5803-5812.
287. Edgar R, Bibi E (1997) MdfA, an Escherichia coli multidrug resistance protein with an extraordinarily broad spectrum of drug recognition. J Bacteriol 179: 2274-2280.
288. Martinez-Martinez L, Pascual A, Jacoby GA (1998) Quinolone resistance from a transferable plasmid. Lancet 351: 797-799.
289. Briales A, Rodriguez-Martinez JM, Velasco C, Diaz de Alba P, Dominguez-Herrera J, et al. (2011) In vitro effect of qnrA1, qnrB1, and qnrS1 genes on fluoroquinolone activity against isogenic Escherichia coli isolates with mutations in gyrA and parC. Antimicrob Agents Chemother 55: 1266-1269.
290. Rodriguez-Martinez JM, Velasco C, Garcia I, Cano ME, Martinez-Martinez L, et al. (2007) Characterisation of integrons containing the plasmid-mediated quinolone resistance gene qnrA1 in Klebsiella pneumoniae. Int J Antimicrob Agents 29: 705-709.
291. Vetting MW, Hegde SS, Wang M, Jacoby GA, Hooper DC, et al. (2011) Structure of QnrB1, a plasmid-mediated fluoroquinolone resistance factor. J Biol Chem 286: 25265-25273.
292. Depardieu F, Podglajen I, Leclercq R, Collatz E, Courvalin P (2007) Modes and modulations of antibiotic resistance gene expression. Clin Microbiol Rev 20: 79-114.

293. Mazzariol A, Cornaglia G, Nikaido H (2000) Contributions of the AmpC beta-lactamase and the AcrAB multidrug efflux system in intrinsic resistance of Escherichia coli K-12 to beta-lactams. Antimicrob Agents Chemother 44: 1387-1390.
294. Mazzariol A, Tokue Y, Kanegawa TM, Cornaglia G, Nikaido H (2000) High-level fluoroquinolone-resistant clinical isolates of Escherichia coli overproduce multidrug efflux protein AcrA. Antimicrob Agents Chemother 44: 3441-3443.
295. Bialek-Davenet S, Lavigne JP, Guyot K, Mayer N, Tournebize R, et al. (2015) Differential contribution of AcrAB and OqxAB efflux pumps to multidrug resistance and virulence in Klebsiella pneumoniae. J Antimicrob Chemother 70: 81-88.
296. Jacoby GA, Strahilevitz J, Hooper DC (2014) Plasmid-mediated quinolone resistance. Microbiol Spectr 2.
297. Rodriguez-Martinez JM, Diaz de Alba P, Briales A, Machuca J, Lossa M, et al. (2013) Contribution of OqxAB efflux pumps to quinolone resistance in extended-spectrum-beta-lactamase-producing Klebsiella pneumoniae. J Antimicrob Chemother 68: 68-73.
298. De Majumdar S, Veleba M, Finn S, Fanning S, Schneiders T (2013) Elucidating the regulon of multidrug resistance regulator RarA in Klebsiella pneumoniae. Antimicrob Agents Chemother 57: 1603-1609.
299. Veleba M, Higgins PG, Gonzalez G, Seifert H, Schneiders T (2012) Characterization of RarA, a novel AraC family multidrug resistance regulator in Klebsiella pneumoniae. Antimicrob Agents Chemother 56: 4450-4458.
300. Doumith M, Ellington MJ, Livermore DM, Woodford N (2009) Molecular mechanisms disrupting porin expression in ertapenem-resistant Klebsiella and Enterobacter spp. clinical isolates from the UK. J Antimicrob Chemother 63: 659-667.
301. Chen FJ, Lauderdale TL, Ho M, Lo HJ (2003) The roles of mutations in gyrA, parC, and ompK35 in fluoroquinolone resistance in Klebsiella pneumoniae. Microb Drug Resist 9: 265-271.
302. Domenech-Sanchez A, Martinez-Martinez L, Hernandez-Alles S, del Carmen Conejo M, Pascual A, et al. (2003) Role of Klebsiella pneumoniae OmpK35 porin in antimicrobial resistance. Antimicrob Agents Chemother 47: 3332-3335.
303. Song W, Suh B, Choi JY, Jeong SH, Jeon EH, et al. (2009) In vivo selection of carbapenem-resistant Klebsiella pneumoniae by OmpK36 loss during meropenem treatment. Diagn Microbiol Infect Dis 65: 447-449.
304. Tsai YK, Fung CP, Lin JC, Chen JH, Chang FY, et al. (2011) Klebsiella pneumoniae outer membrane porins OmpK35 and OmpK36 play roles in both antimicrobial resistance and virulence. Antimicrob Agents Chemother 55: 1485-1493.
305. Heisig P (1996) Genetic evidence for a role of parC mutations in development of high-level fluoroquinolone resistance in Escherichia coli. Antimicrob Agents Chemother 40: 879-885.
306. Khodursky AB, Zechiedrich EL, Cozzarelli NR (1995) Topoisomerase IV is a target of quinolones in Escherichia coli. Proc Natl Acad Sci U S A 92: 11801-11805.
307. Kumagai Y, Kato JI, Hoshino K, Akasaka T, Sato K, et al. (1996) Quinolone-resistant mutants of escherichia coli DNA topoisomerase IV parC gene. Antimicrob Agents Chemother 40: 710-714.
308. Houssaye S, Gutmann L, Varon E (2002) Topoisomerase mutations associated with in vitro selection of resistance to moxifloxacin in Streptococcus pneumoniae. Antimicrob Agents Chemother 46: 2712-2715.
309. Smith HJ, Walters M, Hisanaga T, Zhanel GG, Hoban DJ (2004) Mutant prevention concentrations for single-step fluoroquinolone-resistant mutants of wild-type, efflux-positive, or ParC or GyrA mutation-containing Streptococcus pneumoniae isolates. Antimicrob Agents Chemother 48: 3954-3958.
310. van Vliet AH (2010) Next generation sequencing of microbial transcriptomes: challenges and opportunities. FEMS Microbiol Lett 302: 1-7.
311. Sorek R, Cossart P (2010) Prokaryotic transcriptomics: a new view on regulation, physiology and pathogenicity. Nat Rev Genet 11: 9-16.

312. Croucher NJ, Thomson NR (2010) Studying bacterial transcriptomes using RNA-seq. Curr Opin Microbiol 13: 619-624.
313. Zhanel GG, Chung P, Adam H, Zelenitsky S, Denisuik A, et al. (2014) Ceftolozane/tazobactam: a novel cephalosporin/beta-lactamase inhibitor combination with activity against multidrug-resistant gram-negative bacilli. Drugs 74: 31-51.
314. Cabot G, Bruchmann S, Mulet X, Zamorano L, Moya B, et al. (2014) Pseudomonas aeruginosa ceftolozane-tazobactam resistance development requires multiple mutations leading to overexpression and structural modification of AmpC. Antimicrob Agents Chemother 58: 3091-3099.
315. Kurnasov O, Jablonski L, Polanuyer B, Dorrestein P, Begley T, et al. (2003) Aerobic tryptophan degradation pathway in bacteria: novel kynurenine formamidase. FEMS Microbiol Lett 227: 219-227.
316. Bredenbruch F, Nimtz M, Wray V, Morr M, Muller R, et al. (2005) Biosynthetic pathway of Pseudomonas aeruginosa 4-hydroxy-2-alkylquinolines. J Bacteriol 187: 3630-3635.
317. Bredenbruch F, Geffers R, Nimtz M, Buer J, Haussler S (2006) The Pseudomonas aeruginosa quinolone signal (PQS) has an iron-chelating activity. Environ Microbiol 8: 1318-1329.
318. Farrow JM, 3rd, Pesci EC (2007) Two distinct pathways supply anthranilate as a precursor of the Pseudomonas quinolone signal. J Bacteriol 189: 3425-3433.
319. Olsen LR, Vetting MW, Roderick SL (2007) Structure of the E. coli bifunctional GlmU acetyltransferase active site with substrates and products. Protein Sci 16: 1230-1235.
320. Mehra R, Sharma R, Khan IA, Nargotra A (2015) Identification and optimization of Escherichia coli GlmU inhibitors: An in silico approach with validation thereof. Eur J Med Chem 92: 78-90.
321. Wong A, Kassen R (2011) Parallel evolution and local differentiation in quinolone resistance in Pseudomonas aeruginosa. Microbiology 157: 937-944.
322. Pedersen SS, Jensen T, Hvidberg EF (1987) Comparative pharmacokinetics of ciprofloxacin and ofloxacin in cystic fibrosis patients. J Antimicrob Chemother 20: 575-583.
323. Moriarty TF, McElnay JC, Elborn JS, Tunney MM (2007) Sputum antibiotic concentrations: implications for treatment of cystic fibrosis lung infection. Pediatr Pulmonol 42: 1008-1017.
324. Wright EA, Fothergill JL, Paterson S, Brockhurst MA, Winstanley C (2013) Sub-inhibitory concentrations of some antibiotics can drive diversification of Pseudomonas aeruginosa populations in artificial sputum medium. BMC Microbiol 13: 170.
325. Li X, Mariano N, Rahal JJ, Urban CM, Drlica K (2004) Quinolone-resistant Haemophilus influenzae: determination of mutant selection window for ciprofloxacin, garenoxacin, levofloxacin, and moxifloxacin. Antimicrob Agents Chemother 48: 4460-4462.
326. Heisig P, Tschorny R (1994) Characterization of fluoroquinolone-resistant mutants of escherichia coli selected in vitro. Antimicrob Agents Chemother 38: 1284-1291.
327. Singh R, Swick MC, Ledesma KR, Yang Z, Hu M, et al. (2012) Temporal interplay between efflux pumps and target mutations in development of antibiotic resistance in Escherichia coli. Antimicrob Agents Chemother 56: 1680-1685.
328. Drlica K (2003) The mutant selection window and antimicrobial resistance. J Antimicrob Chemother 52: 11-17.
329. Gullberg E, Cao S, Berg OG, Ilback C, Sandegren L, et al. (2011) Selection of resistant bacteria at very low antibiotic concentrations. PLoS Pathog 7: e1002158.
330. Maechler F, Pena Diaz LA, Schroder C, Geffers C, Behnke M, et al. (2014) Prevalence of carbapenem-resistant organisms and other Gram-negative MDRO in German ICUs: first results from the national nosocomial infection surveillance system (KISS). Infection.
331. Pohl S, Klockgether J, Eckweiler D, Khaledi A, Schniederjans M, et al. (2014) The extensive set of accessory Pseudomonas aeruginosa genomic components. FEMS Microbiol Lett 356: 235-241.
332. Bielecki P, Muthukumarasamy U, Eckweiler D, Bielecka A, Pohl S, et al. (2014) In vivo mRNA profiling of uropathogenic Escherichia coli from diverse phylogroups reveals common and group-specific gene expression profiles. MBio 5: e01075-01014.

333. Kaas RS, Friis C, Ussery DW, Aarestrup FM (2012) Estimating variation within the genes and inferring the phylogeny of 186 sequenced diverse Escherichia coli genomes. BMC Genomics 13: 577.
334. Toledo-Arana A, Dussurget O, Nikitas G, Sesto N, Guet-Revillet H, et al. (2009) The Listeria transcriptional landscape from saprophytism to virulence. Nature 459: 950-956.
335. Mandlik A, Livny J, Robins WP, Ritchie JM, Mekalanos JJ, et al. (2011) RNA-Seq-based monitoring of infection-linked changes in Vibrio cholerae gene expression. Cell Host Microbe 10: 165-174.
336. Szafranska AK, Oxley AP, Chaves-Moreno D, Horst SA, Rosslenbroich S, et al. (2014) High-Resolution Transcriptomic Analysis of the Adaptive Response of Staphylococcus aureus during Acute and Chronic Phases of Osteomyelitis. MBio 5.
337. Vickery K, Deva A, Jacombs A, Allan J, Valente P, et al. (2012) Presence of biofilm containing viable multiresistant organisms despite terminal cleaning on clinical surfaces in an intensive care unit. J Hosp Infect 80: 52-55.
338. Oliveros JC (2007) VENNY. An interactive tool for comparing lists with Venn Diagrams.
339. Comas I, Borrell S, Roetzer A, Rose G, Malla B, et al. (2012) Whole-genome sequencing of rifampicin-resistant Mycobacterium tuberculosis strains identifies compensatory mutations in RNA polymerase genes. Nat Genet 44: 106-110.
340. Zankari E, Hasman H, Kaas RS, Seyfarth AM, Agerso Y, et al. (2013) Genotyping using whole-genome sequencing is a realistic alternative to surveillance based on phenotypic antimicrobial susceptibility testing. J Antimicrob Chemother 68: 771-777.
341. Stoesser N, Batty EM, Eyre DW, Morgan M, Wyllie DH, et al. (2013) Predicting antimicrobial susceptibilities for Escherichia coli and Klebsiella pneumoniae isolates using whole genomic sequence data. J Antimicrob Chemother 68: 2234-2244.
342. Gordon NC, Price JR, Cole K, Everitt R, Morgan M, et al. (2014) Prediction of Staphylococcus aureus antimicrobial resistance by whole-genome sequencing. J Clin Microbiol 52: 1182-1191.
343. Kos VN, Deraspe M, McLaughlin RE, Whiteaker JD, Roy PH, et al. (2015) The resistome of Pseudomonas aeruginosa in relationship to phenotypic susceptibility. Antimicrob Agents Chemother 59: 427-436.
344. Koser CU, Ellington MJ, Cartwright EJ, Gillespie SH, Brown NM, et al. (2012) Routine use of microbial whole genome sequencing in diagnostic and public health microbiology. PLoS Pathog 8: e1002824.
345. Didelot X, Bowden R, Wilson DJ, Peto TE, Crook DW (2012) Transforming clinical microbiology with bacterial genome sequencing. Nat Rev Genet 13: 601-612.
346. Koser CU, Holden MT, Ellington MJ, Cartwright EJ, Brown NM, et al. (2012) Rapid whole-genome sequencing for investigation of a neonatal MRSA outbreak. N Engl J Med 366: 2267-2275.
347. Reuter S, Ellington MJ, Cartwright EJ, Koser CU, Torok ME, et al. (2013) Rapid bacterial whole-genome sequencing to enhance diagnostic and public health microbiology. JAMA Intern Med 173: 1397-1404.
348. Koser CU, Fraser LJ, Ioannou A, Becq J, Ellington MJ, et al. (2014) Rapid single-colony whole-genome sequencing of bacterial pathogens. J Antimicrob Chemother 69: 1275-1281.
349. Pulido MR, Garcia-Quintanilla M, Martin-Pena R, Cisneros JM, McConnell MJ (2013) Progress on the development of rapid methods for antimicrobial susceptibility testing. J Antimicrob Chemother 68: 2710-2717.
350. Barenfanger J, Drake C, Kacich G (1999) Clinical and financial benefits of rapid bacterial identification and antimicrobial susceptibility testing. J Clin Microbiol 37: 1415-1418.
351. Weiss J, Arielly H, Ganor N, Paitan Y (2015) Evaluation of the NanoCHIP Infection Control Panel test for direct detection and screening of methicillin-resistant Staphylococcus aureus (MRSA), Klebsiella pneumoniae carbapenemase (KPC)-producing bacteria and vancomycin-resistant Enterococcus (VRE). Infection.

352. Miller MB, Tang YW (2009) Basic concepts of microarrays and potential applications in clinical microbiology. Clin Microbiol Rev 22: 611-633.
353. Tuite N, Reddington K, Barry T, Zumla A, Enne V (2014) Rapid nucleic acid diagnostics for the detection of antimicrobial resistance in Gram-negative bacteria: is it time for a paradigm shift? J Antimicrob Chemother 69: 1729-1733.
354. Stanssens P, Zabeau M, Meersseman G, Remes G, Gansemans Y, et al. (2004) High-throughput MALDI-TOF discovery of genomic sequence polymorphisms. Genome Res 14: 126-133.
355. Jurinke C, Denissenko MF, Oeth P, Ehrich M, van den Boom D, et al. (2005) A single nucleotide polymorphism based approach for the identification and characterization of gene expression modulation using MassARRAY. Mutat Res 573: 83-95.
356. Dutton-Regester K, Irwin D, Hunt P, Aoude LG, Tembe V, et al. (2012) A high-throughput panel for identifying clinically relevant mutation profiles in melanoma. Mol Cancer Ther 11: 888-897.
357. Mao Y, Tan F, Yan SG, Wu GX, Qiao CL, et al. (2013) High-throughput genotyping of single-nucleotide polymorphisms in ace-1 gene of mosquitoes using MALDI-TOF mass spectrometry. Insect Sci 20: 167-174.
358. Posthuma CC, van der Beek MT, van der Blij-de Brouwer CS, van der Heiden PL, Marijt EW, et al. (2011) Mass spectrometry-based comparative sequencing to detect ganciclovir resistance in the UL97 gene of human cytomegalovirus. J Clin Virol 51: 25-30.
359. Shi A, Chen P, Vierling R, Zheng C, Li D, et al. (2011) Multiplex single nucleotide polymorphism (SNP) assay for detection of soybean mosaic virus resistance genes in soybean. Theor Appl Genet 122: 445-457.
360. Syrmis MW, Moser RJ, Whiley DM, Vaska V, Coombs GW, et al. (2011) Comparison of a multiplexed MassARRAY system with real-time allele-specific PCR technology for genotyping of methicillin-resistant Staphylococcus aureus. Clin Microbiol Infect 17: 1804-1810.
361. Bouakaze C, Keyser C, Gonzalez A, Sougakoff W, Veziris N, et al. (2011) Matrix-assisted laser desorption ionization-time of flight mass spectrometry-based single nucleotide polymorphism genotyping assay using iPLEX gold technology for identification of Mycobacterium tuberculosis complex species and lineages. J Clin Microbiol 49: 3292-3299.
362. Trembizki E, Smith H, Lahra MM, Chen M, Donovan B, et al. (2014) High-throughput informative single nucleotide polymorphism-based typing of Neisseria gonorrhoeae using the Sequenom MassARRAY iPLEX platform. J Antimicrob Chemother 69: 1526-1532.
363. Morelli G, Song Y, Mazzoni CJ, Eppinger M, Roumagnac P, et al. (2010) Yersinia pestis genome sequencing identifies patterns of global phylogenetic diversity. Nat Genet 42: 1140-1143.

7 Danksagungen

In erster Linie danke ich meiner Betreuerin und Gruppenleiterin Prof. Susanne Häußler für die Möglichkeit, in dieser großartigen Gruppe zu arbeiten. Danke für die immerwährende Motivation, die nie endenden Ideen und die Unterstützung während der letzten Jahre.

Weiterhin möchte ich mich bei meinem Mentor Prof. Michael Steinert bedanken und Prof. Dietmar Schomburg danke ich für den Vorsitz der Prüfungskommission.

Den Mitgliedern meines *Thesis Committee* Dr. Ulrich Nübel und Dr. Manfred Höfle danke ich für die anregenden Diskussionen während unserer Treffen und die Unterstützung während meiner Dissertation.

Bei unserer ganzen Abteilung MOBA am HZI und am Twincore möchte ich mich für die die Unterstützung und die tolle Atmosphäre während der letzten Jahre bedanken! Ich danke Agata Bielecka und Tanja Nicolai für die Durchführung der Illumina *library preparation* und Bianca Nouri für die Unterstützung bei der Mutagenese. Weiterhin möchte ich mich für die exzellente Unterstützung unserer Bioinformatiker*innen bedanken. Allen voran Denitsa Eckweiler, Klaus Hornischer, Uthayakumar Muthukumarasamy, Sarah Pohl und Matthias Preuße.

Vor allem aber danke ich Monika Schniederjans, Ariane Khaledi und Agata Bielecka für die wundervolle Stimmung in unserem Büro und die Versorgung mit Tee, Schokolade und guter Laune sowie Mathias Müsken und Stephan Brouwer für die Duelle abseits des Labors auf dem Fußballplatz.

Ich danke allen beteiligten Kooperationspartner*innen, die uns freundlicherweise klinische Proben zur Verfügung gestellt haben: Iris F. Chaberny (Medizinischen Hochschule Hannover, jetzt Universitätsklinikum Leipzig), Axel Kola und Petra Gastmeier (Charité - Universitätsmedizin Berlin), Isabell Hamann und Roger Hillert (Medizinischen Labor Ostsachsen), Daniel Jonas (Universitätsklinikum Freiburg), Wolfgang Witte und Yvonne Pfeifer (Robert-Koch-Institut Wernigerode) sowie Martin Kaase und Sören Gatermann (Nationale Referenzzentrum für Gram-negative Krankenhauserreger Bochum).

Dr. Robert Geffers und der Arbeitsgruppe Genomanalytik am HZI danke ich für die Bereitstellung des Pyrosequencers und die Durchführung der Illumina- Sequenzierung

Meiner Familie danke ich für immerwährende Unterstützung.

Abschließend möchte ich Marcelina danken, dem wichtigsten Menschen in meinem Leben.